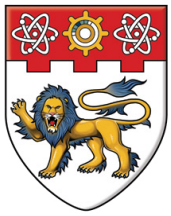

NANYANG TECHNOLOGICAL UNIVERSITY

EXPERIMENTAL INVESTIGATION OF SURFACE MODIFICATION MECHANISM IN VIBRATORY FINISHING PROCESS

Prakasam Pradeep Kumar

School of Mechanical and Aerospace Engineering

Nanyang Technological University, Singapore

2015

Acknowledgments

I would like to start my thesis by thanking the people who helped me reach this stage in my graduate studies. Each and everyone mentioned in this section have played a significant role and just adding them in this section of my thesis would not be sufficient to express my gratitude. I am always indebted to them for their help and support.

First and foremost, I would like to express my sincere gratitude to my supervisors Dr. Sathyan Subbiah (previously Asst. Prof. at NTU, now Assoc. Prof. at IIT-Madras) and Dr. Sylvie Castagne (Asst. Prof. at NTU) for their continuous support and guidance throughout my PhD studies.

Thanks to Dr. Sathyan Subbiah for accepting me in the graduate program under his supervision; for supporting me throughout my studies, and for guiding me to successfully reach the final stage of my graduate school journey. Thanks for his patience during the long technical discussions during our weekly meetings which had molded me not only as a researcher but also as an individual.

Thanks to Dr. Sylvie Castagne for her initial support and guidance as my co-supervisor. But I cannot thank her enough for accepting to supervise me, join her research group and helping me complete my thesis during my final year. Without her help, support and guidance, I wouldn't have reached this stage and this thesis would not have taken its current shape. I would like to express my heartfelt gratitude to her.

I would also like to thank the members of my PhD confirmation panel - Dr. Yeo Swee Hock, Dr. Zhou Kun and Dr. Zhang Yilei for their valuable comments and suggestions during my confirmation examination.

Thanks to the Nanyang Technological University and School of Mechanical and Aerospace Engineering Management for accepting and funding my PhD program through the NTU Research Scholarship.

I acknowledge and sincerely thank the partial scholarship and funding support

received from Rolls-Royce Advanced Technology Center, Singapore. I am grateful to Mr. Kelvin Chan and Ms. Anna Tai from Rolls-Royce for their support and guidance as my project managers. A special thanks to Mr. Kelvin Chan for his technical guidance, support and help throughout my course. I would like to thank Dr. Henry Cheng, Dr. Wang Wei and Mr. Kai Soon Fong from A-STAR for their support and collaboration during their period of secondment with Rolls-Royce. And a special thanks to Dr. Henry Cheng for his suggestions and advice during the final year of my PhD.

I would also like to thank Dr. Chow Cher Wong, Mr. Edwin Ng, Mr. Wee Kin Teo, Dr. Kurichi Kumar, Mr. Thomas Haubold and Mr. Charles Ng from Rolls-Royce for their support in the completion of my PhD thesis. I also want to thank Mr. Gary, Mr. Kai Lee and Ms. Cathlyn for helping me to operate the machines and equipment in Rolls-Royce. I would like to thank Ms. Jacelyn, Mr. Ang Teck Meng, Mr. Poon Weng, Ms. Mei Yoke for helping me operate the lab equipment in NTU. I would like to thank Mr. Vigneashwara Pandiyan and Mr. Tejaswi Abrol for their collaboration and support during their masters dissertation and for helping me perform some of the experiments for my PhD thesis. I would also like to thank Mr. Arvind, Mr. Sudhan, Mr. Saravanan, Mr. Vignesh, Mr. Rajaganesh, Mr. Dinesh, Mr. Siddharth and Mr. Tijo for their valuable suggestions and support as research associates from NTU. Thanks to Dr. Buddhika, Mr. Bala, Mr. Mani, Dr. Rajaneesh, Mr. Shanmugam, Mr. Adnan and Dr. Karthic for their support as fellow PhD students without which my PhD journey wouldn't have been so smooth.

I would like to thank Dr. Tai Kang (Assoc. Prof. at NTU) for his guidance during my Masters Dissertation; for introducing me to Rolls-Royce and for his encouragement to apply for a PhD program. I would also like to thank Dr. Chee Keong Goh from Rolls-Royce for his guidance during my Masters Dissertation.

And last but not the least I would like to thank my friends, parents and my brother for their unconditional love and support throughout my life.

Abstract

Vibratory finishing process is a widely used surface modification and polishing process in the aerospace, marine and automotive industry to alter the surface finish. Although it has been used for a long time, the mechanism of the surface modification and the relationship between process parameters and the surface finish obtained is not clear due to the complexity of surface modification mechanism and uncontrollable nature of process parameters. Thus the design of this process for new components is still undertaken on a trial and error basis. Material removal models and optimization algorithms are available for this vibratory finishing, but the type of mechanism which leads to the final surface is still not clear. From a tribological viewpoint, surface modification can be a result of either of two mechanisms – plastic deformation or material removal. This thesis strives to find the effect of process parameters on these mechanisms and final surface obtained. Specialized techniques involving controlled 1D vibration, wear debris analysis and online acoustic emission measurement have been developed. The surface modification mechanism is measured using a novel method and is related to the final surface finish obtained (Chapter 4). A novel method to collect the wear debris of the workpiece surface is developed and the wear debris collected is related to the surface modification mechanism and final surface (Chapter 5). In 1D vibratory finishing the parallel and perpendicular media motion is separated and the effect of media motion, frequency and amplitude is studied (Chapter 6). The contact between the media particles and workpiece are recorded using an acoustic emission sensor and the results are compared. This technique is proposed as an online monitoring technique for vibratory finishing process (Chapter 7). The vibratory finishing process is studied and reported from a tribological viewpoint which will be of use to the industries to better understand and optimize the process.

Contents

List of Tables

List of Figures

List of Symbols

β constant from geometric properties of chip (Chai and Lawn's model)

ρ density of workpiece

a bowl acceleration

K media cutting factor constant

m_w mass of the workpiece

v_w workpiece velocity

AE Acoustic Emission

CFD Computational Fluid Dynamics

g acceleration due to gravity

h height from which the media is dropped

MR Material Removal

PD Plastic Deformation

Ra Average Surface Roughness

T Time

U specific energy

v velocity

Chapter 1

Introduction

1.1 Overview

Vibratory finishing is one of the widely used surface modification processes in the aerospace, marine and automotive manufacturing industry to alter the surface finish of the components. It is one of the mass finishing processes (explained in section 1.3.3) used to finish more than one part at the same time. It combines the principle of abrasive machining (section 1.3) and mass movement of abrasive media to alter the peaks and valleys of the surface thereby altering the surface finish of the workpiece. The main focus of this thesis is the experimental investigation of surface modification and monitoring of vibratory finishing process.

This chapter introduces the reader to the basic types of abrasive and machining processes to give an overview on where the vibratory finishing process is placed in the manufacturing process cycle and also explains how the process works along with its merits and demerits. A brief review of the published literature is also made to give an overview on the previous scientific work done. Based on these information, the objective and scope of the thesis is introduced at the end of this chapter.

1.2 Machining

A raw material is converted into a finished component by a series of processes. The first process is usually purification of the raw materials which are available freely in nature (like iron ore). After this process, many kinds of process chains are available based on the specific application required. One of the most common cycle includes casting followed by machining and finishing which is explained in this section. The purified raw material is cast into required shapes by melting and pouring the molten material into casts of desired shape. This casting is usually made of sand which has cavities carved into required shapes. The cast material is then made into desired shape by removing material by series of processes called machining.

Machining is a cutting process which use objects with sharp edges called as tools (usually made of hard metals like steel) which in turn cut the cast parts into desired shape. There are four types of variations of this cutting process depending on the orientation and the type of tool used.

1. If the workpiece is fixed to a rotating chuck and a single stationary tool is forced on the workpiece removing material forming a cylindrical or an elliptical part, the process is called **turning**, and usually the tool will have a single cutting edge.

2. If the tool is rotated and the workpiece is fixed creating a flat surface, the process is called **milling**, and the tool will usually have more than two edges.

3. Another type of machining process which make holes by using a cylindrical tool is called **drilling**.

4. If the formed hole is enlarged or machined to a required dimension, the process is called **boring**.

These are the four basic types of machining processes. They can be subdivided into many types depending on the application. Cutting tools are very efficient in

removing material but achieving close tolerances (that is, making the shape conform to the required dimension) and high quality surface finishes require high precision, which is expensive to implement on mass scale manufacturing. Hence a new type of cutting tools called abrasives were invented about a century ago. Machining processes which uses abrasives to remove material is usually called Finishing or Polishing. This is explained in the next section. The three typical parts of widely used manufacturing processes cycle are Casting, Machining and Polishing. Figure 1.1 shows a typical manufacturing process cycle.

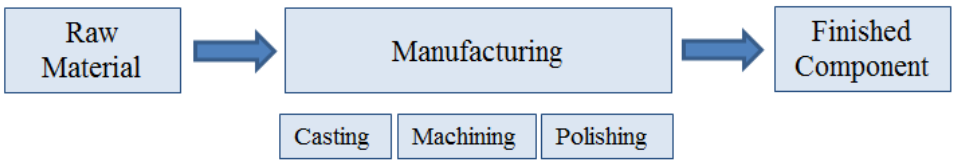

Figure 1.1: Typical Manufacturing Process Cycle

1.3 Abrasive Machining Process

As explained earlier, machining processes which use abrasives are called abrasive or finishing or polishing processes. This section will explain abrasives process and tools in detail. Abrasives are small miniature cutting tools made of naturally occurring or artificial hard minerals. These abrasives are formed into different shapes like wheels by bonding together with materials like feldspar or coated on top of a strong paper or cloth belt. There are many types of naturally occurring abrasives in forms such as crystalline silicon carbide (SiC), aluminum oxide (Al_2O_3) and also natural diamond (any diamond not of gem quality). In addition to this, scientists have also developed some artificial abrasives like artificial diamonds and cubic boron nitride (CBN). Table 1.1 lists the knoop hardness and the application of these abrasives.

Each of these abrasives has its own applications. Diamonds are the hardest abrasives and can cut any material other than steel, due to chemical reactivity between the diamonds and steel. Aluminum oxides are usually used for cutting

Table 1.1: Comparison of properties of different abrasives (Jackson and Davim, 2010)

Abrasive	Knoop Hardness (HK)	Application
Diamond	7000	Machining of very hard materials such as glass, stone, ceramics and other abrasives
Cubic boron nitride (CBN)	4700	Grinding of wear resistant materials such as high-speed steel and low-carbon steel
Silicon carbide (SiC)	2480	Grinding of hard non-ferrous metals
Aluminum oxide (Al_2O_3)	2100	Grinding of hard ferrous metals

steel but they are not suitable for non-ferrous materials for which silicon carbide is used. Artificial diamonds and CBN are harder than aluminum oxide and silicon carbide but are more expensive. Thus the abrasives are selected based on the application and economic viability.

1.3.1 Types of abrasive tools

There are two types of abrasive tools based on the material to which the abrasives are attached

- Bonded abrasives
- Coated abrasives

Bonded abrasive tools are formed by pouring a mix of abrasive and bond into a mold and compacting them at high temperature. There are two types of bonded abrasives based on the material used for bonding - vitrified and resinoid. Vitrified type uses clay type bonding material and resinoid type uses organic type bonding material. After baking (vitrified at about 2000ºF;

resinoid at 300ºF to 500ºF) they are finished to required tolerances. Figure 1.2a shows the different types of commercial bonded abrasives available in the market.

(a) Bonded Abrasives

(b) Coated Abrasives

Figure 1.2: Types of Abrasive Tools (Groover, 2010)

Coated abrasive tools are formed by coating a long paper or cloth with many layers of abrasives by using adhesives. Because of this, coated abrasives were widely used for industrial application only after the invention of suitable materials for cloth and paper (which can withstand the machining force) and water-proof adhesives (for use with lubricants). Figure 1.2b shows the different coated abrasives available in the market.

In addition to these two types of abrasive tools, abrasives are also available freely and they are used in various methods based on which there are many types of

abrasive processes.

1.3.2 Types of Abrasive Processes

Abrasive processes can be divided two categories based on the abrasive tool used.

- Fixed abrasive processes
- Free abrasive processes

Fixed abrasive processes use abrasives usually fixed to the tool. Processes employing bonded abrasives such as grinding, honing and super-finishing and coated abrasives such as belts, discs and flap wheels are categorized under fixed abrasive processes. Grinding is the fundamental type of fixed abrasive process. This process was initially developed from machining processes like turning and milling by replacing the cutting tools with grinding wheels. Grinding wheel is a bonded abrasive tool. Depending on the orientation of the grinding wheel and workpiece, the grinding machines are called by different names such as cylindrical grinders, center-less grinders, double-disk grinders and surface grinders. The grinding wheel is modified into stone shaped into required profiles in honing and super-finishing. The grinders are replaced by belts or flexible coated abrasives, when the application requires a large coverage area and specific applications like edge modification, as wheels generally polish a small area and cannot be used easily for curved surfaces. As mentioned earlier, these flexible abrasive tools were widely used only after the invention of strong backing material and water-proof adhesives.

Free abrasive processes use abrasives freely flowing in the process such as lapping, polishing, blasting and mass finishing. These processes use either raw abrasives mixed with a liquid in form or a slurry or abrasives bonded with materials like ceramic or plastic but freely flowing on the surface. These processes are generally used for finishing operation as the material removal will not be as high when compared to fixed abrasive processes. Fixed abrasive process are used for rough finishing and free abrasive processes are used for fine finishing of surfaces.

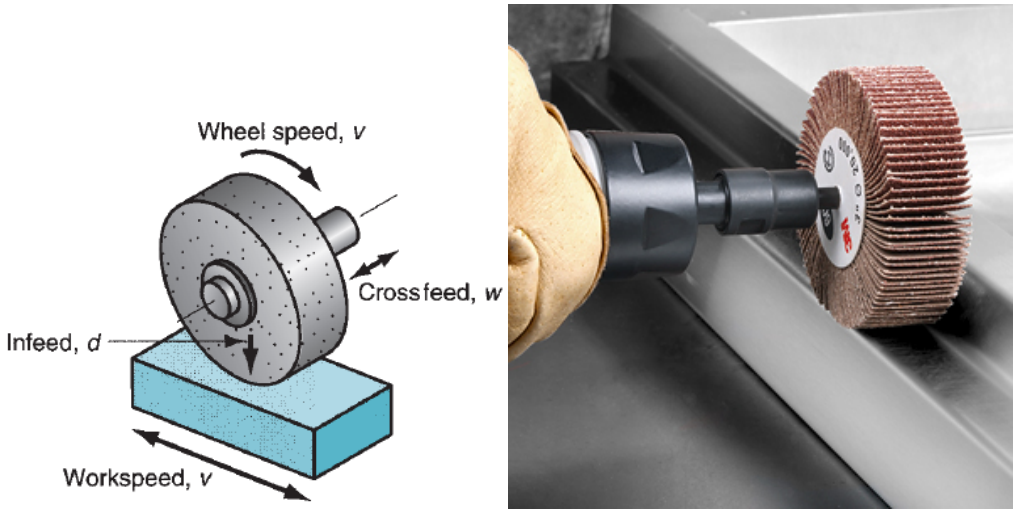

(a) Schematic of grinding process (b) Flap wheel Polishing Process

Figure 1.3: Fixed Abrasive Processes (Groover, 2010)

Each of these free abrasive processes has its own application. Lapping, chemical and mechanical polishing are usually used to achieve very smooth surface finishes in the range of few micro meters to even some cases anon-meter finishes. The size indicates the size of the surface imperfections formed by the process. Mass finishing is a type of widely used loose abrasive processes generally used for finishing large number of components.

1.3.3 Mass Finishing Process

Mass finishing processes are used for finishing more than one part at the same time. It is mainly used for cleaning, deburring and surface finishing of industrial materials.

There are four basic elements of mass finishing (Kyle Elmblad and Petkovich, 2002) as shown in figure 1.4.

1. Part: This is the workpiece which is to be polished. This includes a wide variety ranging from toys, jewelry, medical tools and implants, turbine blades, fasteners, gears, hinges, aircraft components etc. Parts can either be fixed inside the machine or freely moving along with the media inside the chamber as shown in figure 1.4.

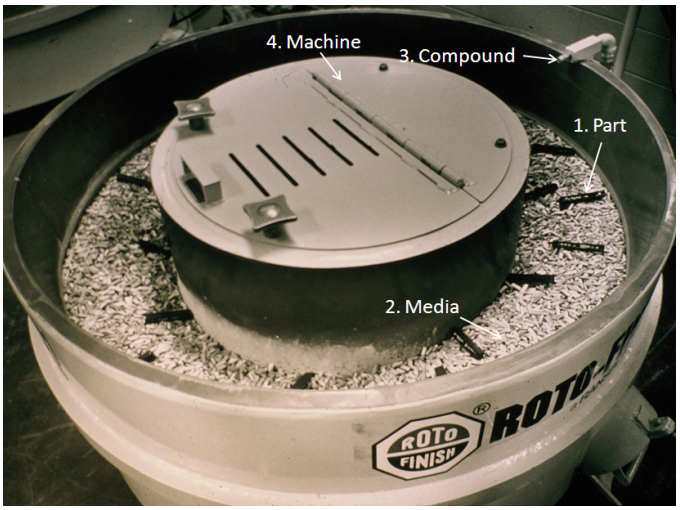

Figure 1.4: Elements of Mass Finishing (Gillespie, 2007)

2. Media: The media is the main element responsible for the finishing action on the part. It also separates the parts from touching each other, if they are freely floating. Media is chosen based on the application, type, composition, shape and size. It is classified into two types. Abrasive and non abrasive. Abrasive media is generally composed of a ceramic base bonded with abrasive material like Silicon,Titanium or Aluminium Carbide and is available in various grades of abrasivity and shapes. Even though vibratory finishing is basically an abrasive process, a wide range of non-abrasive media particles made of plastic, ceramics are also used as it gives a better surface quality and texture when compared to the abrasive media. Hence abrasive media is used for achieving the requisite surface finish and the non abrasive media is used to achieve the specific surface roughness.

3. Compound: This is usually water mixed with soap or detergent and this is mixed along with the media during the process. This is used to carry away the broken down media and abraded particles of the part. It also cleans the surface and brightens the part. There are also compounds used commercially which chemically modify the surface of the parts.

4. Machine: There are three types of mass finishing machines: rotary, vibratory and centrifugal. Rotary machines are the oldest and have a rotating barrel containing the media and the parts. The rotary action causes the media and the parts to roll, causing the finishing action. Vibratory machines have a rotating shaft

attached to a bowl which is fixed to ground by means of springs. Eccentric weights are attached to the ends of the shafts which make them wobble when it rotates, which in turn vibrates the assembly. In other types a vibratory motor is directly attached to the bowl or tub. Bowl type machines are generally used for smaller workpieces, while tub type machines are used for larger workpieces. The third type, centrifugal machines have a rotating disk in the bottom of the barrel which makes the media and parts spin inside the barrel. This process is 6-20 times more aggressive (Kyle Elmblad and Petkovich, 2002) than barrel and vibratory process. But the drawback of this process is that only small parts can be processed using these machines. Vibratory machines are widely used than the other two types of mass finishing machines due to ease of automation, continuous processing and versatility to polish a wide range of parts.

1.3.4 Salient features of mass finishing

The salient features of mass finishing processes are

- Uniform surface finish throughout the workpiece
- Ability to debur the internal edges
- Saturation of surface to specific value after a particular time

These are the main reasons why this process is still used in industries, in spite of its slow material removal rate when compared to other abrasive processes. The first two features to finish the component uniformly and debur the internal edges can be attributed to the free movement of abrasives. The third feature which causes a saturated surface finish makes the process predictable and opens further scope for optimization. Figure 1.5 shows the saturation of surface roughness of different surfaces to a same level after a period of vibratory finishing.

In order to predict and model this saturation, it is necessary to understand which mechanism causes this saturation. Even though it is common knowledge that the running-in or the state of equilibrium of media roughness and surface

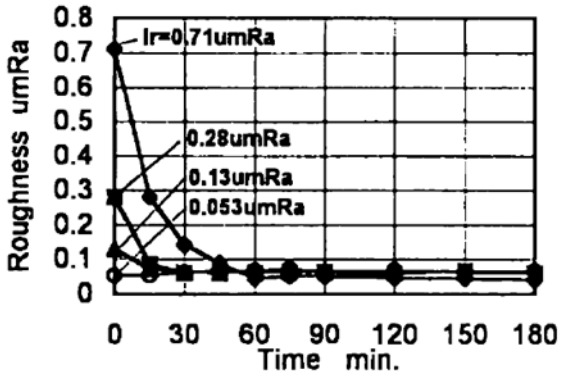

Figure 1.5: Saturation of surface roughness with time (Hashimoto and Debra, 1996)

roughness causes this saturation, the mechanism of material removal which causes this equilibrium is not known yet. A prediction model can be built based on mechanism which can be used for the process optimization.

1.4 Current State of Research

Although the vibratory finishing process has been used commercially since 1960s, very few works [Gillespie (1975); Sofronas and Taraman (1979)] have been published, prior to the experimental investigation of vibratory finishing done by Wang et al. (2000). After that many works by Baghbanan et al. (2003); Ciampini et al. (2007); Yabuki et al. (2002); Ciampini et al. (2008, 2009); Mohajerani and Spelt (2009); Naeini and Spelt (2009, 2011); Mohajerani and Spelt (2010) have been published which tries to characterize and model the vibratory finishing process both experimentally and analytically. But the basic surface modification mechanism has not been studied in detail except for the work done by Yabuki et al. (2002) where they have presented the different types of contacts occurring in vibratory finishing process (All these works are explained in detail in chapter 2). This does not explain why and how the surface is saturating after a specific time of polishing. Hence this thesis strives to understand the surface modification mechanism in vibratory finishing process.

1.5 Objective and Scope

The main objective of this thesis is to understand the surface modification mechanism which causes the surface saturation and the factors affecting the mechanism for vibratory finishing process.

The experimental investigation of surface saturation is performed in four steps.

1. **Experimental investigation of surface topography:** In the first part of the investigation, the surface modification mechanism is studied from the surface topography of the finished surface. Experiments and measurements have been conducted with industrial grade vibratory finishing components as explained in chapter 3. Three workpiece materials - Ti-6Al-4V Titanium Alloy, duplex stainless steel and T6061- Aluminum Alloy have been used. A detailed analysis of surface modification mechanism of Ti-6Al-4V alloy and its relation to surface roughness saturation is presented in chapter 4. This is followed by wear debris analysis in chapter 5.

2. **Wear Debris Analysis:** The surface modification mechanism found from the previous step is confirmed by studying the shape and size of wear debris particles formed by the industrial grade finishing machines only for a duplex stainless steel workpiece, since the wear debris collection was not possible for other two materials. The results of this investigation are presented in chapter 5.

3. **Effect of process parameters on surface modification:** The effect of process parameters such as frequency and amplitude of vibrations on the surface modification mechanism is studied. To study this, a specialized setup have been developed as explained in chapter 3 and the results are presented in chapter 6.

4. **Online (live) monitoring:** The wear debris analysis is followed by measuring and analyzing the live acoustic emission signals emitted by the workpiece to

monitor the surface modification mechanism for workpieces made of Ti-6Al-4V titanium alloys. The results of this investigation are present in chapter 7.

The studied surface modification mechanism is eventually correlated with the surface saturation in each of these investigations.

1.6 Limitations

As mentioned in the previous section, the performed activities can be divided into four categories. Experiments in each category are designed in such a way that the findings will not only fill the knowledge gaps in literature but also be useful for the industry at the same time. Hence a more practical approach is followed in conducting and analysis of the current research. Because of this, the range of materials, processing conditions, parameters used and experiments conducted will be tending more towards the industry standards. Hence this work will be different from a purely academic research, since the results and solutions presented caters directly to the industry, while answering some research questions at the same time.

1.7 Organization of thesis

This thesis is divided into eight chapters. The first chapter introduces the reader to the process, and subsequently introduces the objective and scope of this thesis. The second chapter explains the detailed literature review performed to formulate the hypothesis and methods required for the investigations. The third chapter presents a detailed description of the various machines and equipment used for the investigations. The next four chapters present the results and significant findings of the four investigations performed to study the surface modification mechanism. The final chapter concludes the thesis, summarizing the findings and presenting the scope for future research in this topic.

Chapter 2

Literature Review

This chapter reviews experimental and modeling efforts reported in literature to understand the vibratory finishing process. In addition to this, the literature review conducted to perform the investigations have also been included.

2.1 Experimental Investigations in Vibratory Finishing

This section explains the experimental methods and results collected from the various studies published in literature related to vibratory finishing process.

2.1.1 Process output trends

The major output characteristics which are measured in vibratory finishing process are the material removal rate and surface roughness of the workpiece. This section strives to explain how these output characteristics vary with the process parameters.

Early research of vibratory finishing was undertaken and reported by Gillespie (1975), Sofronas and Taraman (1979) and Hashimoto and Debra (1996). Gillespie (1975) studied the deburring application of vibratory finishing in detail. Experiments were performed in a vibratory tub with three types of media and two sets of

workpieces made of stainless steel and aluminium. The change in output characteristics such as material removal, dimensions of the workpiece, surface roughness, burr thickness and height with respect to time for the two workpieces and three sets of media were reported. A capability model to decide the applicability of the vibratory finishing process for various processing conditions using the available experimental data was presented in this work. The capability model developed was only applicable for the two workpieces and the three sets of media. Later a book on mass finishing that presents detailed information about all the mass finishing processes and the parameters were written by Gillespie (2007).

Hashimoto and Debra (1996) measured the material removal and surface finish of the workpiece subjected to vibratory finishing and found that the material removal depends on the initial surface roughness and it increased as the initial roughness increased. The final surface roughness of the workpiece was found to be saturating after a period of finishing and the final roughness obtained was a function of initial surface roughness. This is shown in figure 2.1. The modeling part is explained in detail in section 2.2.3. Sofronas and Taraman (1979) modeled the output characteristics such as edge radius and height reduction, surface roughness reduction with respect to initial hardness, media and processing time using design of experiments and regression based analysis. This is also explained in section 2.2.3. After these works, the investigation of vibratory finishing was started by Wang et al. (2000) in which a series of experiments was performed and the effect of media and lubrication conditions on surface roughness and hardness of two sets of workpiece was studied. Three types of spherical ceramic media with different diameters (7mm, 9mm, and 11mm) and three lubrication conditions such as dry, water wet and detergent wet conditions were tested. It was found that the hardness was maximum for the larger media due to larger kinetic energy and surface roughness changed according to the lubrication conditions and it was in the order of dry, water wet and detergent wet conditions. The results obtained for one of workpiece are shown in figure 2.2 and 2.3. An experimental investigation of vibratory finishing

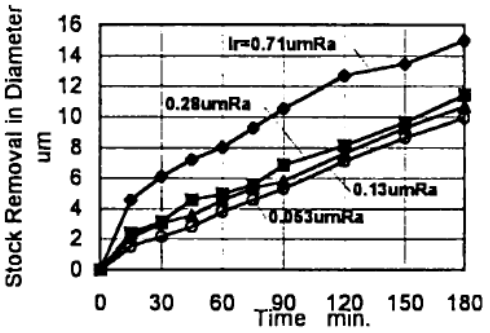

(a) Variation of Material Removal Rate with time

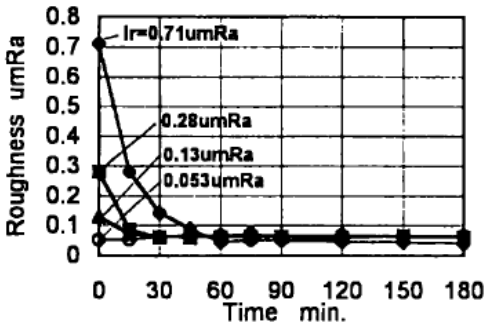

(b) Variation of Surface Roughness with time

Figure 2.1: Variation of Output parameters studied (Hashimoto and Debra, 1996)

process was done by (Domblesky et al., 2003). In this work, a detailed study showing the effect of process parameters such as media, workpiece material and bowl acceleration has been reported. Material removal rate and surface roughness of the workpiece were measured to evaluate the effectiveness of the process. The machine used for testing was a vibratory bowl which had exchangeable roll and feed weights which varied the acceleration of the machine. The acceleration directly influenced the material removal rate of the workpiece as shown in figure 2.4. The material removal rate increased linearly with acceleration. However the surface roughness did not change considerably with increase in acceleration.

The hardness of the workpiece and density difference of media and workpiece material had a major influence on the finishing performance. Soft, dense materials will have a higher material removal rate than the harder, less dense materials as shown in figure 2.5. On the other hand, a better surface finish was achieved for harder materials which had less material removal as shown in figure 2.6.

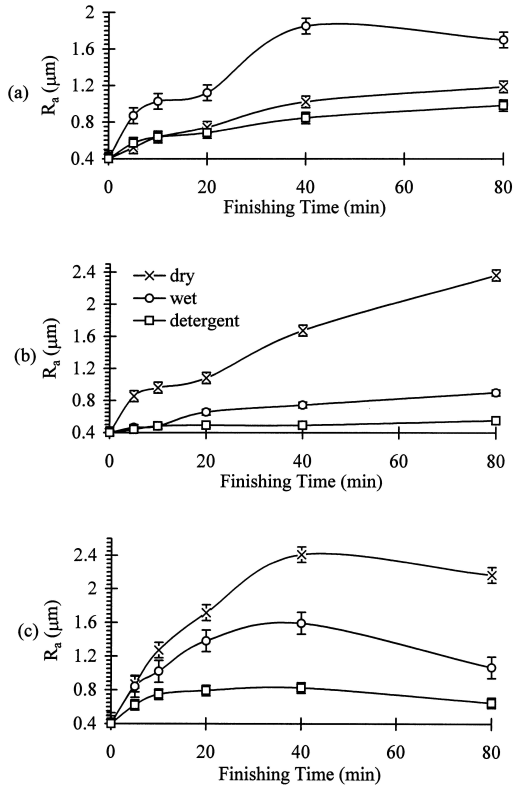

Figure 2.2: Surface finish trends of workpiece for various sizes of media a-7mm, b-9mm and c-11mm and lubrication conditions against finishing time (Wang et al., 2000)

Baghbanan et al. (2003) performed experiments on a tub type of vibratory finishing machine which has more aggressive action than that of the vibratory bowl. Output characteristics such as hardness, material removal, curvature and surface roughness of two workpieces were measured with respect to time, for dry and wet conditions. Figure 2.7 shows the results obtained for one of the workpieces. The hardness was found to be increasing with time, while the mass change increased in dry conditions. This increase in mass is attributed to the accumulation of media wear debris on the workpiece surface in dry conditions. The plastic deformation that produced strain hardening is said to generate a curvature on the workpiece which increases with time. The surface roughness of the workpiece improves after a certain time in dry finishing due to the removal of media wear debris which is not seen in wet conditions.

Vibratory finishing process was also studied in detail by Sangid et al. (2011a,b) but the workpiece was clamped instead of freely flowing with the media. This is

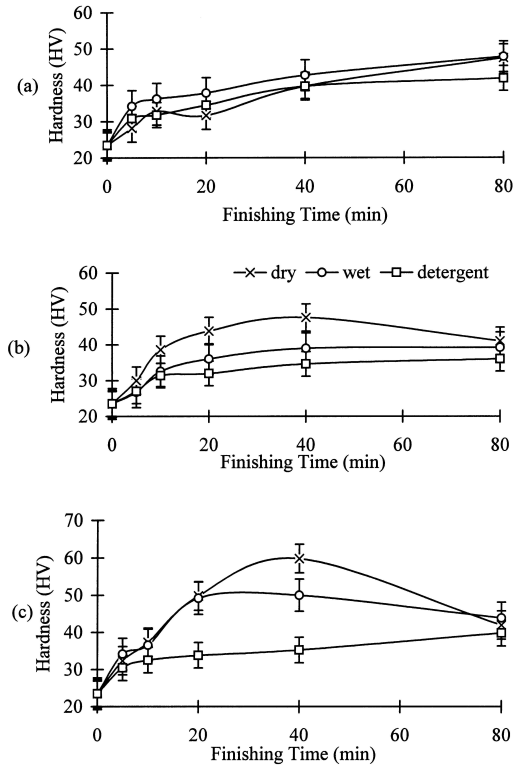

Figure 2.3: Hardness trends of workpiece for various sizes of media a-7mm, b-9mm and c-11mm and lubrication conditions against finishing time (Wang et al., 2000)

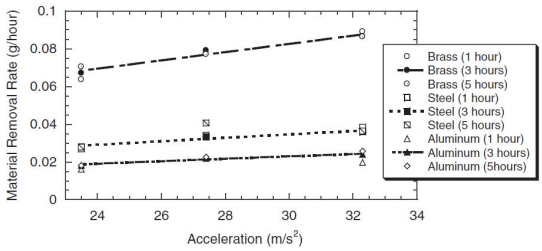

Figure 2.4: Effect of acceleration on Material Removal Rate (Domblesky et al., 2003)

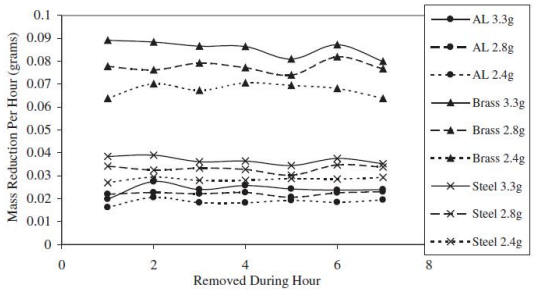

Figure 2.5: Material removal trend with respect to workpiece hardness (Domblesky et al., 2003)

a similar work to that of other works by Ciampini et al. (2007); Cariapa et al. (2008); Ciampini et al. (2009), where the media motion is analyzed with clamped

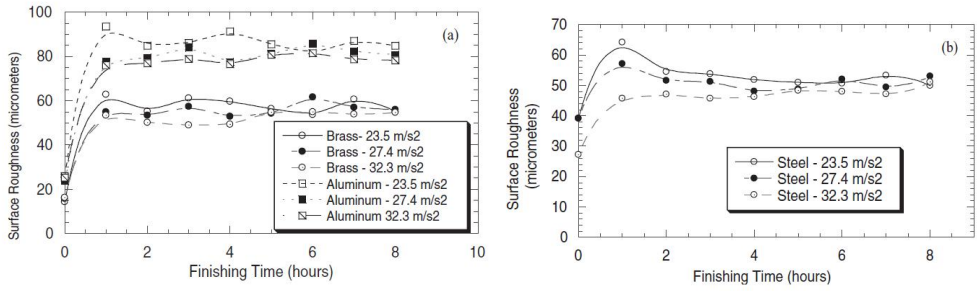

Figure 2.6: Surface finish trends with respect to workpiece hardness (Domblesky et al., 2003)

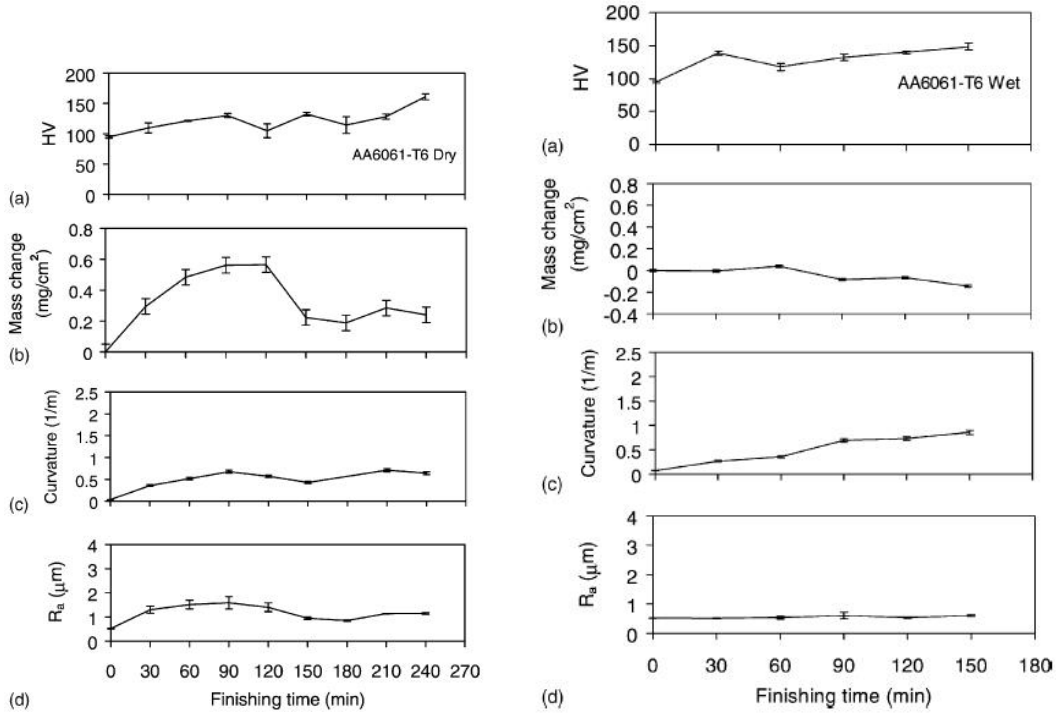

Figure 2.7: Output Patterns of tub vibrator in Dry and Wet Conditions (a) Hardness (HV) (b) Mass charge (c) Curvature (d) Surface Roughness (Ra) against finishing time (Baghbanan et al., 2003)

workpiece. Process parameters such as frequency and amplitude for a tub vibratory finisher have been varied and the resulting changes in residual stress and surface roughness of the workpiece have been calculated. From these studies it is concluded that high frequency vibrations increase the residual stress, and amplitude does not have a major influence on the residual stress and hence the fatigue life of the workpiece. It is also reported that high frequency produced a rougher surface than the unfinished component, although increasing the residual stress. This is shown in figure 2.8.

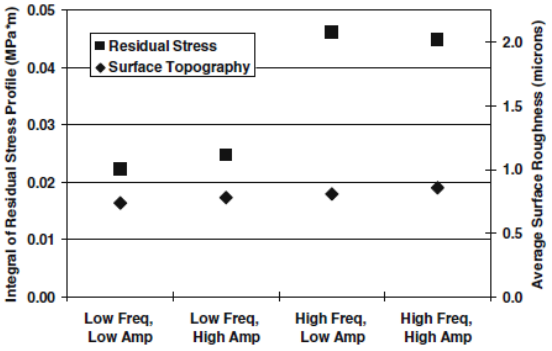

Figure 2.8: Effect of frequency on Surface Roughness and Residual Stress (Sangid et al., 2011a)

In addition to this, the effect of position, orientation and surface shadowing of workpiece inside the tub and its effect on residual stress and surface roughness of workpiece have also been studied by Sangid et al. (2011a). The results of these studies show that changing the position of workpiece does not change the fatigue life and the surface roughness, but the orientation affects the residual stress and surface roughness. A workpiece which is oriented at right angle to the media motion has more residual stress and a rougher surface than that of workpiece oriented parallel to media motion. When two workpieces are very close together such that one prevents the media from freely hitting the other, it is called shadowing. This effect was tested and it was found that upto 25mm shadowing had a detrimental effect on surface roughness and residual stress. All these effects are shown in figure 2.9.

A comparison of residual stress and surface roughness of an unfinished, vibrostrengthened (that is vibratory finished with clamped workpiece) and shot peened workpieces has been made by Sangid et al. (2011a). The results show that the shot peened workpieces have the highest residual stress followed by vibrostrengthened workpieces and unfinished workpiece.

Mohajerani and Spelt (2009) studied the mechanism of edge rounding of brittle materials such as borosilicate glass and silicon nitride using an abrasive ceramic and non-abrasive steel media, for both vibratory bowl and vibratory tub finishing machines. The material removal occurred only in the edges of the brittle materials. The flat surfaces were found to be very slightly affected due to the process. The

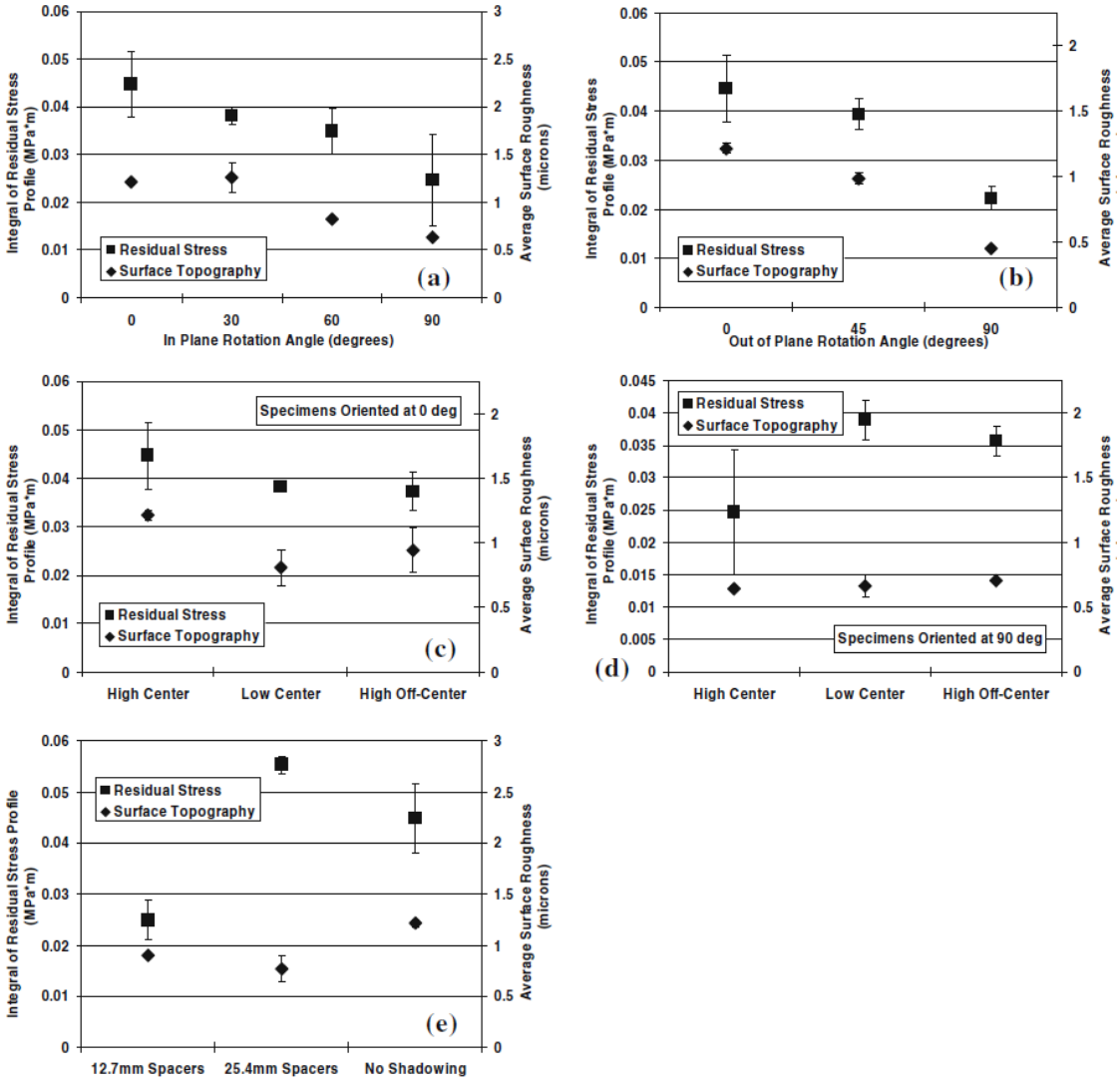

Figure 2.9: Effect of Orientation (a,b), Position (c,d) and (e) Shadowing on Surface Roughness and Residual Stress (Sangid et al., 2011a)

main reason for the edge wear was found to be the chipping action due to the impact of media balls, followed by the abrasive wear due to the abrasive particles of media. From a series of experiments, it is concluded that the edge wear of glass specimen occurs in both vibratory bowl and tub machines only for abrasive ceramic media. Flat surfaces experienced similar wear only in more energetic tub vibrator. The same behavior was seen for silicon nitride but to a lesser extent due to the higher fracture toughness of silicon nitride. The edge wear was also not found to be dependent on the media flow direction or the flow pattern. The rate of edge wear was calculated based on the chipping length and area of the wear edge and it varied with time as shown in figure 2.10.

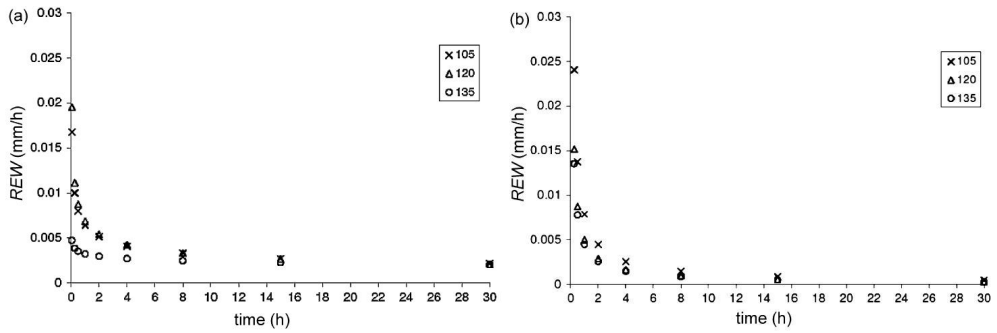

Figure 2.10: Edge wear in brittle materials in a-tub finisher b-bowl finisher for various edge angles (Mohajerani and Spelt, 2009)

The output characteristics such as material removal rate has been studied in form of edge wear rate, diameter loss and mass loss of the workpiece. Surface roughness of the workpiece finished was also measured for various periods of finishing and processing conditions. There is also another set of works which tries to characterize the vibratory finishing process with the use of Almen strips which are generally used in characterization of shot peening processes. The next section explains in detail about the works published in this respect.

2.1.2 Almen Strip Characterization

Almen strips are generally used in shot peening process to characterize the process parameters such as shot density, radius, velocity, impact frequency, impact coverage, elastic modulus and yield stress. The almen strips are clamped and subjected to processing, and the change in curvature is calculated after the process. Baghbanan et al. (2003) tested Almen strips under various boundary conditions for vibratory tub and bowl finishing machines. Figure 2.11 shows the almen strip curvatures obtained for Aluminium and Copper workpieces under wet and dry conditions. It was found that the curvature was more for the tub vibrator than the bowl vibrator and wet conditions gave more curvature.

Ciampini et al. (2008) also characterized the vibratory finishing process using Almen strips. They built a custom experimental setup to isolate the effect of vibratory bowl on the almen strips and expose it only to the action of media. Instead

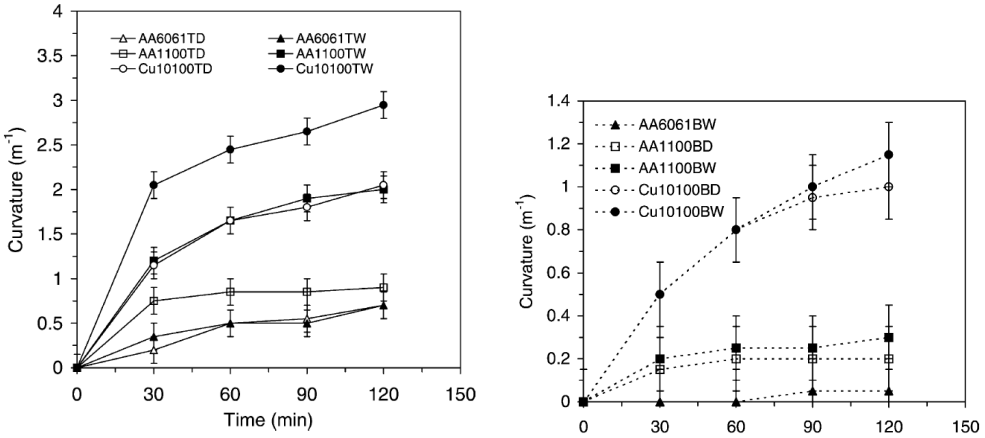

(a) Tub finisher (b) Bowl finisher

Figure 2.11: Almen strip curvatures obtained for various conditions (Baghbanan et al., 2003)

of the force sensor, almen strips were used as a workpiece here. The change in arc height of the almen strips were measured and a parameter known as Almen Intensity was calculated for two loading conditions (91kg and 112 kg) and three types of almen strips were used in the experiments. The results show that the curvature saturates after 120mins of processing time and the intensity increased for increased loading conditions indicating the increased force and frequency components with media loading.

2.1.3 SEM Analysis of finished surfaces

Wang et al. (2000) have performed a Scanning Electron Microscopy analysis for the dry and wet finishing processes and reported their findings. Figure 2.12 shows the images captured using the SEM. In dry finishing process, the mechanism of material removal seems to be normal impact and in wet finishing, scratching occurs. This is believed to be due to a decrease in friction in wet conditions.

Similar observations have been made by Ciampini et al. (2007) and Yabuki et al. (2002), who identified an additional mechanism of rolling shown in figure 2.12c.

Thus, a brief but sufficient analysis of experimental works done to characterize the output characteristics of vibratory finishing is done in this section. The next section deals with the measurement of intermediate parameters.

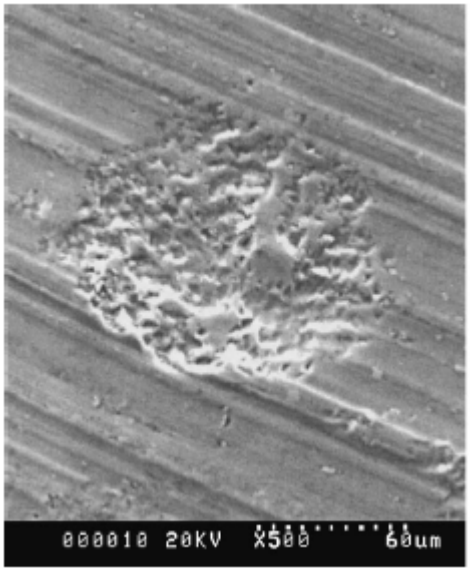

(a) Impact crater (Wang et al., 2000)

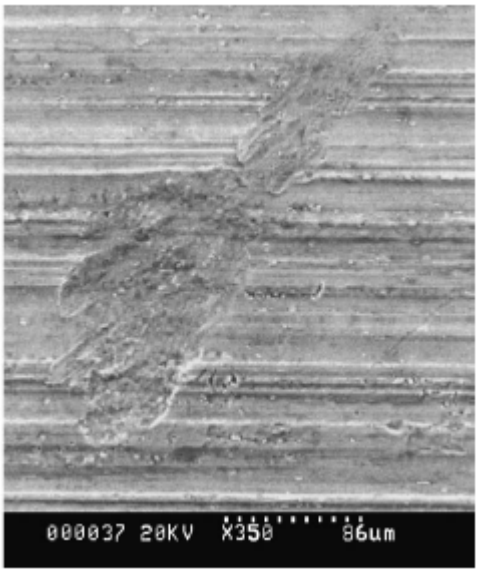

(b) Scratch formed (Wang et al., 2000)

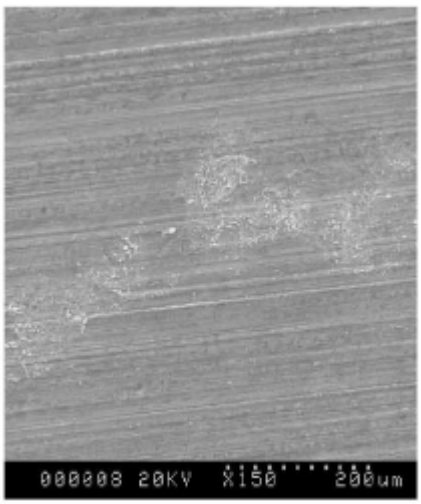

(c) Rolling Contact (Yabuki et al., 2002)

Figure 2.12: SEM Analysis of finished surfaces showing different types of contacts

2.1.4 In process Measurements

2.1.4.1 Contact Force Measurement

Wang et al. (2000) measured the contact forces of the media and compared it with the surface finish of the workpiece. A load cell type of force sensor made of strain gauge was used to measure only the normal contact forces as shown in figure 2.13. The force signals obtained were highly variable in random bursts as one media rolled over another. The force sensor output was digitized only at 500 Hz, which

was high enough only to measure 7 values during an impact. Hence the authors have stated that the maximum force obtained may not be the accurate value of force. They have also stated that the contact force is a measure of compliance of the surface and cannot be treated as a constant parameter to quantify the end surface conditions. Nonetheless, from the results obtained it is evident that there is not much difference in maximum impact force for dry and wet conditions. The impact force increased with media size only for dry condition and there was no change for wet conditions.

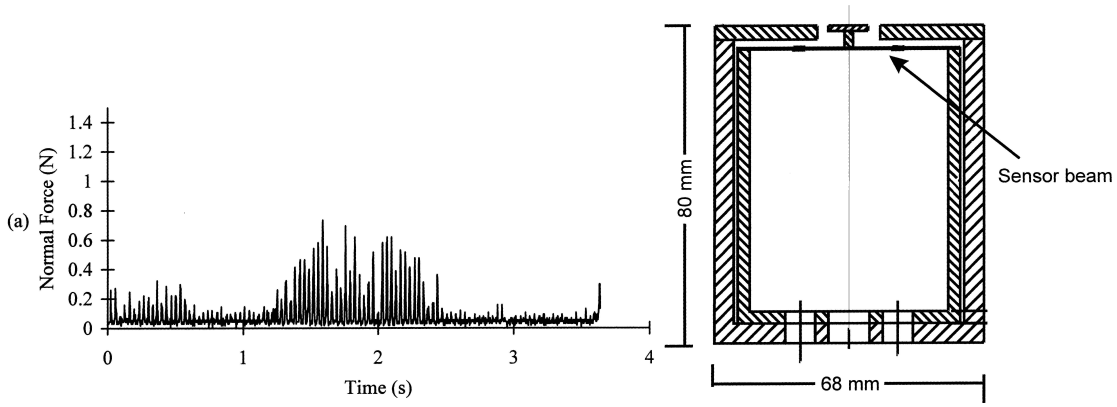

(a) Force signals with time (b) Sensor used

Figure 2.13: Contact Force Measurement (Wang et al., 2000)

Yabuki et al. (2002) further explored the contact forces in the vibratory finishing process using a new setup for measuring the forces. The setup consists of one normal and three tangential capacitive force sensors to measure the normal as well as the tangential forces. Figure 2.14 shows the sensor and force signals measured. The force signals were digitized at 50 kHz as compared to 500 Hz in the previous research by Wang et al. (2000).

From the measurement of normal and tangential contact forces, the values of coefficient of friction between the media and the workpiece for dry and wet conditions were calculated. In a separate setup, a scratch and rolling test were performed using the same media used in the process and the force signals were recorded. From comparing the force signals obtained from tests with that of vibratory finishing process, media contact occurring in the process have been identified and classified

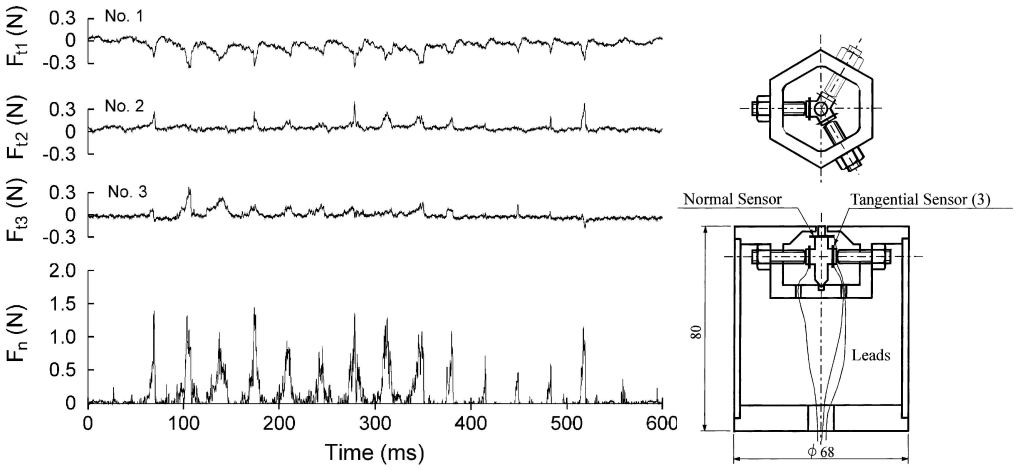

(a) Force Signals with time (b) Sensor used

Figure 2.14: Forces signals obtained from the four sensors (Yabuki et al., 2002)

into three types: 1. Normal impact; 2. Sliding contact; 3. Relative impact, in which one media is in contact with workpiece and another media impacts on it. The figure 2.15 shows the types of tests performed to simulate these conditions and the corresponding force signals and craters created on the workpiece.

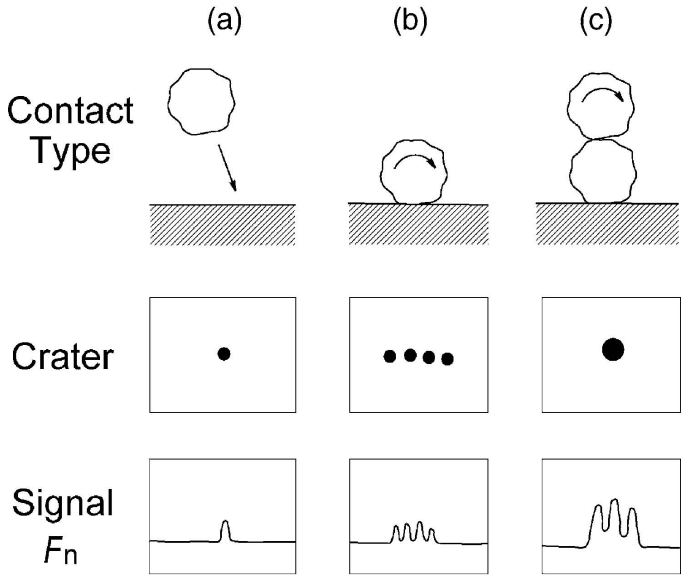

Figure 2.15: Types of media contact (a) Normal impact (b) Sliding contact (c) Relative impact (Yabuki et al., 2002)

The process was also videotaped using a small camera to visualize the motion of media particles. This camera was mounted onto a hollow cylindrical workpiece covered at one end with a glass window and a flat aluminium plate was attached normal to it, so that the media impact on the plate could be recorded. The three

types of contacts proposed from the observation of force values are confirmed by the video obtained from the camera. Figure 2.16 shows the images captured by the camera showing the three types of contacts.

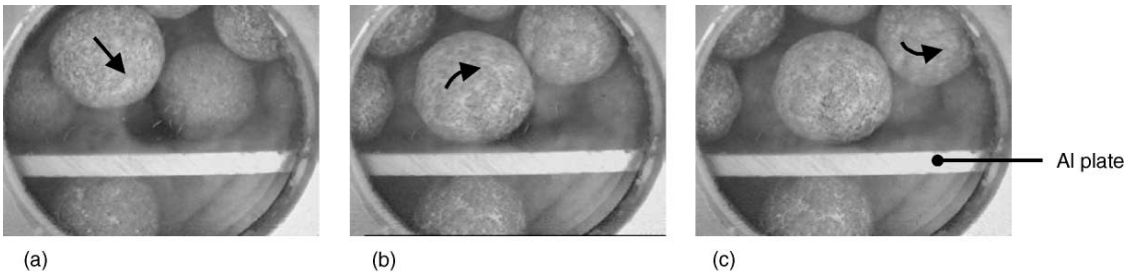

Figure 2.16: Images captured for the video camera showing the three types of media contacts (a) Normal impact (b) Sliding contact (c) Relative impact (Yabuki et al., 2002)

The values of coefficient of friction from these tests have been compared with the coefficient of friction calculated for the vibratory finishing process and the type of motion between the media and workpiece in the vibratory finishing process was identified. It was found that sliding type of media contact on the workpiece did not occur in dry condition. Only impact type of contact occurred and the maximum impact force was observed only in the dry condition. This was attributed to the decrease in coefficient of friction when lubrication was introduced.

Baghbanan et al. (2003) performed force measurement studies for a vibratory tub finisher which has more vibratory force than the bowl finisher using the same sensor setup as Yabuki et al. (2002). Their principal finding was that, the nature of normal and shear forces of both the bowl type and tub type vibratory finishing machines were just the same except for the magnitude of forces which was higher for the tub vibrator. Further, there were more normal impacts than the sliding in dry conditions as observed by Yabuki et al. (2002). The results are shown in figure 2.17. Hence, both the tub vibrator and bowl vibrator can be generalized into a same category as the nature of force are the same. This study also proves that impact force can be used as a consistent process parameter for characterizing the vibratory finishing process regardless of the equipment.

Ciampini et al. (2007) proposed that the impact force measured was a function

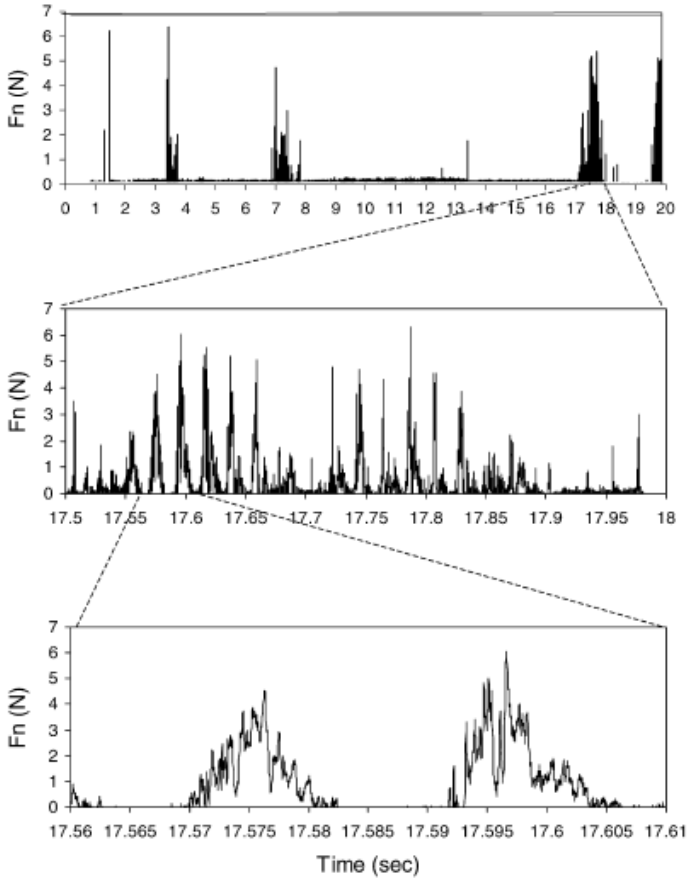

Figure 2.17: Contact force trends for tub vibratory finisher (Baghbanan et al., 2003)

of compliance of the sensing system and not the actual representation of the impact force experienced by the workpiece. Hence the impact velocity was calculated from the impact force measurement and the finishing process was characterized using impact velocity for the same tub vibratory finisher used by Baghbanan et al. (2003). The relationship between impact velocity and force was determined in a separate setup where the media balls dropped on a force sensor from known heights. The impact velocity was calculated from the equation 2.1,

$$v = \sqrt{2gh} \tag{2.1}$$

where v is the velocity, g is acceleration due to gravity and h is height from which the media is dropped.

A new type of force measurement setup has been used by Ciampini et al. (2007), by fixing a single component piezoelectric force sensor to a wall isolated from the

vibrations of the tub. The force sensor was mounted on to a sensor mount assembly which was protected from the media by a housing as shown in figure 2.18.

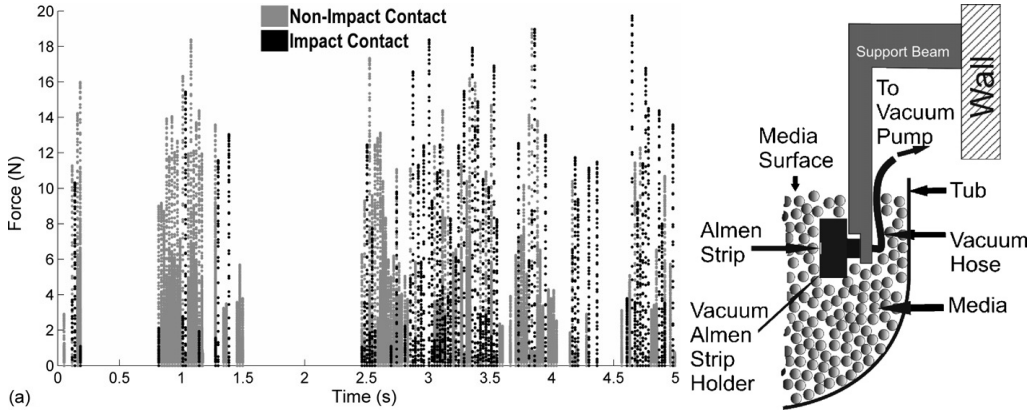

(a) Force signals with time (b) Sensor used

Figure 2.18: Measured force signals and fixed force measurement setup(Ciampini et al., 2007)

From the measurement of force values (figure 2.18), it was found that there are two types of contacts: impact and non-impact. The impact contacts had a ringing effect after the impact and the impact duration was very short. Whereas, the non-impact contacts occurred in a longer duration and did not have the ringing effect. This is shown in figure 2.19.

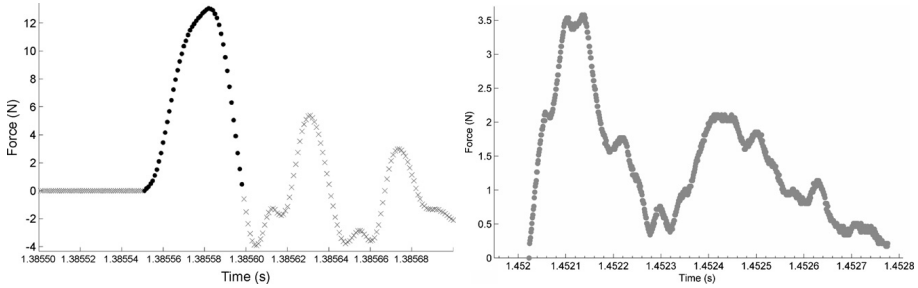

(a) Impact contact (b) Non-impact contact

Figure 2.19: Impact force profile for two types of contacts in Vibratory Finishing (Ciampini et al., 2007)

In addition to this, a statistical analysis of the occurrences of impacts of various velocities have been performed. It was found that the impacts with velocities higher than 0.2m/s did not occur so frequently and did not take part in the material removal mechanism as much as that of the lower velocity impacts.

The researchers conclude that the impact force cannot be modeled further and predicted due to its dependency on the compliance of the workpiece or sensing device. Hence, only the impact velocity have been modeled and predicted. This research project starts off from here, by modeling the impact force taking the compliance of the workpiece into account through modeling and validation of compliant contact force.

2.1.4.2 Media motion and Impact velocity measurement

Wang et al. (2000) used a small video camera, mounted to a hollow cylindrical workpiece of 50mm diameter to record the media motion. From the video capture using this setup they calculated the average contact time of a media particle and workpiece. They found that the media was in contact for only 30% of the total finishing time. Also the average relative speed of the media and workpiece was calculated as 11, 7 and 4 cm/s for dry, water-wet and detergent-wet conditions respectively. Yabuki et al. (2002) also recorded the media motion to study the contact mechanism of media and workpiece, which was explained in section 2.1.4.1.

Sangid et al. (2011b) used a high speed camera setup and a separate fixture made of plexiglass to visualize the media motion attached to vibratory tub finishing machine as shown in figure 2.20.

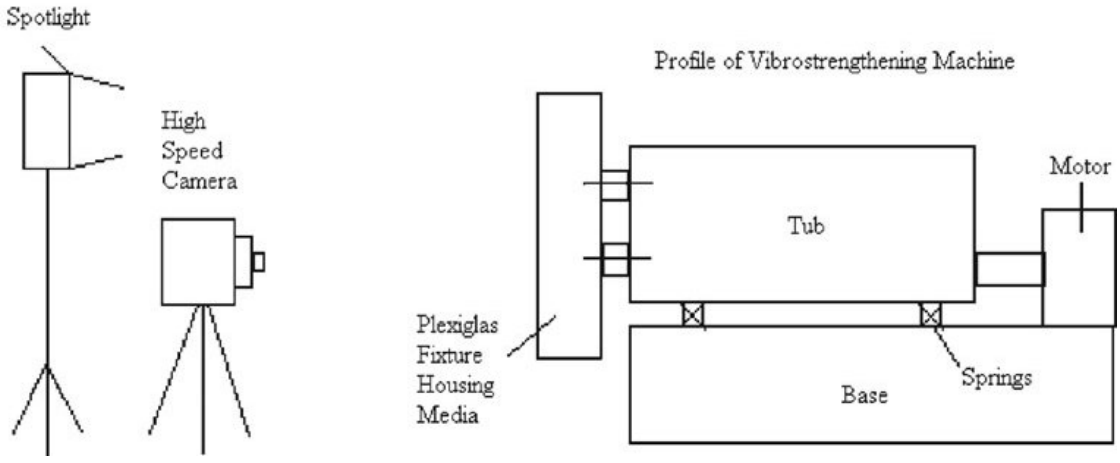

Figure 2.20: High Speed Camera setup to measure media velocity (Sangid et al., 2011b)

The increase in residual stress with increase in frequency of vibration, shadowing

of surfaces and effect of position of workpiece are all attributed to the media impact velocity which was calculated experimentally using the high speed camera. The impact velocities were calculated at various points of the tub.

The absolute velocity of media and velocity with respect to tub were calculated for various depths as shown in figure 2.21. It was found that the absolute velocity increased with depth and the relative velocity decreased. This is because the motion of the tub is fixed on the top and free to move in the bottom. The media particles at the bottom are accelerated by the moving tub, hence their absolute velocity is high, but relative velocity is low. But the media particles at the top do not have any external acceleration other than the media particles at the bottom. The tub motion is confined at top, hence the absolute velocity of media is low and relative velocity is high.

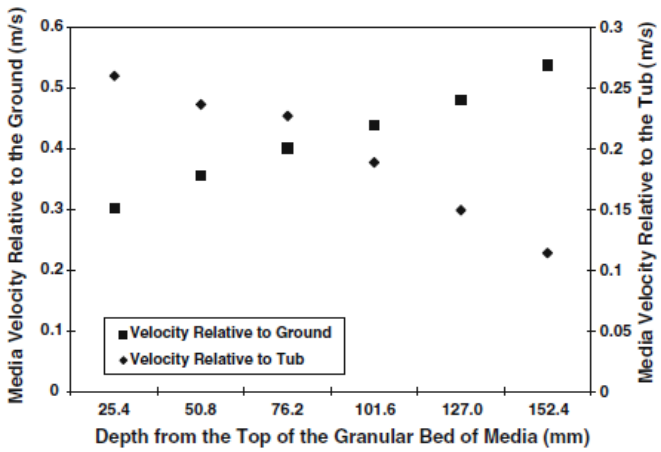

Figure 2.21: Absolute and Relative velocities of media to Ground and Tub (Sangid et al., 2011b)

Naeini and Spelt (2009) installed two glass plates in between the walls of the tub for recording the motion of the media particles as shown in figure 2.22. Two accelerometers were attached to the tub to measure the frequency and amplitude of the tub vibrations.

The velocity of media was measured at four locations inside the vibratory tub and this velocity was used to calibrate and validate the discrete element model developed to predict the velocity which is explained in the next section of this report. The calculated values of velocity at different positions tested for two different

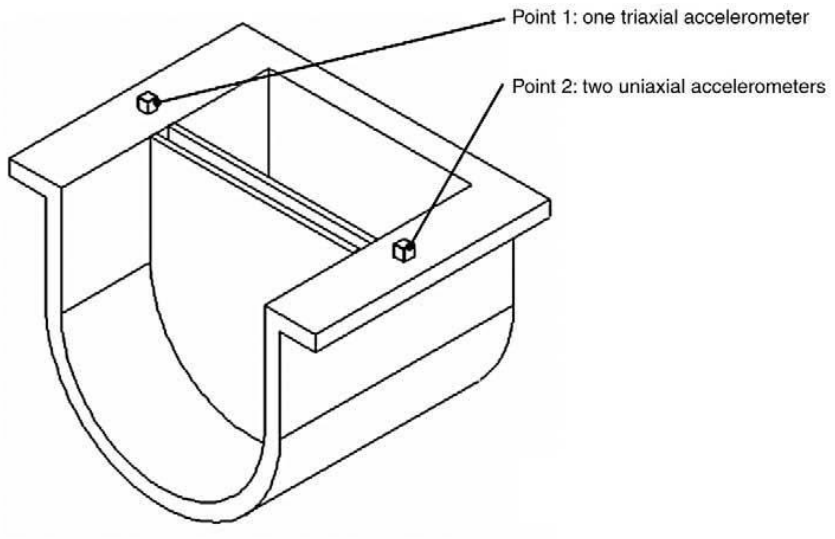

Figure 2.22: Experimental method for 2D DEM (Naeini and Spelt, 2009)

media conditions are shown in figure 2.23.

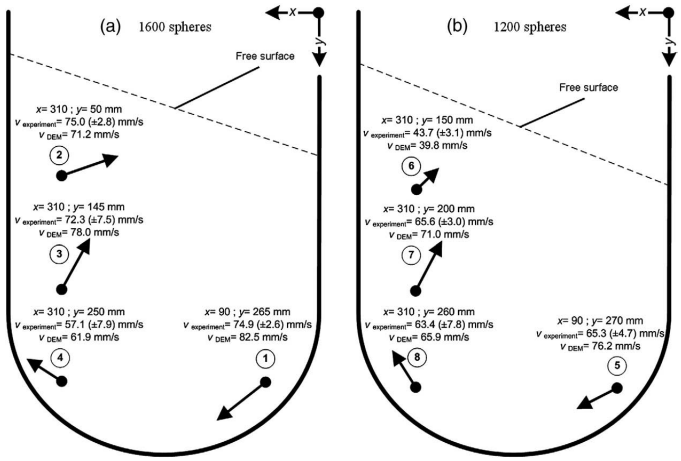

Figure 2.23: Media velocity calculated at different locations (Naeini and Spelt, 2009)

Hashemnia et al. (2013) developed a new type of laser probe measurement technique to measure the impact velocities of media particles in a tub type vibratory finishing machine. The laser was fixtured inside the moving media particles as shown in figure 2.24. Local impact velocities were recorded at various positions within the flow and with different probe orientations. The resent laser impact velocity measurements were compared with those obtained in a previous study using an impact force sensor.

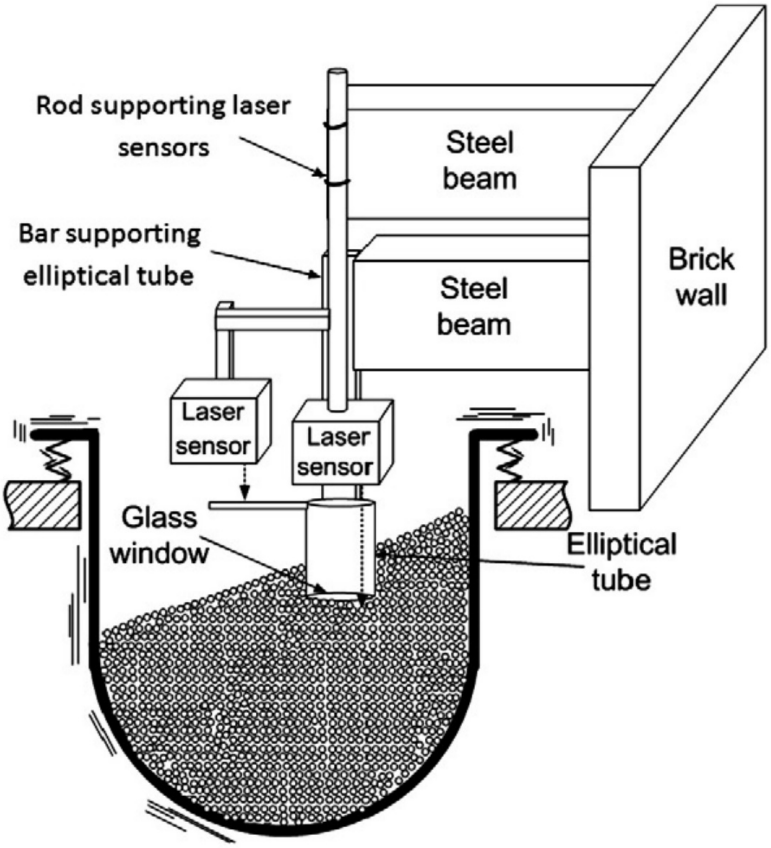

Figure 2.24: Laser probe measuring impact velocities developed by Hashemnia et al. (2013)

2.2 Modeling efforts

The experimental measurements of intermediate parameters such as impact velocity and output characteristics such as material removal rate, surface roughness and residual stress of the workpiece explained in the previous section was modeled using various methods. This section explains each of the works done in this respect.

2.2.1 Modeling of media motion and impact velocity

Naeini and Spelt (2009), used Discrete Element Method (DEM) to model the flow of media in a tub vibrator. DEM was initially developed by Cundall (1971) to model the flow of particles in the field of geotechnical engineering. DEM was later used to model the particle flow in many works. The modeling is based on the basic equations of motion and contact force models.

Naeini and Spelt (2009) predicted the impact velocity of the media using DEM, as it was pointed out earlier [Ciampini et al. (2007)] that the impact force cannot be treated as a parameter due to its dependency on the compliance of the measuring surface and the media. Hence the impact velocity is predicted using this method. In this work, a single layer of steel spheres were used as media in a tub vibratory finisher.

Contact force model was implemented for the vibratory finishing process using the published values for contact parameters by Naeini and Spelt (2009). Later, these parameters were optimized using a mathematical formulation. The velocity is taken as a function of spring, damping and relative damping coefficients. Hence to find out three variables, three equations are required. The velocity is measured experimentally at three points and three equations are solved by using the initial parameters obtained from the literature and optimized values are obtained. These optimized values are then used to validate the model with the experimental data. The initial set of parameters predicted the velocity of media at 4 points inside the tub with an accuracy of 70% and the optimized parameters had an accuracy of 90%. This is shown in figure 2.25.

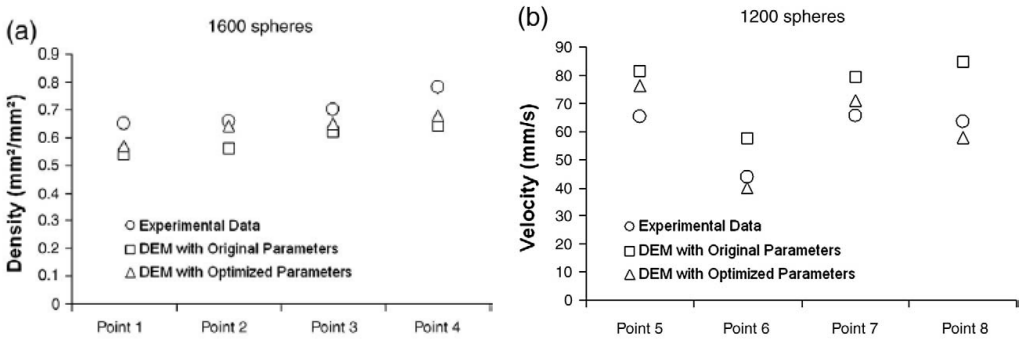

(a) 1600 Spherical Media (b) 1200 Spherical media

Figure 2.25: Comparison of DEM results (Naeini and Spelt, 2009)

Later, Naeini and Spelt (2011) used this 2D model to predict the flow of 3D movement of media. They increased the number of layers of media by increasing the gap between the glass plates and used two types of media viz. spherical steel and glass. The motion of the media was captured to calculate the media veloc-

ity through high speed camera, the effect of amplitude of vibration and the wall material was studied. From these studies they found that the velocity of the steel media matched those of experiments than the glass media. The bulk circulation of the media is calculated in a fluid mechanics approach using the velocity of the media. From the experimental study the following results were obtained. As the bed depth increases the circulation increased due to the increase in density of the media. The amplitude increase did not cause much change in the circulation, whereas the change in wall material changed the friction coefficient between the wall and the media. This affected the shear force between the wall and media and hence the circulation. The same tub was modeled in DEM and the motion was input into it and the velocity of media was predicted and matched the trends obtained in the experiments, but the values were smaller than the experimental results. This finding is attributed to the lack of rolling friction in the DEM model. In addition, they also predicted the shear force of the media using the media velocity.

2.2.2 Modeling of Material Removal Rate of Workpiece

Domblesky et al. (2004) experimentally investigated the vibratory finishing process, which was explained in the first part of this section, also developed an empirical material removal model based on their experimental results. They developed an empirical equation for material removal rate which is shown in the equation 2.2

$$MRR = K\left(\frac{\rho}{U}\right) a m_w v_w \tag{2.2}$$

where m_w is the workpiece mass, a is the bowl acceleration, v_w is the workpiece velocity, U is the specific energy, σ is the density of the workpiece and K is the constant depending on the media cutting factor determined from experiments. The specific energy is defined as the power required for unit volume removal of material from the workpiece. From this model, they were able to confirm the time independent nature of material removal and they identified the parameters which affected the material removal rate. Domblesky et al. (2004) also confirmed that

the material removal does not depend on the ratio of (ρ/U) factor of the equation. Instead it depended on the factor $m_w v_w$. This was a parametric modeling method rather than predictive modeling.

Cariapa et al. (2008) developed a predictive material removal model for the centrifugal disk mass finishing machine, based on the theories of fluid dynamics and numerical analysis (CFD). They carried on the experiments using a centrifugal disk mass finishing machine and used the experimental results to validate the material removal model. The material removal model developed can predict the material removal of the workpiece based on the ratios of density and hardness of the metal coupon and ceramic media. The media particles were assumed to follow a fluid motion. Cariapa et al. (2008) calculated the viscosity of the media particles, by finding the force exerted by the media on a workpiece connected to a force sensor through a nylon string. The material removal model was able to predict the process with maximum deviation of 16%. The surface roughness patterns of the workpiece were also studied, but there seemed to be no relationship between surface roughness and material removal rate. Cariapa et al. (2008) have concluded by saying that there is a need for a surface roughness study. Hence, this model based on fluid dynamics was developed only for Centrifugal type mass finishing machine. Such a type of material removal model has not been developed for vibratory finishing machine to the knowledge of the author.

Edge rounding of Borosilicate glass and silicon nitride using vibratory finishing and its modeling was studied by Mohajerani and Spelt (2009, 2010) and the mechanism of edge wear of brittle workpieces using ceramic abrasive and steel media was reported. From this they formulated a relationship between edge angle and wear rate. The wear of the edges was modeled numerically by a new method. Forces were applied randomly from a distribution of forces which was calculated from the measured chip lengths. Then this force was compared to force required for chipping based on Chai and Lawn's model (equation 2.3).

$$F = \beta K_c h^{3/2} \left(\frac{cos\theta}{1 + \gamma sin(\theta + \phi)} \right) \tag{2.3}$$

where β and K_c are constants calculated from the geometric and material properties of the chip, h is the distance of point of force from the edge, θ and ϕ are the angles of the force applied and the edge. If the randomly applied force value was greater than this value, then surface was modified by calculating the chip length (equation 2.4) formed due to that force.

$$c = \frac{\gamma h \cos\theta}{1 + \gamma \sin(\theta + \phi)} \tag{2.4}$$

where γ is the ratio of chip length and crack length d, when θ and ϕ are zero. All these parameters are shown in figure 2.26

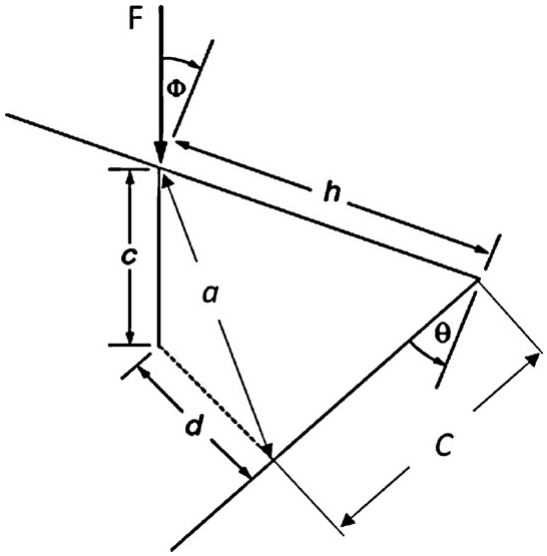

Figure 2.26: Comparison of predicted and experimental data (Wear vs. Time)(Mohajerani and Spelt, 2010)

This length of chip was removed from the surface accordingly. This process was repeated for 'n' number of times which was calculated based on the experimental data. Wear rate of edges was calculated based on this model and the values predicted matched to the experimental value to an acceptable level. Some of the results are shown in figure 2.27.

The main drawback of this model is that the parameters of the model are

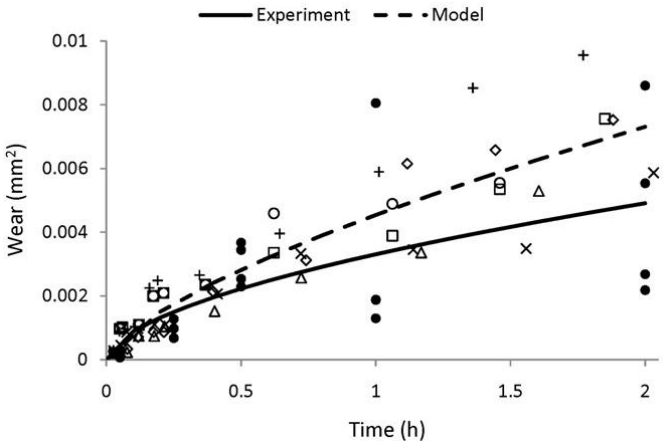

Figure 2.27: Comparison of predicted and experimental data (Mohajerani and Spelt, 2010)

calculated from the same experimental data which is to be predicted using the model. Hence, the applicability of the model will be limited to only this set of values and not be general.

This model was developed only for brittle materials. It is clear from the fact that the edge wear depends on the chipping force due to impact of workpiece. This chipping force is the impact force of the media on the workpiece.

2.2.3 Modeling of Surface Roughness of Workpiece

Sofronas and Taraman (1979) studied the effect of variables of vibratory machining process such as workpiece hardness, projection width, processing time, media size and vibration frequency on three responses such as projection height reduction, edge radius and surface finish reduction. They have used Response surface methodology to formulate a relationship between the above mentioned parameters. A design of experiments has been performed in central composite method having 33 sets of experimental values. From the study, the vibration frequency (F) is identified as the most important parameters followed by media size (M) and the processing time (T). Brinell hardness of the workpiece is found to have no effect on the surface finish change of the workpiece. The reduction in surface finish was given S which is given in the equation 2.5.

$$S = 4.2 \times 10^{-9}.T^{0.15}.M^{0.75}.F^{2.93} \tag{2.5}$$

Hashimoto and Debra (1996) developed a mathematical model for the material removal rate and surface roughness of the workpiece, using the change in surface roughness and process time as parameters. According to the experiments performed the surface roughness does not change after a certain period of finishing and hence the constant value reached (D_r) and the initial roughness (I_r) are used as parameters along with the process time as given in the equation 2.6.

$$Ra = (I_r - D_r).e^{-t/T} + D_r \tag{2.6}$$

where, t is the time at which the Ra is to be calculated and T is the time at which the Ra value becomes constant $\{(I_r - D_r)e^{-1} + D_r\}$.

These are the surface roughness models available for vibratory finishing model. As seen above, the calculations made are very basic in nature and does not consider the individual effect of material removal mechanism occurring in vibratory finishing process in detail. The experiments done by Domblesky et al. (2003) confirm that the surface roughness saturates after a certain time of finishing and have stated that it does not depend on bowl acceleration. Experiments in centrifugal disk mass finishing done by Cariapa et al. (2008) have also confirmed that the change in surface roughness does not follow a specific pattern. Hence, the effect of parameters other than acceleration and media are yet to be related with surface roughness of the workpiece. The factors identified which affects the surface roughness are the initial media roughness and the workpiece material.

A detailed analysis of surface evolution of brittle edges was done by Mohajerani and Spelt (2010). The surface evolution was applicable only for the edges of the brittle workpieces as the flat surface of the brittle workpieces did not wear much. And the predicted surface was used to measure the surface roughness of the edges. But such a technique has not been used for flat or curved surfaces of ductile

materials. All these issues will be addressed in this thesis.

2.2.4 Modeling of Residual Stress of Workpiece

In addition to material removal and surface roughness, researchers have also tried to model the residual stress of the workpiece using various method. This section gives a brief description of works performed in this respect.

Sangid et al. (2011b) developed a computational model for predicting the fatigue life of the workpiece with surface roughness and induced residual stress as the input parameters. The dimensions of the micro notches (a,b and c shown in figure 2.28) present in the surface were used to calculate the stress intensity factor of the surface (K_t). This was related to the stress required to propagate the crack in the surface (S_{open}).

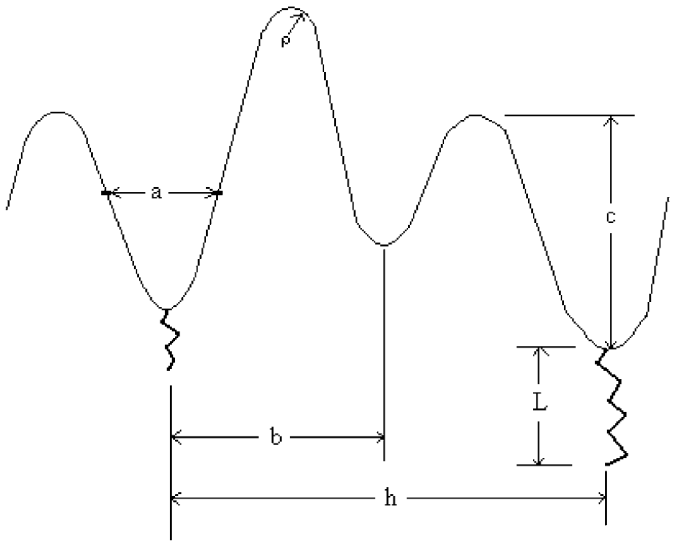

Figure 2.28: Schematic of structure showing the dimensions of the micro-notches and crack length Sangid et al. (2011a)

The effect of residual stress on the crack tip was modeled using the fatigue ratio (R) which in turn was related to the stress required to propagate the crack. The residual stress of the machined surface and the surface topography were measured and input into the model to find the ratio of stress required to open the crack to the maximum stress applied (S_{max}). This is shown in equation 2.7.

$$\frac{S_{open}}{S_{max}} = \left\{ \frac{S_{stable\,open}}{S_{max}} - \left[A \left(\frac{S_{max}}{\sigma_y} \right) + B \right] e^{\left[\frac{l/c}{(S_{max}/\sigma_y)^D} \right]} \right\} (1 - F) + F.R \qquad (2.7)$$

where A, B, C, D and F are empirical constants related to stress intensity factor (K_t) and surface topography (a, b, c); l is the length of the crack; σ_y is the yield stress. When this ratio reaches more than 1, the crack is said to be growing and the crack length is calculated from the critical stress intensity factor of the material. When the crack reaches a critical value, the material is said to have attained failure. The main drawback of this model is that it does not take into account the crack initiation stage of material failure and it considers only a single crack. This model is similar to work done by Mohajerani and Spelt (2010), where they have modeled the a crack growth for brittle edges.

Ciampini et al. (2009) modeled the curvature of almen strips using LS-DYNA in ANSYS. In this model, they have characterized the effect of media impact velocity on residual stress of the almen strips. The velocity distribution measured experimentally by Ciampini et al. (2007) was used as input to the model. They have modeled workpiece using 1D axisymmetric formulation. The limitation of this model was that, it did not take into account of the elastic wave energy absorption by the almen strip support, which led to the overestimation of the plastic deformation per impact when compared to the experimental measurements by Ciampini et al. (2008). This model gave the deformation of the Almen strip due to varying degrees of coverage of stochastically located impacts with random velocities.

A detailed review of the works published related to vibratory finishing is done in the previous sections of this report. The next section will explain the basic term "wear" used to represent material removal and different types of wear.

2.3 Wear Mechanisms

Wear is the removal of unwanted solid material from the workpiece, as defined by John and Burwell. Traditionally wear is seen as undesirable from a design stand-point, while in surface modification processes, controlled wear is desired. Primarily different types of wear mechanisms causes fracture, chemical dissolution and melting of material surface causing the wear which are controlled by the specific tribosystem (Bhushan, 2000). There are four basic types of wear mechanisms,

1. Adhesive Wear
2. Abrasive Wear
3. Fatigue Wear
4. Corrosive Wear

Adhesive and abrasive wear occur due to plastic contact between solids, and the latter two - fatigue and corrosive wear occurs due to either plastic or elastic contact between solids. The first three types of wear - adhesive, abrasive and fatigue can occur either due to deformation and fracture, termed as mechanical wear or due to melting and friction termed as thermal wear. Corrosive type of wear occurs due to chemical reaction between the reacting solids. Figure 2.29 shows the different types of wear mechanisms and the terms associated with the different types as illustrated by Bhushan (2000).

In vibratory finishing, only the first three types of wear mechanisms are possible, as there is no chemical reaction between the components. In addition, only abrasive wear mechanism is predominant as the media is usually a bonded abrasive tool. But due to to complex action of media around the bowl, three types of contacts occur Yabuki et al. (2002) - rolling, scratching and impacts which can cause other types of wear mechanisms in addition to abrasive wear. Hence from the four types of wear, only the first three types are explained in detail in the following section.

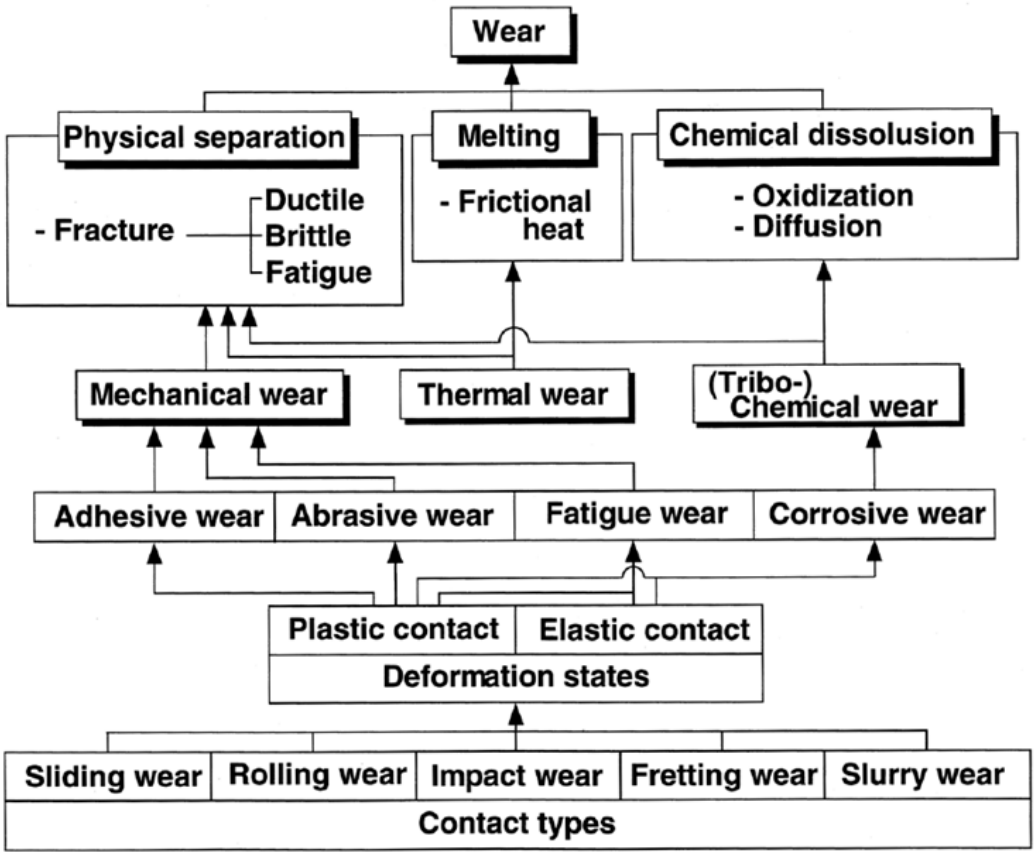

Figure 2.29: Types of Adhesive Wear Mechanisms (Bhushan, 2000)

2.3.1 Adhesive Wear

Adhesive type of wear occurs when two surfaces with similar properties contact each other. When the bonding strength between the surfaces is greater than the force applied, the tangential shear causes the plastic deformation of material at the contact region. When this plastic deformation exceeds the ultimate failure strength of the material, material fracture and hence wear occurs as shown in figure 2.30a.

This wear can in-turn occur by two types of mechanisms viz - compression and tension. When the wear particles are compressed due to the tangential shear caused by the adhesion, flake like shear tongues are formed as shown in figure 2.31a. Whereas when the wear particles are pulled out due to tension, more plastic deformation occur which results in wedge shaped wear particles as shown in figure 2.31b. A detailed analysis of different types of wear particles resulting from various mechanisms is presented in the wear debris analysis part (section 2.5) of this

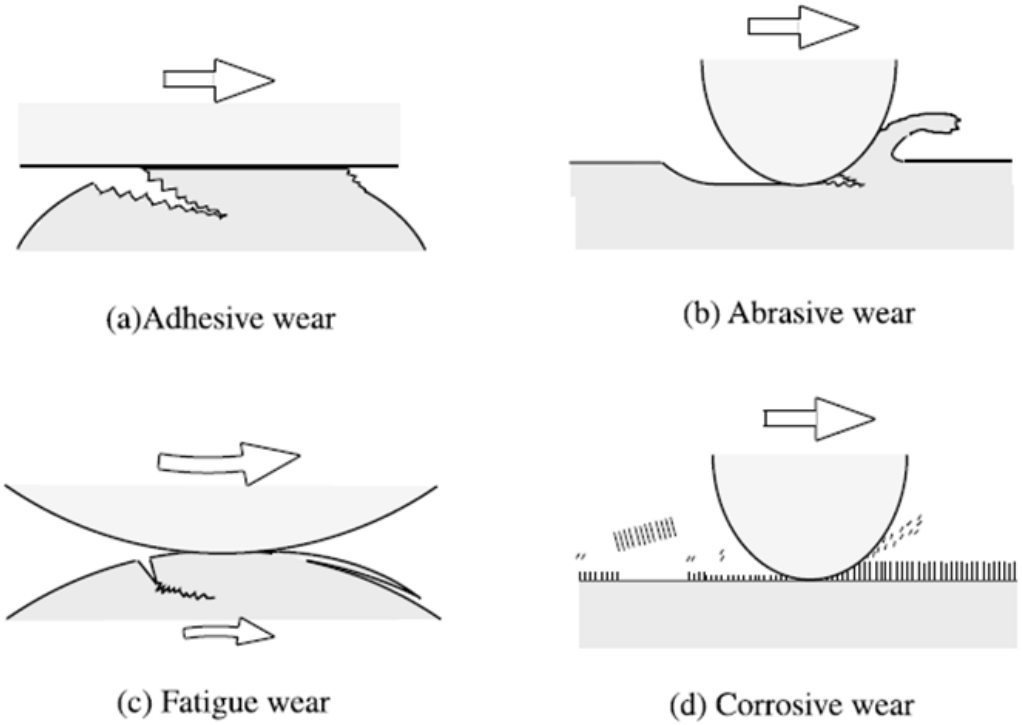

Figure 2.30: Different types of wear mechanisms (Bhushan, 2000)

chapter.

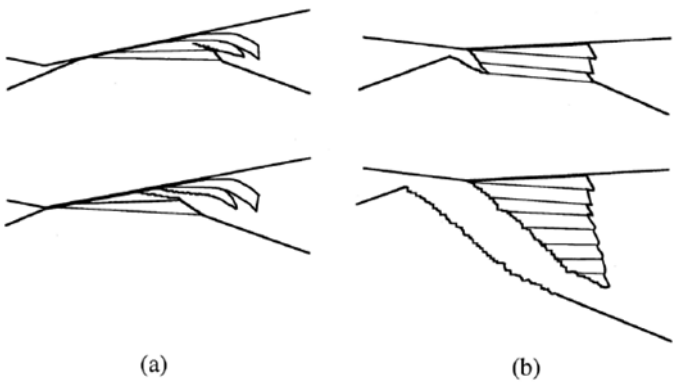

Figure 2.31: Types of Adhesive Wear Mechanisms (Bhushan, 2000)

2.3.2 Abrasive Wear

Abrasive wear can be defined as a material removal mechanism in which, the asperities (projections) of hard body, penetrates and remove material from the surface of the softer body (Gates, 1998). On a micro scale, abrasive wear occurs in three modes viz,

1. Cutting
2. Wedge Formation
3. Ploughing

Figure 2.32 shows the schematic and the actual SEM images (obtained by Hokkirigawa and Kato (1988)) of these three modes. Cutting, as the name implies, is characterized by the cutting of material along with formation of ribbon like chips and usually occurs in low friction conditions. Wedge formation occurs when there is a high friction and adhesive wear causing plastic deformation and a cracked area in form of a wedge at the end of the worn area. Ploughing is characterized by the plastic deformation of material, which pushes the material on to the sides forming grooves as shown in the figure 2.32. Hence, abrasive wear can cause only material removal (micro-cutting) or only plastic deformation (ploughing) or a mixture of both (wedge formation).

The occurrence of these three types of wear modes is controlled by the parameters of the tribosystem such as the cutting depth, force applied, hardness of the material and the radius of the cutting tool. Hokkirigawa and Kato (1988) have further investigated this behavior and correlated the occurrence of these modes with respect to two parameters namely:

- Degree of penetration, D_p
- Degree of wear, β

which are defined by the equations 2.8 and 2.9.

$$D_p = R\sqrt{\frac{\pi H}{2W}} - \sqrt{\left[\frac{\pi H}{2W}\right] R^2 - 1} \tag{2.8}$$

$$\beta = \frac{\triangle V_g - \triangle V_r}{\triangle V_g} \tag{2.9}$$

where, H is the hardness of the materials, R is the radius of the cutting tool, W is load applied, $\triangle V_g$ and $\triangle V_r$ are the volumes of the groove and ridges formed

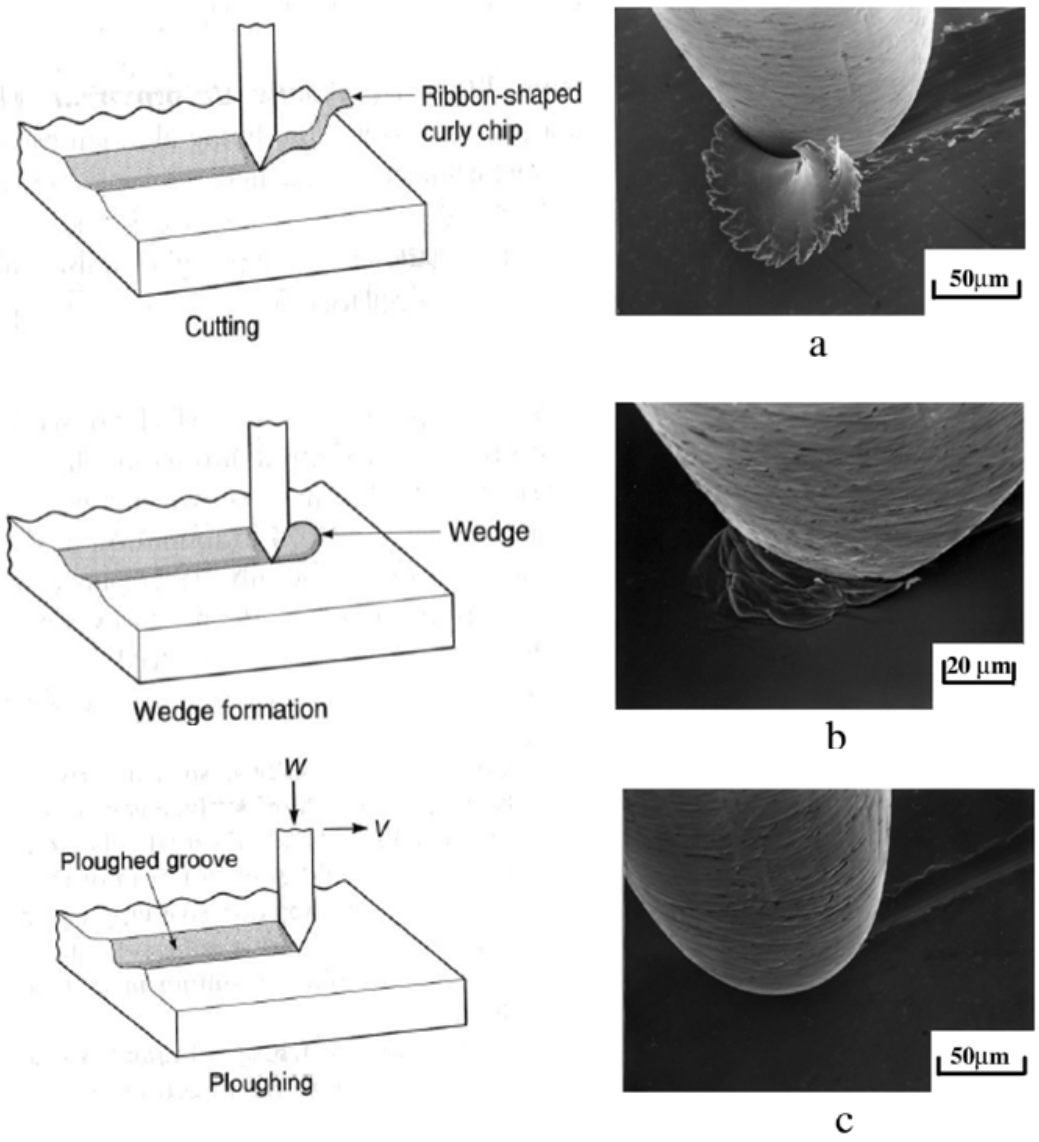

Figure 2.32: Abrasive Wear Modes with SEM image representation (a) Cutting (b) Wedge Formation (c) Ploughing (Hokkirigawa and Kato, 1988)

due to the abrasive wear mechanism as shown in figure 2.33.

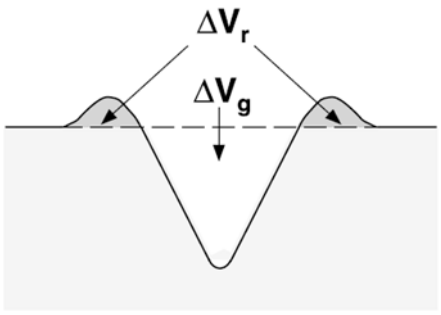

Figure 2.33: Degree of Wear (Hokkirigawa and Kato, 1988)

The correlation between the above parameters, degree of penetration and degree of wear is shown in figure 2.34. As shown in figure 2.34, when the degree of penetration and degree of wear is less, ploughing occurs. Low degree of penetration and low degree of wear represent very light loading conditions under very less friction (as degree of penetration is inversely proportional to the load W, equation 2.8). When both the values increases, wedge formation starts and ultimately results in the cutting mode of abrasive wear. Hence, when the process stop with low force and friction, ploughing is the predominant mechanism and when the process stops at an intermediate force and friction, wedge formation occurs. And when the process continues with heavy loading and friction, cutting occurs. Vibratory finishing parameters fall under the first category as the force applied and the amount of material removed is very less compared to other abrasive processes. Hence ploughing mode of abrasive wear can be expected. But this theory has not been reported so far. This thesis tries to fill that gap by investigating the types of surface modification mechanisms in vibratory finishing.

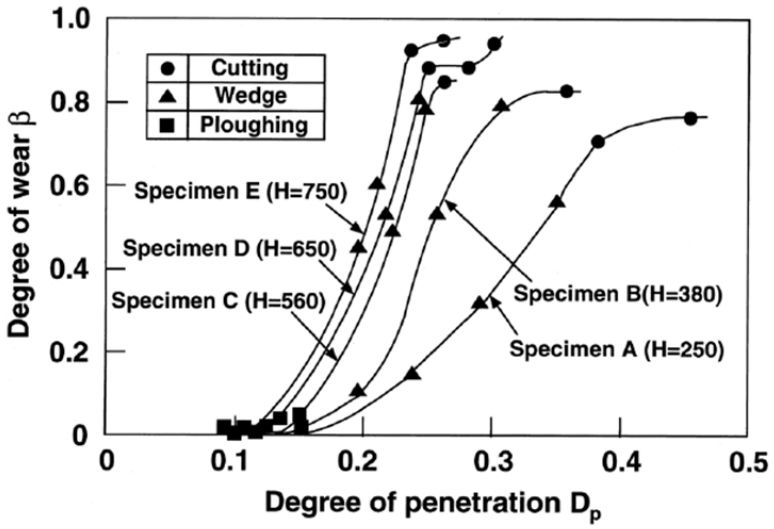

Figure 2.34: Correlation between Degree of wear and Degree of penetration (Hokkirigawa and Kato, 1988)

2.3.3 Fatigue or fretting wear

The next type of wear occurs when there are repeated number of contacts on the surface, in spite of the applied force being less than the ultimate critical stress of the material. This is because of the action of the microscopic defects in the material like slip planes, inclusions and vacancies in the grain boundaries, which when acted upon by a repeated number of small forces, will decrease the yield and ultimate stress of the material. Sometimes it also causes work hardening of the material subsurface before failure (Kayaba and Suzuki, 1976). Fatigue wear can occur due to two types of contacts - elastic and plastic. Elastic type of contact usually occurs when there is a presence of rolling element. When the number of rolling cycles exceeds a critical number, the wear particles are formed in form of flakes. This mechanism is also called spalling.

Plastic contact causes ploughing type of abrasive wear without forming any wear particles. But when this ploughing is repeated over time above a critical number, the plastic flow causes a thin surface layer to protrude in the direction of sliding as shown in the figure 2.35. This thin layer increases as the number of cycles increase (Akagaki and Kato, 1988). In vibratory finishing, there are multiple passes of media impacts, rolling and scratching on the workpiece. Hence this type of fatigue wear mechanism is possible in vibratory finishing.

As mentioned earlier, in addition to these three types of wear, corrosive wear occurs due to chemical action between the contacting surfaces. Since there is no chemical reagent used in the vibratory finishing process of interest, this type of wear is not discussed in detail. Moving forward, the different types of wear mechanisms which occur in processes similar to vibratory finishing have been studied. As mentioned in Chapter 1, Introduction, vibratory finishing is one of the different types of abrasive finishing processes. The following section gives a brief introduction on the wear mechanisms which occur in such processes.

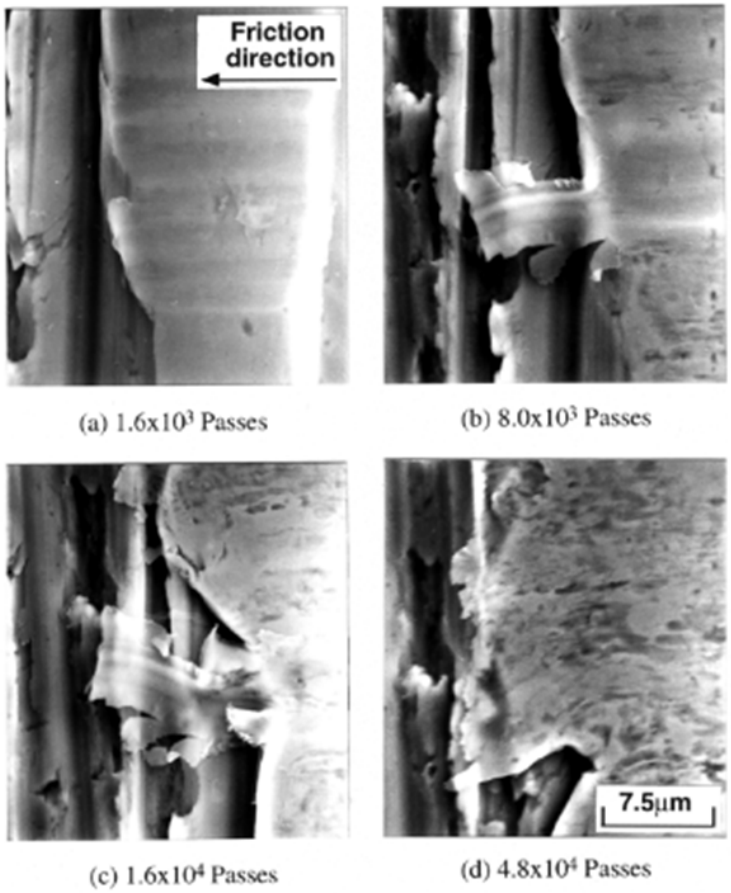

Figure 2.35: Fatigue wear in plastic mode (Akagaki and Kato, 1988)

2.4 Process Specific Wear Mechanisms

As mentioned in chapter 1, there are two types of abrasive processes.

- Fixed abrasive process
- Free abrasive process

Fixed abrasive processes are those in which the abrasives are bonded to a medium such as paper or feldspar and usually fixed to a force applying tool. Whereas free abrasive processes are those in which the abrasives (either bonded or raw) are free to move with respect to the workpiece causing the surface modification. There are many types of fixed and free abrasive processes. Grinding is one of the basic types of fixed abrasive processes which uses bonded abrasive tools for removing material from the workpiece. The mechanism of material removal of grinding is explained in

this section. There are three types of material removal or wear mechanisms which occur in grinding.

- Ploughing
- Chipping
- Breaking

Ploughing as explained previously is one of the abrasive wear modes which results in only plastic deformation forming ridges. The material loss is negligible during this plastic deformation while in some cases, the ridges are removed due to further abrasive action. Chipping is the cutting mode of abrasive wear, where the volume of chip removed is equal to volume of the trace formed by the abrasive. Breaking occurs by the initiation and propagation of cracks in the subsurface of the material. Plowing and chipping are applicable to ductile materials, whereas breaking occur most commonly in brittle materials. However, a combination of all these mechanisms occur in any grinding process, but which of them predominates depends on the material and the system characteristics. Figure 2.36 shows the three modes of material removal in grinding process.

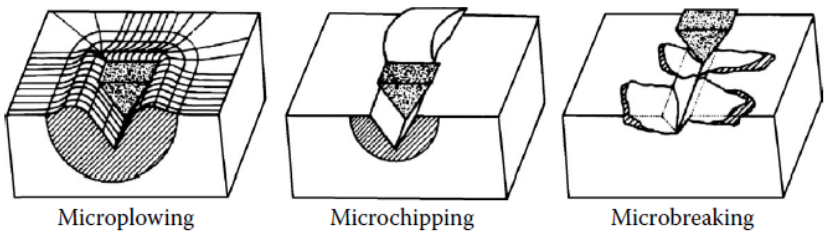

Figure 2.36: Different modes of wear in grinding (Marinescu et al., 2006)

As mentioned in the scope of this thesis our focus is only towards the ductile materials which are currently used in the aerospace industry, and hence the mechanisms related to ductile materials will be discussed further. Figure 2.37 explains the cutting mechanism as explained by Kuchle (2009). When the contact between the abrasive and surface occur, the high cutting angle of the abrasive grain causes

the media to flow and form three regions as shown in figure 2.37. The initial contact first forms an elastic region and as the contact depth increases, a plastic region starts forming and when the plastic region crosses a critical depth of cut, material removal occurs forming chips.

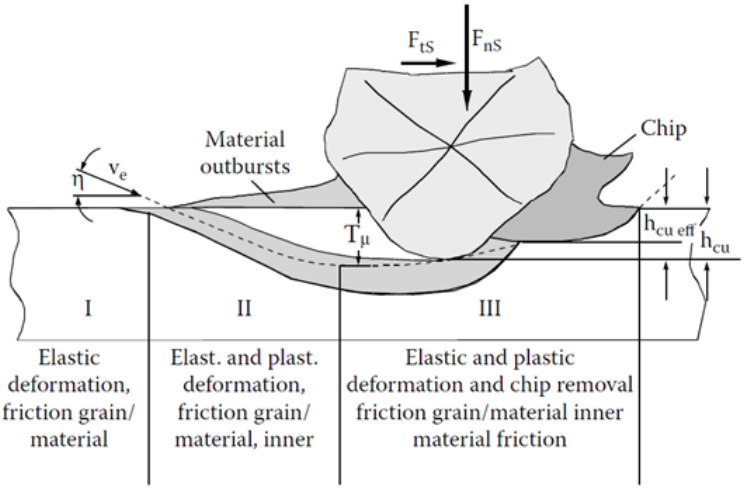

Figure 2.37: Normal cutting mechanism in Grinding (Kuchle, 2009)

This mechanism has further been investigated in detail by Marinescu et al. (2006). This three stages can further divided into 6 phases as shown in figure 2.38. In the first phase only deformation occurs which results in a groove formation. This is continued by a formation of chip in the form of a parallelogram shape due to the shearing and cutting action of the abrasive grain. The next phase results in formation of thread shaped chips which are formed due to the curling of the parallelogram chips formed in the previous stages, due to the thermal and mechanical forces acting on the chip after it is formed. For small feeds, the process ends here forming thread shaped wear debris particles. When the feed rate is large, cutting continues further causing the shear and deformation in the contact zone increasing the contact temperature. This causes local melting and melted regions are transferred to the chips. Hence a tadpole shaped chips or wear debris particles are formed in the fourth phase. When there is a further contact, the next phase results in a mixture of chips formed in shapes such as threads and curls. When there are no lubricants present, the molten region results in spherical chips which

are categorized under phase 6 (figure 2.38). There are different kinds of chips or wear debris particles, due to different experimental and operating conditions. Hence investigating the wear debris particles can also give an indication of the surface modification mechanism. This is one of the four parts of the thesis. Section 2.5 will explain in detail the different types of wear debris formed by different types of mechanisms.

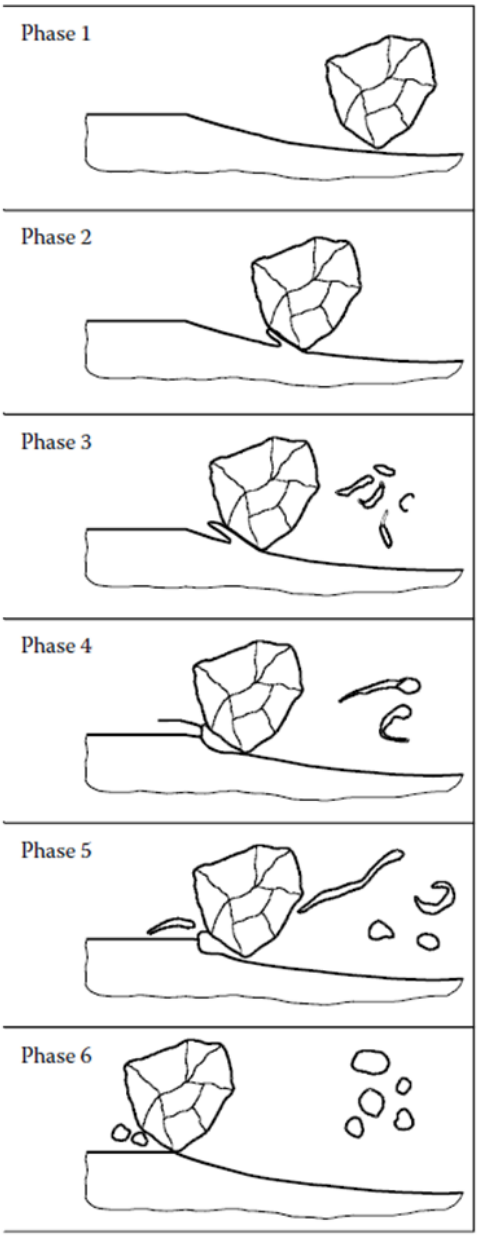

Figure 2.38: Six Phases of Grinding Chip Formation (Marinescu et al., 2006)

Hence in grinding the contact between abrasive and work surface will not only result in normal abrasive and adhesive wear, but also cause thermal reaction in the surface causing local melting. This is because of the continuous contact and high forces involved. Whereas in vibratory finishing the force applied is very less and contact is intermittent. Hence the occurrence of these types of wear will be less prominent in vibratory finishing. Grinding being a basic type of abrasive process was chosen for this study to get an overview of the basic types of wear mechanisms. In addition to this, there are many other research publications dealing with wear mechanisms of related processes like lapping and polishing. In addition to the basic mechanisms occurring in grinding (cutting, ploughing, breaking, melting), the rolling action of free abrasives causes fatigue and fretting wear on the surface. The knowledge obtained from these literature works are used to investigate the wear mechanisms which causes the surface modification leading to the saturation in vibratory finishing process. Chapter 4 continues from here, analyzing the investigation methodology and results obtained.

2.5 Wear Debris Analysis

Any machining process in general will result in chips being formed due to removal of material. Wear Debris Analysis refers to the analysis of these chips or debris particles generated by the wear process. As discussed in the previous section, different types of wear mechanisms occur in a variety of conditions. The wear debris generated by these processes vary depending on the system characteristics such as the contact angle, material properties of the contacting materials such as hardness and forces involved. The following section explains the different types of wear debris generated by different types of processes and also various methods available to identify and characterize the wear debris particles.

2.5.1 Wear Debris Classification based on type of Wear

Abrasive Wear: Ribbon shaped particles are formed when there is an occurrence of material removal which results in chips. Chips are formed when the metal is being cut from the surface of the material by the plowing action of the harder material on the soft one. This type of wear is categorized under abrasive wear. Figure 2.39 shows the ribbon shaped particles obtained from the abrasive wear. The shape is independent of the force applied. Even the nano-scale forces will result in similarly shaped particles but in nanometer scale as reported by Zhao and Bhushan (1998).

Figure 2.39: Ribbon shaped particles formed by micro cutting (Rigney, 1992)

Adhesive Wear: When there is a material transfer from one surface to another as in terms of adhesive wear, there is a formation of wear track , which results in the formation of lumps as shown in figure 2.40. These lumps breaks off after a while forming discrete wear debris particles.

Plastic Deformation: Wedge shaped particles are formed when there is an occurrence of plastic deformation. The plastically deformed layers cause the material to flow over the surface leading to the formation of sheared layers. These sheared layers are further removed from the surface by repeated contacts as shown in figure 2.41. Platelet shaped particles are formed mainly by rolling action of the surface. This is another type of plastic deformation mechanism occurring on the surface.

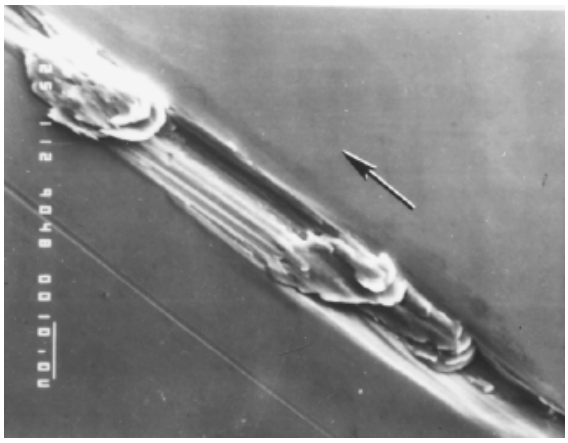

Figure 2.40: SEM image of Wear Track formed by Adhesive Wear (Glaeser, 1981)

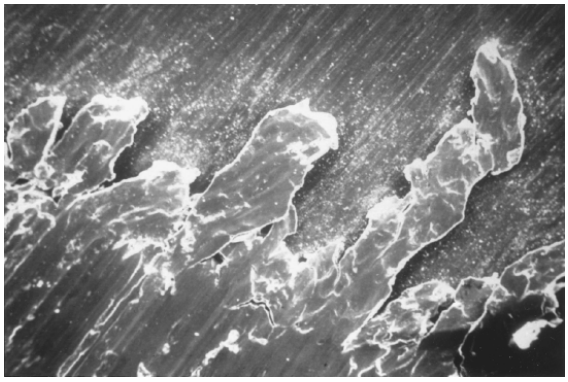

Figure 2.41: Plastically deformed layers forming lips or extrusions (Bhushan, 2001)

Melting: Spherical shaped particles are formed by very high contact temperature which causes melting on the surface. The melted particles are cooled down rapidly causing spherical shaped particles. These kind of particles are typical to grinding process where the contact temperature is very high causing the melting of the particles formed. These particles also have a dendritic microstructure as shown in figure 2.42.

Irregularly shaped particles are formed by a combination of two or more of the above mechanisms. For example, those particles formed partly by abrasion and partly by melting will have half ribbon and half spherical structure similar to a tadpole. These kind of wear debris particles are generated by grinding process as described earlier by Marinescu et al. (2006) in section 2.4. A comprehensive review of different types of wear debris particles and their sources have been made by Fitch (2013) which is shown in figure 2.43.

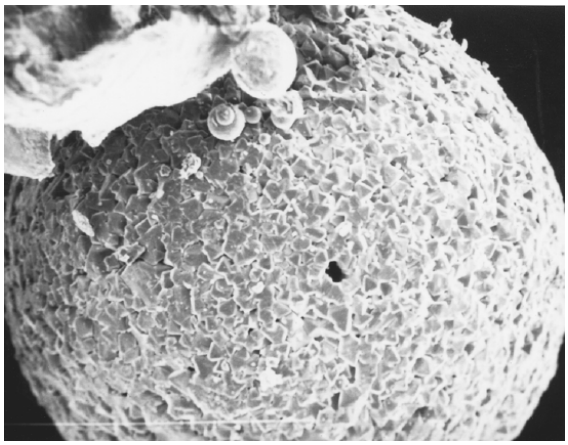

Figure 2.42: Spherical Wear Debriss formed by melting with dendritic microstructure(Bhushan, 2001)

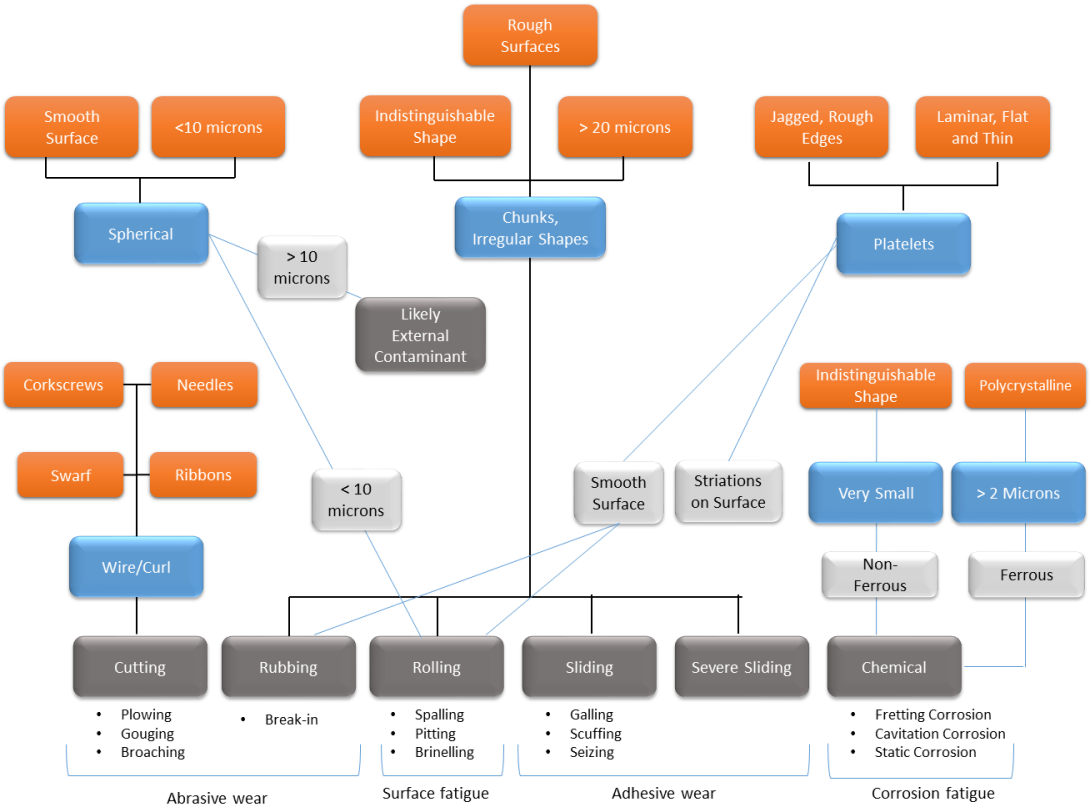

Figure 2.43: Different types of wear debris particles and their sources(Fitch, 2013)

2.5.2 Characterization Methods

There are many characterization methods available for the analysis of wear debris particles. The following methods form the basis for a number of wear debris apparatus such as particle counters and analyzers [Roylance and Hunt (1999)].

Spectrometric analysis is performed by analyzing the result of excitation

either in the source of electrons or light emitted from the materials. This method is used to measure extremely small particles of less than 8μm. But this type of analysis will not be able to give the exact shape and size of the wear debris particles which are required to ascertain the surface modification mechanism.A schematic of spectrometric analysis is shown in figure 2.44.

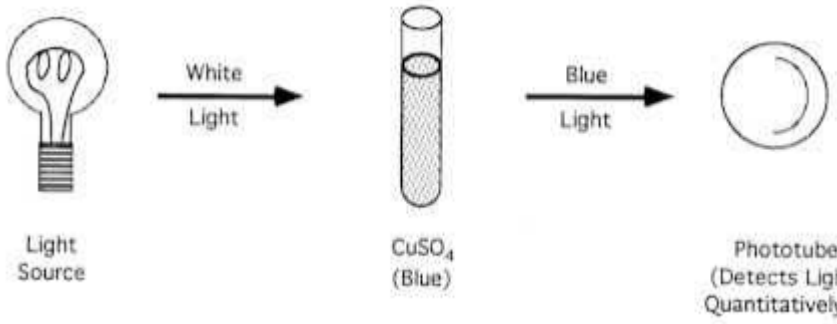

Figure 2.44: Schematic of Spectrometric Analysis(Roylance and Hunt, 1999)

Particle counting refers to physically counting the number of particles present in the analyzed sample. This method can be performed using the reflection of laser light or pore blockage from the collected wear debris particles. The laser light reflection works on the same method as the spectrometric analysis. The sample containing the wear debris particles are passed through a transparent tubing, on which a laser light is passed. This light will be captured by a photodiode which converts the light into electrical signals. An estimate of the size and number of particles are obtained from this reading.

Pore blockage is performed by passing the fluid containing the wear debris across a thin film having pores of usually 10μm. The flow rate is maintained at a constant value and the pressure differential across the film is measured. When there is a presence of wear debris, the pressure differential changes from which the number and size of the wear debris particles are calculated. When compared to the optical technique, pore blockage does not suffer from false positive readings due to presence of dust and other particles along with the wear debris. A schematic of this method is shown in figure 2.45.

Ferrous density analysis refers to the analysis of ferrous quantity present in

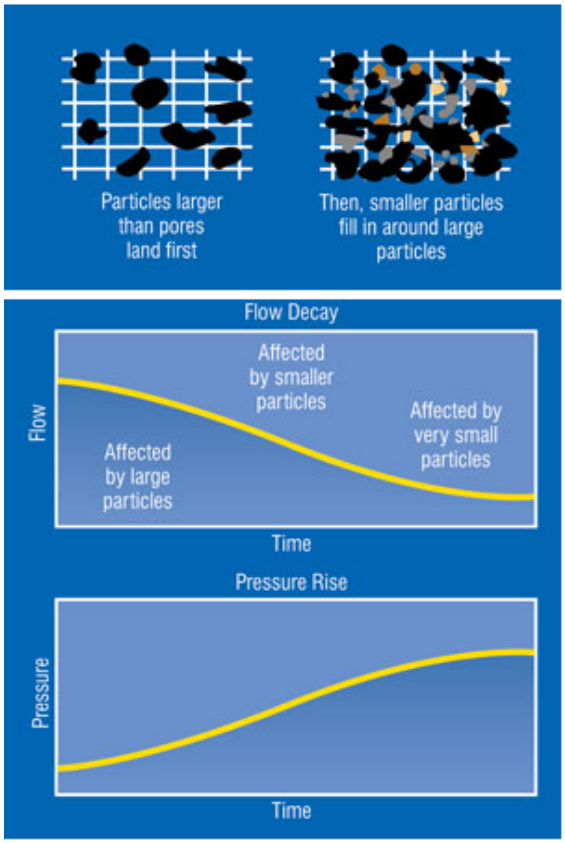

Figure 2.45: Pore Blockage Method (Spurlock, 2006)

the collected sample. This method works only for ferrous materials. The ferrous density is usually measured using a method called direct reading ferrography. This method works on the basis of magnetic force. A high power magnet is placed near a tube filled with fluid containing wear debris particles. Large wear debris particles are attracted towards the magnet while smaller particles remain. A light is then passed through the tube from which the size of the particles are deduced.

Analytical ferrography also refers to the optical analysis of ferrous particles using a microscope or scanning electron microscope collected using magnetic force, but the shape, size and characteristics of the wear debris particles can be obtained in this method.

2.6 Online Monitoring

This section explains in detail the works which were studied to develop an online monitoring technique for understanding the surface modification mechanism in vibratory finishing. An extensive literature review of all the methods feasible to monitor vibratory finishing was performed. This is explained in the following section.

For any type of vibratory finishing process there are 28 input process parameters available according to Gillespie (1975) which is shown in the table 2.1.

Table 2.1: Process parameters of Vibratory finishing Process (Gillespie, 1975)

Compound	Media	Machine	Workpiece	Loading
Composition	Size	Frequency	Material	Amount of media
Grit Size	Shape	Amplitude	Initial roughness	Amount of abrasives
Grit material	Material	Basic Design	Surface area	Amount of water
Emulsifying Agent	Coarseness of the grit	Shape	Toughness	Volume of parts
	Composition	Capacity	Geometry	Weight of parts
	Weight		Location	
			Size	
			Weight	

All these parameters have a major influence on the mechanics as well as the final surface finish obtained. All these input parameters are mostly machine settings and material properties and cannot be related to the mechanics of material removal occurring in the process through a physical model. In order to relate these to the surface modification mechanism, a new set of intermediate parameters which can be

measured in-situ during the process and that can be related to the mechanics as well the surface modification mechanism are introduced. These parameters are termed 'sense parameters'. The input process parameters are first correlated to the sense parameters which are in turn correlated to the surface modification mechanism.

2.7 Sense Parameters

There are many sense parameters which can be measured during the process. A comprehensive list of parameters which can be measured and their significance is reported in the following section.

2.7.1 Force

The machining or cutting force occurring in a process is the basic parameter for quantifying any mechanical material removal process. The aspects of the cutting forces such as,

- Magnitude of the cutting forces and their components
- Directions and locations of action of those forces
- Pattern of the forces: static and or dynamic

are essential for the determination of the following:

- Estimation of cutting power consumption
- Evaluation of role of the various machining parameters
- Study of behavior and machinability characterization of the work materials
- Condition monitoring of the machining tools

This cutting force can be measured using different types of sensors such as:

- Piezoelectric sensors which converts the mechanical displacement of a piezoelectric crystal into electric signals

- Strain gauge based load cells which employ the strain gauges which are based on the electric resistance change when there is a strain occurring in the device.

If the cutting force is measured along normal and tangential directions, the coefficient of friction due to the cutting can be calculated. The relationship between the surface texture and coefficient of friction is well known. Menezes et al. (2008) have studied the influence of various roughness parameters on coefficient of friction under lubricated conditions. They found that the coefficient of friction varied considerably with different surface roughness values.

The different curves are obtained for different materials. In addition to this they also identified the mean slope of the profile as the most suitable surface roughness parameter which changes with relative to that of the coefficient of friction. There are numerous other works relating the effect of cutting forces on surface finish of the machines surface. Hence the measurement of coefficient of friction can be used to monitor the surface evolution of work surfaces, from which corresponding surface roughness can be obtained. This cutting force has been measured on-line for vibratory finishing process by previous researchers which was already explained in section 2.1.4.1. Contact force was used to characterize the type of contact occurring by calculating the coefficient of friction. But the value of contact force was not correlated with the surface roughness obtained. Also contact force has not been measured at various time intervals of the process.

2.7.2 Velocity

The cutting speed or velocity is the next important parameter after cutting force to determine the dynamics of the process. In case of sliding contact, the velocity affects the coefficient of friction, which in turn affects the surface finish of the work surfaces. The velocity of polishing depends on the media shape, size and material. The cutting or material removal takes place in vibratory finishing mainly through impacts and hence the velocity of media measured is termed as the impact velocity. This was also previously explained in section 2.1.4.2.

The impact velocity has been measured experimentally for both bowl and tub vibratory finishing machines and for various input processing conditions. Impact velocity was used to characterize the input motion occurring at various heights of the tub. Thus, both contact force and impact velocity have been used only as tools to understand the process characteristics for various processing conditions and not as a tool to monitor the process and control the surface finish obtained. This is clear from the lack of correlation between the contact force, impact velocity and the surface finish at various time intervals.

2.7.3 Contact Pressure

Contact pressure is a term often used in contact mechanics to represent the pressure developed at the junction where two bodies are in contact. The contact pressure can be measured using specialized sensors like Tekscan shown in figure 2.46 which can measure the pressure distribution over an area. But the contact pressure can also be theoretically obtained from the contact force measured and by estimating the area of contact between the media and workpiece.

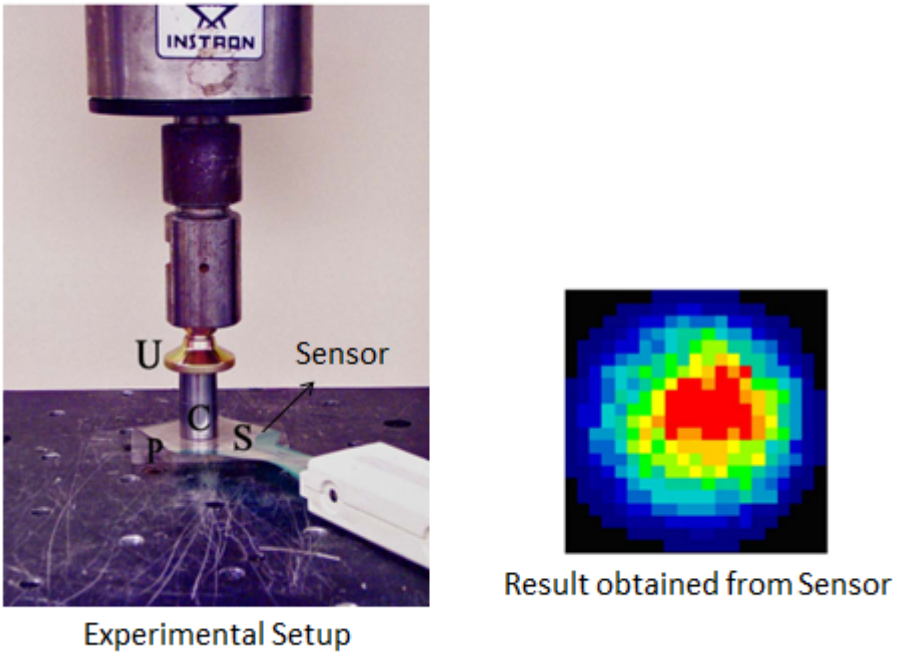

Figure 2.46: Tekscan pressure sensor setup used and Result obtained by Bachus et al. (2006)

2.7.4 Strain rate

The strain of the surface due to the media action can be measured using strain gauges which are based on resistance change. When there is a change in displacement of the sensor, which has a Wheatstone resistance bridge inside, the resistance changes which produce a difference in the current supplied to the strain gauge. But the same technology is used in load cell based force measurement, where these strain gauges are attached to a fixed mass in all three directions. The mass along with the gauge is called the load cell. The force is estimated from the strain value obtained from the load cell. Hence the measurement of strain is also included in the force measurement by using a load cell.

2.7.5 Temperature

Temperature is one of the four basic units of measurement: length, mass, time and temperature. During the machining process, a considerable amount of the machine energy is transferred into heat through plastic deformation of the workpiece surface, the friction between the tool and the workpiece. Researchers suggest that 99 per cent of the work done is converted into heat. This results in an increase in the tool and workpiece temperatures. Temperature occurring at the workpiece tool interface can be measured using many methods [Longbottom and Lanham (2005)] such as thermocouples, PVD (physical vapor deposited) films and thermal cameras. Figure 2.47 shows the thermocouple placed inside the workpiece material cut into two halves developed by Huda et al. (2002). So these methods are also not non-destructive. All these methods holds good only for dry processes. The presence of coolant in the process will be a major hindrance and the values obtained will vary drastically. Vibratory finishing being a wet process uses the compound which is basically a detergent mixed with water to clean the surface after machining. Hence the measurement of temperature is not feasible for monitoring and controlling the process.

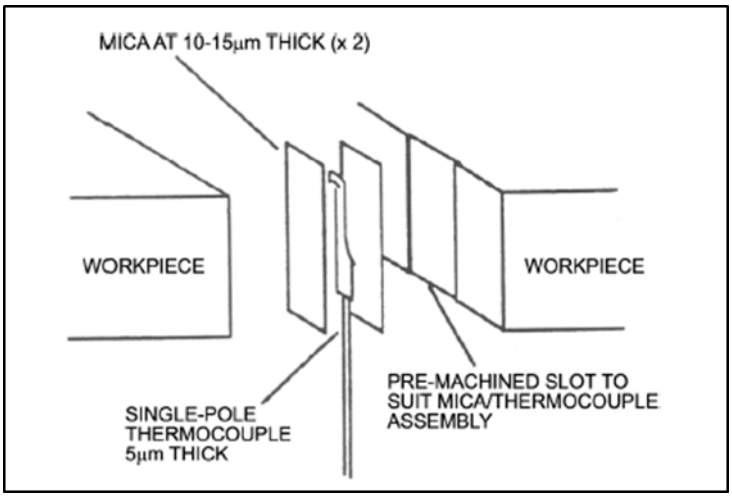

Figure 2.47: Thermocouple based temperature measurement (Huda et al., 2002)

2.7.6 Eddy current

The parameters such as force, velocity, contact pressure, strain and temperature discussed above are the derivatives of basic units of measurement such as displacement, time, mass and temperature. Now some methods used for Non-Destructive Testing (NDT) will be analyzed for use as sense parameters for characterizing the surface obtained using vibratory finishing process. Eddy current is the method which employs the detection of flaws by measuring current produced in any electrically conductive material that is subjected to an alternating magnetic field which is generated by passing an alternating current through a coil [Willcox and Downes] as shown in figure 2.48. When there is a flaw on the surface, the magnetic flux changes as shown which is reflected in the measured eddy current. This method is currently used to characterize the surface and subsurface flaws, conductivity measurement, coating thickness measurement and also for estimation of residual stress of the material. Measurement of this eddy current is completely electrical and requires the coil and measurement devices alone. Hence it can be easily applied to the workpiece subjected to vibratory finishing. But the information which can be obtained from these signals may represent many quantities such as the conductivity, flaws, material composition, hardness and permeability. Thus there is a high possibility of these signals to overlap and the effect of one parameter to be masked

by other. Generally this method is used only for surface breaking conditions and slightly sub-surface flaws. Hence in spite of its ease of installation, due to its limited applicability it cannot be used for the monitoring of vibratory finishing process.

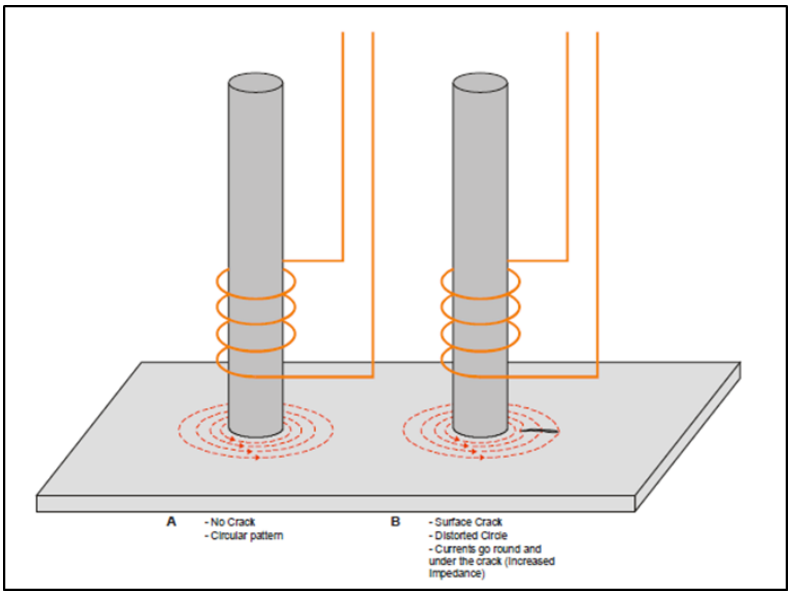

Figure 2.48: Eddy current method (Willcox and Downes)

2.7.7 Radiography

Radio-active isotopes are materials which emit radiations due to unstable nucleus. Tracers are a common application of radioisotopes. A tracer is a radioactive element whose pathway through which a chemical reaction can be followed. Tracers are commonly used in the medical field and in the study of plants and animals. When this tracer is mixed along with the media the path of media and the velocity of media can be detected using suitable gamma ray detectors. Radio-active tracers have been recently used to measure the wear and corrosion. It has been used by researchers to study the wear rate of piston rings inside the internal combustion (IC) engines [Eberle et al. (2005)]. It has also been used in tribo-metrology to measure the wear rate of materials having a very low wear which cannot be quantified by normal means [Franek et al. (2008)]. Figure 2.49 shows the radio-active tracer used to study the performance of IC engines. This type of measurement is feasible in small scale applications. But in vibratory finishing this will require a big scale

gamma detector which is not feasible practically. When the technology is developed to make it smaller and cheaper this method can be used to measure the media flow characteristics.

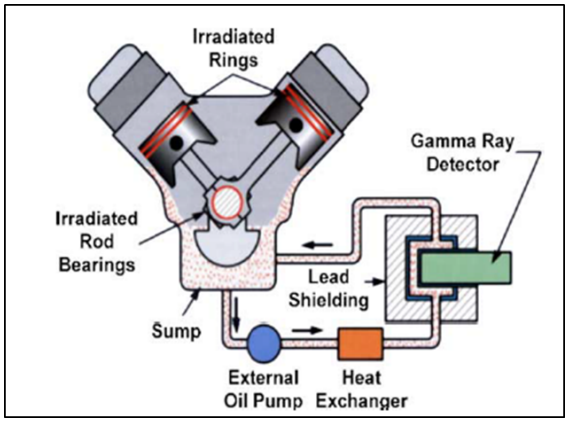

Figure 2.49: Radio-active measurement using gamma ray detector (Eberle et al., 2005)

2.7.8 Ultrasonic Signals

Ultrasonic signals are the high frequency signals of sound which are out of the human hearing range. This method is similar to SONAR, where an ultrasound generated from a source is passed through the work material and the reflected sound is measured by a transducer. The surface quality and flaws are detected from the measured signals [Willcox and Downes] as shown in figure 2.50.

This method can also measure 3D flaws inside the workpiece. But it requires a reference surface which can be used for comparison. In other words, a strong calibration method is required. This method has been widely used to measure the thickness of plates, detection of flaws and even for the monitoring of surface roughness by Coker and Shin (1996) as shown in figure 2.51. Hence it is possible to monitor the surface roughness effectively by using ultrasonic signals measured from the workpiece material.

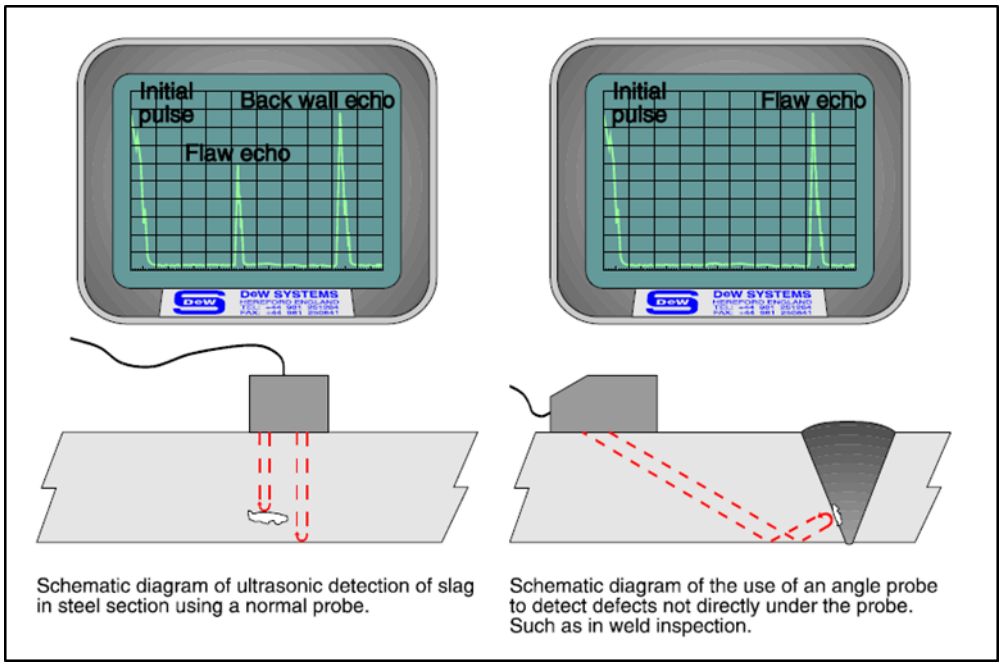

Figure 2.50: Ultrasonic measurementt (Willcox and Downes)

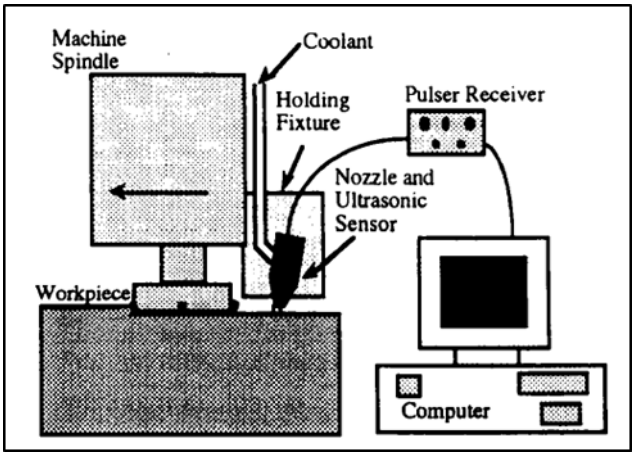

Figure 2.51: Surface roughness monitoring using Ultrasonic signals (Coker and Shin, 1996)

2.7.9 Acoustic Emission

Acoustic emission (AE) is the measure of stress waves induced inside a workpiece when there is a deformation in the workpiece material. They are basically a part of the incident energy which propagates into the material as shown in figure 2.52. The source of acoustic emission can also be a flaw originating inside the workpiece material. Forster and Scheil [Miller and McIntire (1987)] published the first experiments specifically designed to detect AE in metal in 1936. AE signals are one of the most widely used techniques for the online monitoring of machining processes.

This section deals with a brief literature review of selected works in this respect.

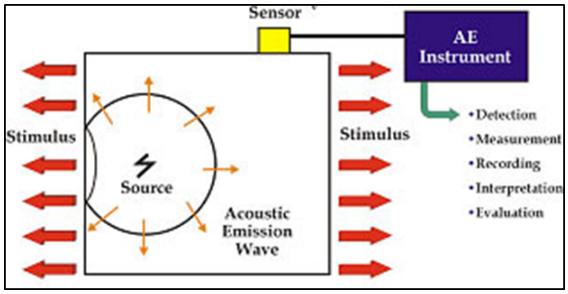

Figure 2.52: Acoustic Emission source and measurement (PAC)

Li (2002) has performed a detailed review of works published for acoustic emission based tool wear monitoring during turning. In this work, he has reviewed 35 journal papers and conference proceedings which deal with the acoustic emission based monitoring. It is concluded at the end of the review that the AE based monitoring is the current trend in the area of online process monitoring due to the high sensitivity of the AE signals. The main issue is to filter the noise and analyze the obtained signals using a suitable signal processing method. Pawade and Joshi (2012) used the AE signals to characterize the surface generation in high speed turning of Inconel 718 based on the AE counts, energy and mean frequency amplitude. The measurement setup is shown in figure 2.53.

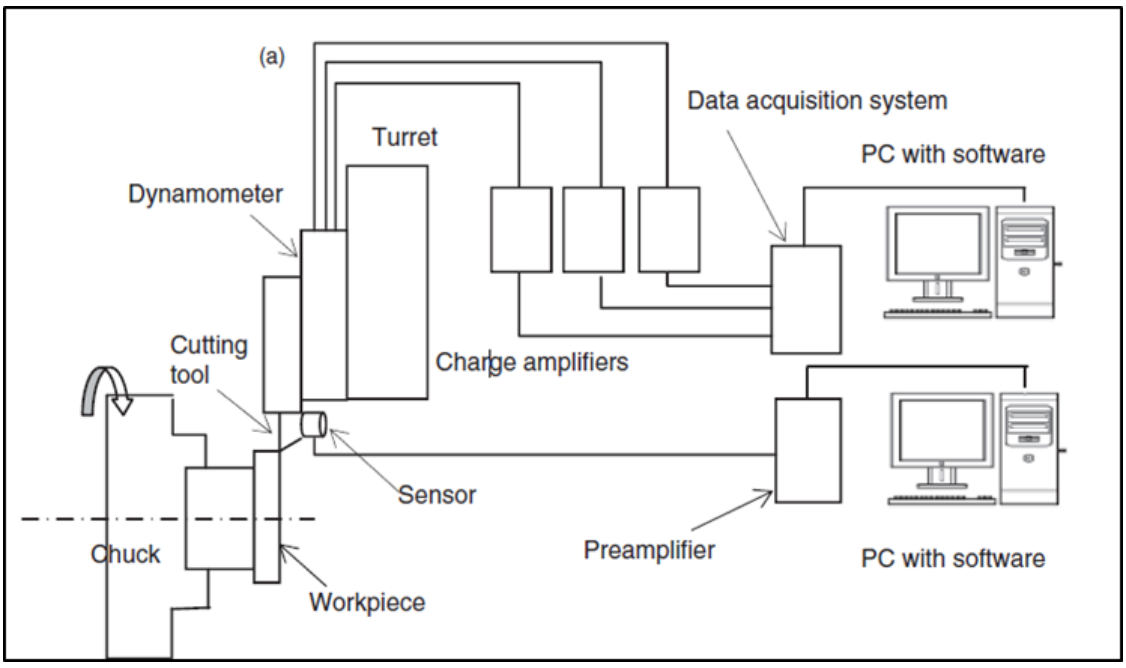

Figure 2.53: Measurement setup used by Pawade and Joshi (2012)

Further the AE signals were analyzed as a function of cutting speed, feed rate, depth of cut and tool geometry. It was found that the AE energy signals varied for different values of surface roughness obtained as shown in figure 2.54.

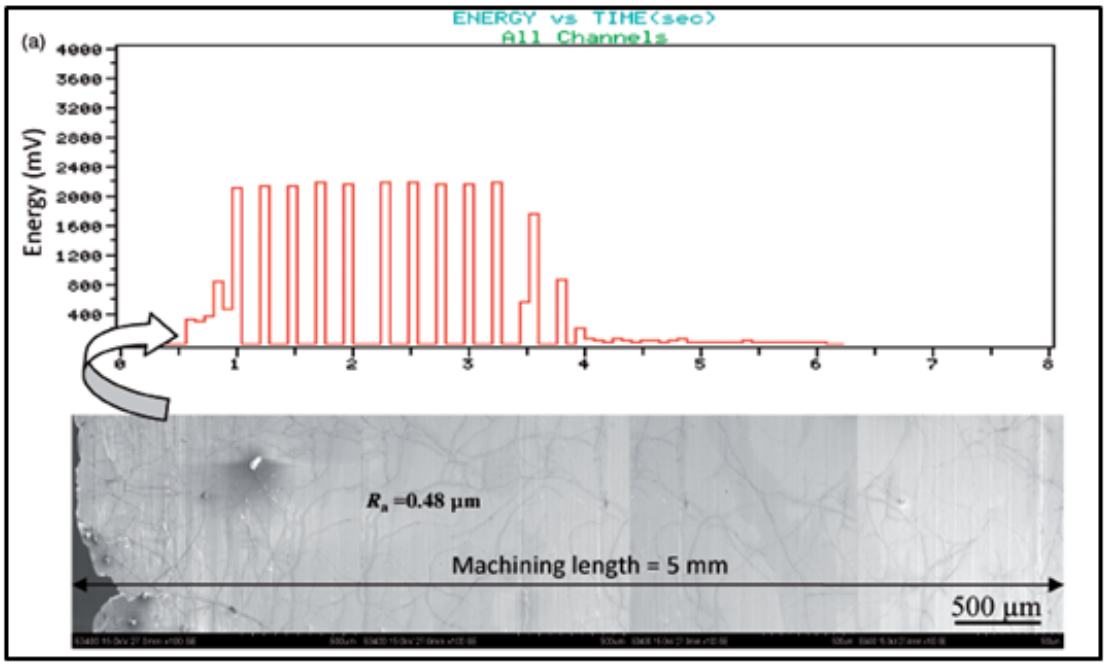

Figure 2.54: Variation of AE energy with surface roughness (Pawade and Joshi, 2012)

Beggan et al. (1999) measured the AE signals for a cutting process and measured the RMS value and the surface roughness of the turning process as shown in figure 2.55. They also modeled the AE and surface roughness using theoretical equations derived from the physical and geometric considerations. From that they found that the deviation of AE signals from the predicted values and surface roughness from the predicted values followed a same trend as shown in figure 2.56.

From this they proposed that the deviation of AE signal from its predicted value can be used to predict the actual value of surface roughness from its predicted value.

Webster et al. (1994) measured the acoustic emission of workpiece subjected to abrasive grinding process using a sensor fixed under the workpiece as shown in the figure 2.57. The raw AE signals as well as RMS, RLS and kurtosis of the raw signals were measured. In addition to AE, force measurement was also done. When the results were compared to the final surface obtained, the ratio of RMS value of

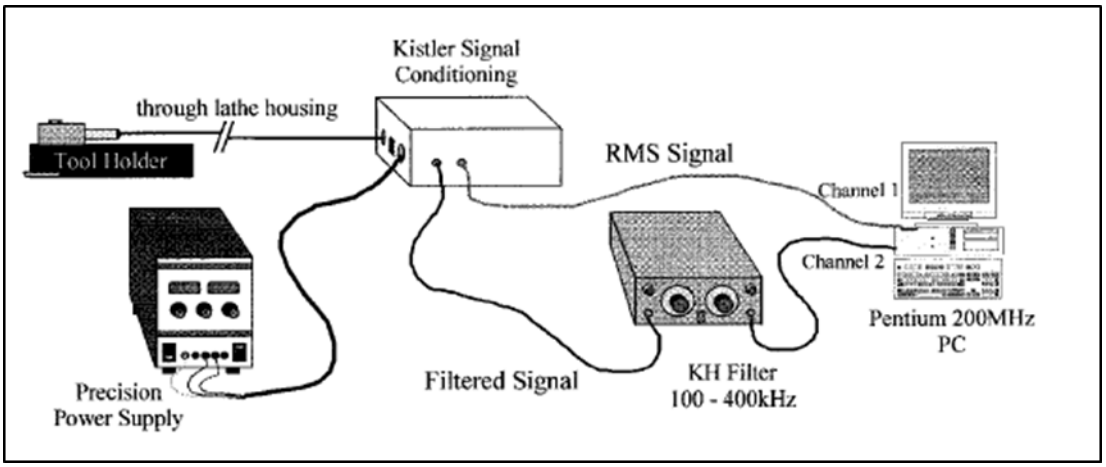

Figure 2.55: Measurement setup used by Beggan et al. (1999)

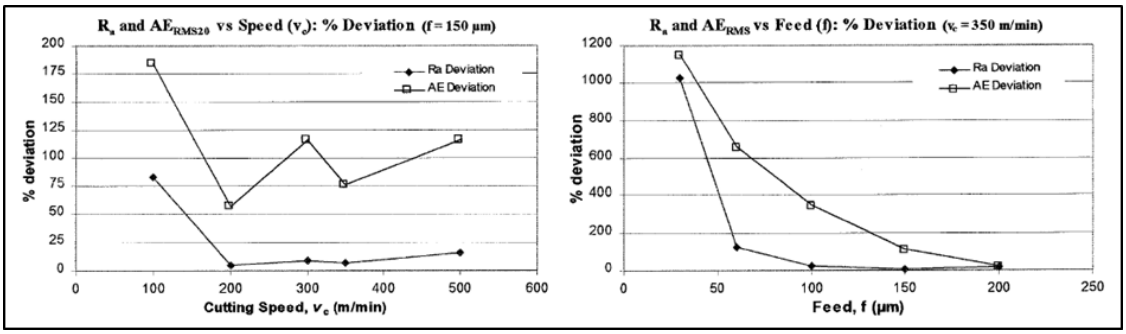

Figure 2.56: Correlation of deviation of AE and Ra from theoretical values (Beggan et al., 1999)

AE and the force measured for different grinding dress lead and the average surface roughness correlated.

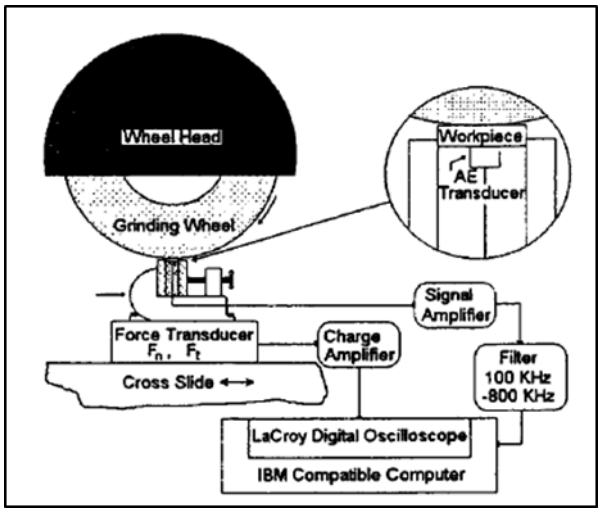

Figure 2.57: AE measurement setup used by Webster et al. (1994)

In a recent study made by Hase et al. (2012) AE signals have been used to

characterize the adhesive and abrasive type of wear mechanisms occurring in controlled laboratory conditions as shown in figure 2.58. They measured the frequency spectrum of AE signals recorded from this process and characterized the process using the spectrum obtained. They found that the signals corresponding to adhesive wear had only a single peak in the low frequency region due to the vibrations, whereas the abrasive wear signals had multiple peaks in low frequency region as shown in figure 2.59.

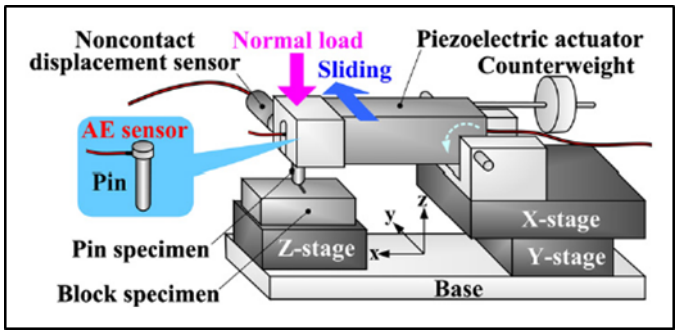

Figure 2.58: Measurement setup used by Hase et al. (2012)

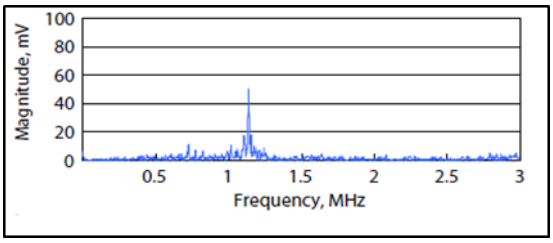

(a) Adhesive Wear

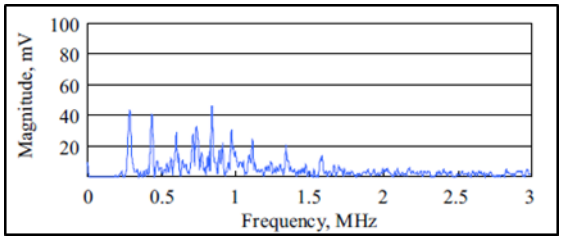

(b) Abrasive Wear

Figure 2.59: Correlation of AE signals with wear mechanism (Hase et al., 2012)

From this they proposed that the type of wear mechanism occurring in any process can be analyzed from the frequency spectrum of AE signals measured from the process. Hence, in addition to surface roughness, the type of wear also can be predicted using AE signals. AE signals have also been used by Jiaa and Dornfeld

(1990) to identify the different regions of sliding wear. The signals have been correlated with the wear mechanism occurring during the sliding, which has been identified from the SEM analysis of the work surfaces.

Ivantsiv et al. (2009) measured the mass flow rate of abrasive jet machining using acoustic emission signals. In their work, they have selected AE peak count and power spectral density of acoustic emission signals to characterize the abrasive jet machining process. AE peak count has been used to predict the number of particle impacts per unit time and the power spectral density at specific frequency was used to predict the mass flow rate.

In addition to these works there are other works by Chang et al. (1996), Inasaki (1998), Buttle and Scruby (1990), Dornfeld et al. (2003), Ferrer et al. (1999) and numerous others relating the use of acoustic emission for the monitoring of machining process and surface characterization. But AE signals were never measured for vibratory finishing processes. It can be used as an effective parameter to monitor the process mechanics, as well as to characterize the media workpiece interaction. Hence, it is selected as the final and the most important sense parameter in this project. In addition to this there are some works which use the fusion of AE and force and relates it to the surface roughness which is explained in the following section.

2.7.10 Force and Acoustic Emission Fusion

Webster et al. (1994)used a combination of force and acoustic emission and correlated the ratio with the obtained surface roughness. Oh and Lee (2011) also used a force and acoustic emission based measurement for the prediction of surface roughness in magnetic abrasive finishing. Factors such as rotational velocity of the polishing quill, gap, abrasive size and feed rate were changed and the corresponding change in Ra was measured along with the force and acoustic emission values. When these values were fed into an artificial neural network, the combined force and acoustic signals predicted the surface roughness with an error percentage

of 2.86%. Azouzi and Guillot (1997) examined the feasibility of intelligent sensor fusion technique to estimate online surface roughness. An artificial neural network was used to make the sensor selection based on the experimental data. Scheffer et al. (2003) presented a schematic diagram for integrated measurement including vibrations, acoustic emission and cutting forces as shown in figure 2.60.

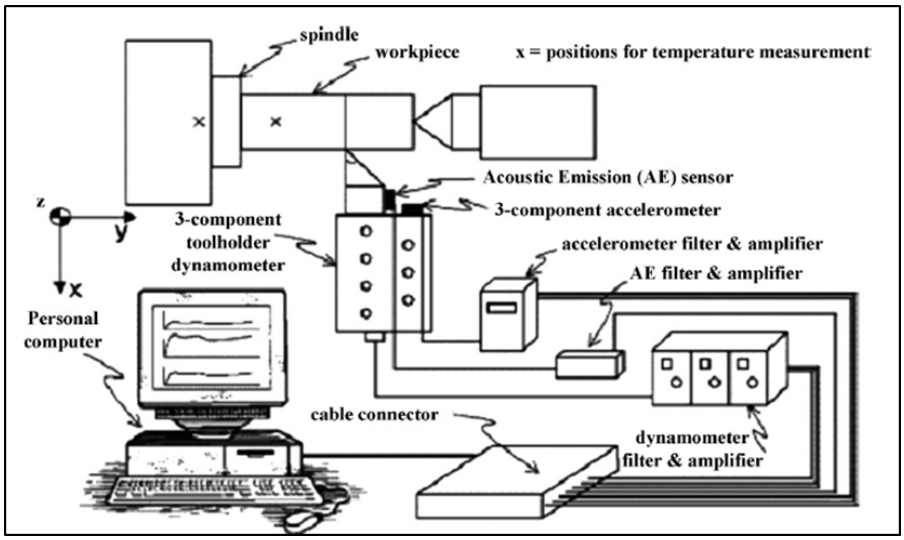

Figure 2.60: Schematic of fusion of force, AE and vibration setup (Scheffer et al., 2003)

2.8 Gaps Identified from Literature

A detailed literature review on vibratory finishing has been performed and the works related to the surface modification, wear debris analysis and acoustic emission have also been studied. Table 2.2 presents the gaps identified from the various sections presented in this chapter.

Table 2.2: Gaps identified from Literature Review

Parts of Literature Review	Gaps Identified
Section 2.1 to 2.4	The mechanism of material removal or surface deformation which causes the surface modification in vibratory finishing is not studied yet.
Section 2.5	There is no knowledge about the wear debris particles generated by vibratory finishing process.
Section 2.1	There is no setup to precisely control the frequency and amplitude of vibrations.
Section 2.6, 2.7	Testing for the process is still performed on a trial-and-error basis. There is no online monitoring technique available.

This thesis aims to fill these four gaps presented in table 2.2 and the activities performed are converted into four work chapters of this thesis. The next chapter introduces the various materials and equipment used for conducting the experiments presented in this thesis.

Chapter 3

Materials and Equipment

3.1 Overview

This chapter explains the workpiece materials, equipment, fixtures and experimental methods used in the experiments performed.

3.2 Workpiece Material

Three workpiece materials including titanium alloy, aluminum alloy and stainless steel alloy were used. The physical and chemical properties of the materials are explained in this section.

3.2.1 Grade 5 Titanium Alloy Ti-6Al-4V

Grade 5 Titanium alloy Ti-6Al-4V was used to fabricate the titanium workpieces used in the experiments. This material is the most commonly used aerospace alloy for fabrication of components like blades, discs, rings and airframes. It is mainly used for its high strength-to-weight ratio. The chemical composition of this alloy by weight is presented in table 3.1.

Component	Composition
Aluminum, Al	6.2
Vanadium, V	4.2
Iron, Fe	0.05
Carbon, C	0.02
Nitrogen, N	0.010
Hydrogen, H	0.001
Oxygen, O	0.06
each	< 0.10
total	< 0.40
Titanium, Ti	Balance

Table 3.1: Chemical composition of Ti-6Al-4V alloy used by weight percentage

3.2.2 Aluminum Alloy T6-6061

Aluminum alloy 6061-T6 was used for experiments involving aluminum workpieces. This alloy is the commonly used aluminum alloy for fabrication of aircraft fittings, couplings, pins, valves and valve parts. It is mainly used for its good workability, high resistance to corrosion and easy availability. The chemical composition of this alloy by weight is presented in table 3.2.

Component	Composition
Aluminum, Al	95.8
Chromium, Cr	0.04
Copper, Cu	0.15
Iron, Fe	0.7
Magnesium, Mg	0.8
Manganese, Mn	< 0.15
Silicon, Si	0.4
Titanium, Ti	< 0.15
Zinc, Zn	< 0.25
Other, each	< 0.05
Other, total	< 0.15

Table 3.2: Chemical composition of T6061 Al alloy used by weight percentage

3.2.3 Duplex Stainless Steel

2205 Duplex Stainless Steel was used for performing the wear debris experiments due to the magnetic nature of the materials which can be easily separated by magnetic separation method. The alloy is used in variety of applications like pressure vessels, heat exchangers, marine and oilfield equipment. The chemical composition of the alloy by weight percentage is presented in table 3.3.

Component	Composition
Carbon, C	0.02
Chromium, Cr	22
Iron, Fe	68.71
Molybdenum, Mo	3.1
Nickel, Ni	6
Nitrogen, N	0.17

Table 3.3: Chemical composition of 2205 Duplex Stainless Steel used by weight percentage

3.3 Industrial Vibratory Finishing Setup

3.3.1 Walther Trowal MV32

Walther Trowal Multi-Vibrator 32 (MV32) vibratory finishing bowl was used for the experiments. This is an industrial grade vibratory finishing bowl with a capacity of 530 liters and a drive power of 13kVA. This vibratory bowl has three vibratory motors - two on the sides and one below the bowl as shown in figure 3.1. The angle of inclination of the motors with respect to the bowl can be modified according to which the media motion inside the bowl varies. The most commonly used angle of motors are 10° and 45° with respect to the vertical axis of the machine. The 10° motor angle is recommended for grinding application whereas the 45° motor angle is recommended for polishing application. Since the machining parameters were not considered to be studied in this thesis, an intermediate angle of 20° was selected for conducting the experiments.

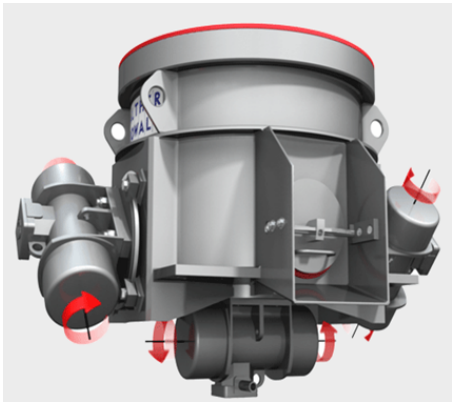

(a) Schematic

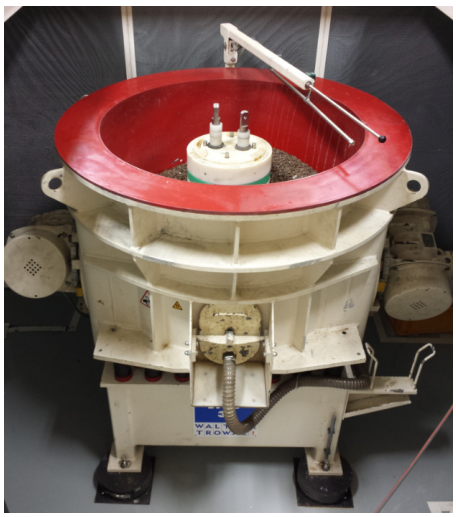

(b) Actual Setup

Figure 3.1: Walther Trowal MV32 vibratory finishing machine

A fixture is used to hold the workpiece inside the bowl as shown in figure 3.2. This fixture is made of Delrin^{TM} material so that the media particles do not abrade the fixture components.

3.3.2 Raytech AV75

AV75 is a table top vibratory bowl finisher from Raytech Industries. This small bowl has been used for performing the wear debris experiments in this thesis. This bowl is usually used to polish small components like screws, nuts and bolts. But it has also been used widely in jewelry and other minor polishing application.

The component was fixed inside the bowl using a fixture as shown in figure

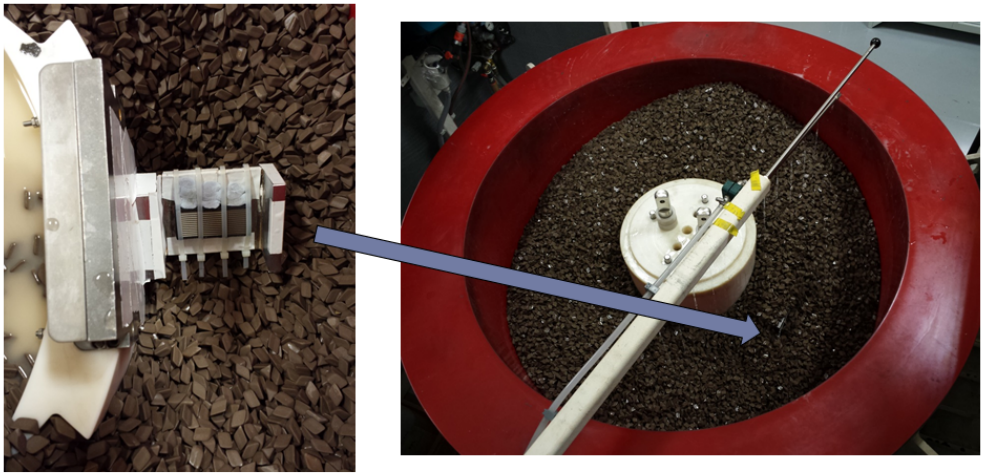

Figure 3.2: Experimental Setup used in MV32

Figure 3.3: Raytech AV75 bench-top vibratory bowl

3.3. In addition to this a small chamber was attached to the bowl for conducting controlled wear debris experiments.

3.3.3 Media

Ceramic Tristar

Ceramic tristar media (Figure 3.4) is the trade name for the ceramic media with a shape of an angle cut extruded triangle. This media was used to perform all the experiments presented in this thesis except for the accelerated wear debris experiment described in later in chapter 5. This media is usually used for its

abrasive nature and polishing applications.

Figure 3.4: Ceramic Tristar Abrasive Media

Plastic Conical

Plastic conical media (as shown in figure 3.5) is used for the wear debris analysis experiment mainly to reduce the amount of media wear as the plastic media does not have the tendency to wear as much as the ceramic media. This media was used for the accelerated experiment described later in chapter 5.

Figure 3.5: Plastic Conical Media

3.3.4 Compound

A water based detergent compound Trowal ARF was used for all the experiments conducted. This compound is mainly used to remove the wear debris particles,

clean the surface and give a smooth and shiny finish to the component.

3.4 Masking tape used for surface modification method

A vinyl tape usually used for insulating electric wires, was used to mask the workpiece surface for conducting the masked surface experiments. This tape was chosen based on the protection it offered to the surfaces from the action of media and its adhesive capability to remain intact without being removed by the action of media.

3.5 Surface Profile Measurement

Surface profile measurement were performed using a contact stylus profilometer from Mitutoyo. Model Surftest Extreme SV-3000 CNC. All measurements were taken after calibrating the stylus and equipment with a standard reference measurement.

3.6 Surface Characterization Equipment

Surface characterization was performed to analyze the surface topography of the finished surface and the wear debris particles at various time intervals. In addition to surface topography analysis, material characterization was also performed using EDX tool available in the SEM.

3.6.1 Scanning Electron Microscope

The following parameters were taken into consideration to obtain high quality pictures of the metallic debris:

Accelerating Voltage: In order to obtain fine surface structure images, lower accelerating voltage (10-15 kV) was used to maintain an optimum balance between

image quality and to find out the chemical composition of particles while doing EDX. Also, the smaller the probe current diameter on the specimen, the higher the magnification and resolution will be. However, the image smoothness depends on the spot size or probe current.

The probe diameter directly depends on the spot size. As the probe diameter is reduced, the spot size is reduced. It is therefore, important to select a probe current suited for the magnification and observation conditions (accelerating voltage, specimen tilt, etc.) and the specimen. Since, small spot size gives grainy images; spot size in the range of 25-35 was used for taking pictures.

In order to avoid/reduce specimen charge up the most important precautions were taken care of i.e. reducing the spot probe current, lowering the accelerating voltage and maintaining an apt working distance to ensure high resolution of the images.

Point by point scanning was done to ensure that the particles being observed were metallic or not by using EDX. An estimate of metallic particles in the sample being observed was made by analysing every spectrum analysed while hunting for metallic particles (retrieved from the EDX projects stored in the computer). Following which, the size and shape analysis was done carefully to observe if there was any change in size of the debris particles and a trend of similar kinds of shape.

3.7 2D Vibratory Finishing Setup

3.7.1 Hydrodynamic Shaker

An electro-magnetic shaker system which is used for high frequency testing of structures was modified to provide the necessary frequency and amplitude for testing the effect of process parameters described in chapter 6. The shaker system operates on compressed air which pushes the electromagnetic core which in-turn switches on and off causing to and fro vibratory motion. Different hole patterns on the vibrating bed facilitate in attaching different fixture designs on to the armature. The

electro-magnetic shaker system is computer controlled. This machine is capable of operating in a frequency range of upto 3000 Hz. The whole set up is controlled by a controller and there is a feedback loop system comprising of an accelerometer which is attached to the vibrating bed of the shaker system from which output is relayed back to the system which ensures that the system operates according to the input parameters given. The accelerometer feedback from the vibrating bed is also verified using the controller and software set up, making the system more reliable. The setup of hydrodynamic shaker is shown in figure 3.6.

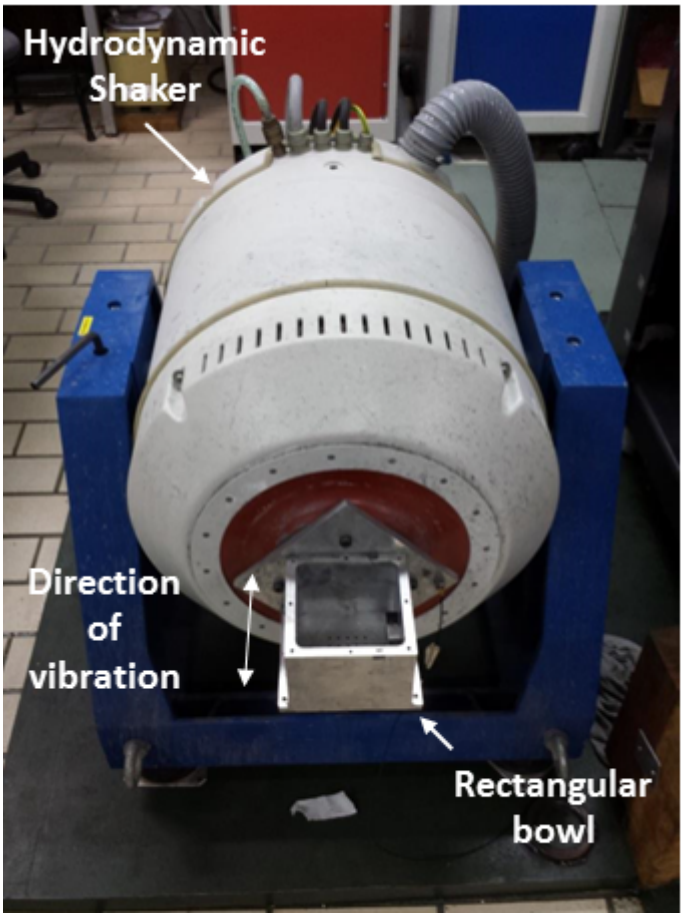

Figure 3.6: Hydrodynamic Shaker Setup

3.7.2 Chamber used for Analysis

A small rectangular chamber of volume 0.9 liters (100x100x90 mm^3) was made from a single aluminium block. The bowl was fabricated with a single aluminium block in order to reduce the number of parts involved in making the bowl as the

bowl would be subjected to vibration. The aluminium block had the provisions of screwing it to one face of the fixture plate, making it viable to be vibrated and attached to the vibrating bed of the shaker system. Figure 3.7 shows the chamber clamped in the shaker system. The workpieces can be fixed in either parallel or perpendicular to the direction of motion of vibrations as shown in the figure 3.7.

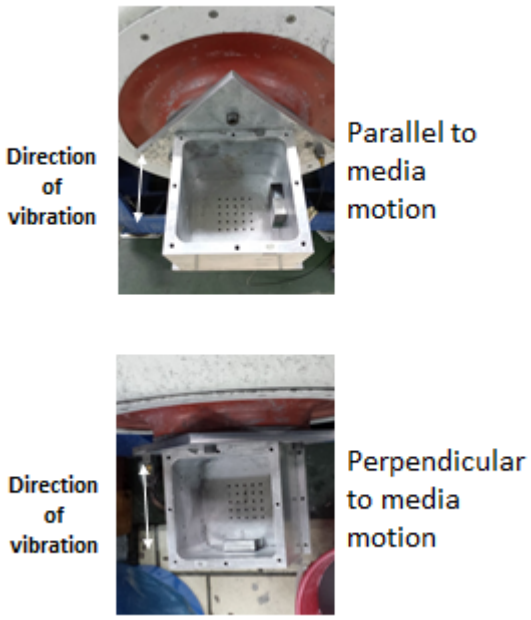

Figure 3.7: Chamber used with two clamping directions

3.7.3 Media and Compound

The same tristar media and trowal ARF compound were used for conducting these experiments.

3.7.4 Recording of Media Motion

The media motion is recorded using an high speed camera setup and an transparent acrylic chamber instead of the chamber described in the previous subsection.

3.8 Acoustic Emission Measurement

3.8.1 Sensor

Sensor is a device which consists of a transducer that converts any form of an input signal to an electrical signal that can be converted into digital form for storage and comparison. Acoustic Emission was selected as a parameter to measure in this thesis. PAC (Physical Acoustic Corporation) acoustic emission sensor was used for the measurement of acoustic emission. PAC ISWD Intrinsically safe differential sensor was used for the experiments described in this thesis.

Figure 3.8: PAC ISWD Acoustic Emission Sensor

ISWD (**I**ntrinsically **S**afe **W**ide-band **D**ifferential) is the ATEX (Appareils destinés à être utilisés en **AT**mosphères **EX**plosibles) certified Acoustic Emission (AE) sensor from Physical Acoustic Corporation (PAC) which can be used even in the most severe environments as the components are fully protected from any form of wear and tear. These sensors were selected as they can be used directly inside vibratory bowl in the presence of abrasive media with very minimal protection. But nevertheless, both the sensors were protected by a stainless steel chamber which is explained in the section 7.4.

3.8.2 Preamplifier

The electrical signals generated by the sensors are not sufficient enough to be input into the analog to digital converter. Hence it is amplified by a system called preamplifier. The preamplifier used for this thesis was PAC 2/4/6 preamplifier with 100KHz to 1200KHz bandpass filter which is shown in figure 3.9. This amplifier

comes with three settings of gain and a gain of 20dB was set for all the experiments performed.

Figure 3.9: PAC 2/4/6 Preamplifier

3.8.3 Data Acquisition System (DAQ)

As mentioned in the previous section, the signals which are preamplified are converted into the analog to digital converter which is also the data acquisition system (DAQ). PAC PCI-2 18 bit A/D converter was used. This DAQ was installed in a desktop PC and was used along with PACWin^{TM} software suite. Figure 3.10 shows the layout of the components used for the measurement of acoustic emission signals.

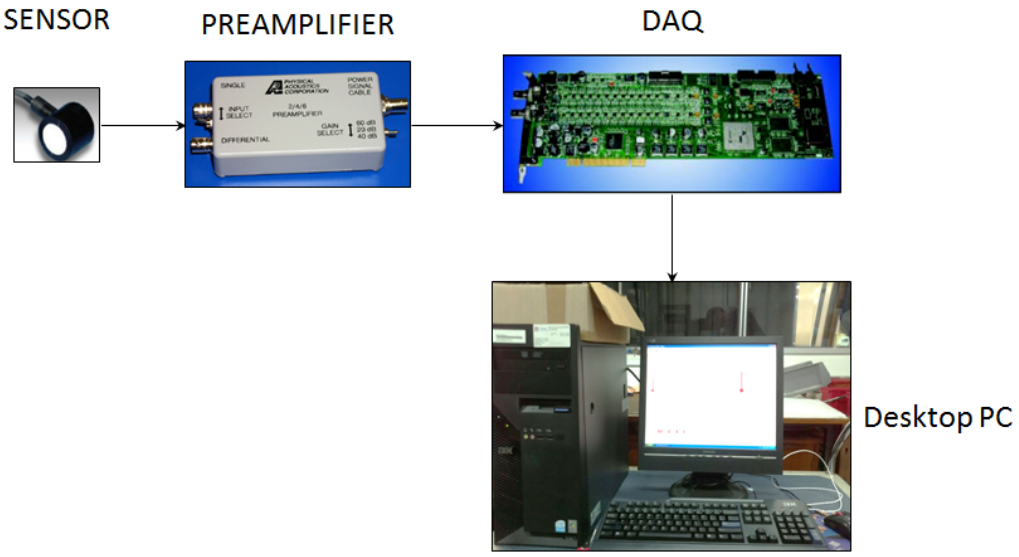

Figure 3.10: Layout of Acoustic Emission Measurement Setup

3.8.4 Couplant

The sensor is attached to the workpiece surface using a coupling medium or a couplant. The nature of couplant determines the effeciency of energy transferred from the workpiece to the sensor. There are many types of couplants available. Epoxy based adhesive is used as a couplant in this thesis. This was used as the adhesive which eliminates the requirement of a separate fixture for the sensor with the workpiece.

3.8.5 Anti-vibration Pad

The acoustic emission setup is connected to the vibratory finishing machine using a mechanical fixture fastened by screws and bolts. Hence they are susceptible to transferring the vibrations from the machine to the sensor. In order to mask or filter these vibrations, an anti-vibration pad manufactured by MISUMI of 3mm thickness have been used in the experiments.

3.9 Summary

Hence this chapter explains in detail the different materials and equipment used for conducting the experiments presented in this thesis. In addition to these equipment a lot of software tools like Matlab, Minitab, Microsoft Excel and Solidworks were used extensively for performing calculations, executing algorithms and designing the experiments and fixtures.

Thus the introductory part of the thesis ends here and the main contents starts from the next chapter which explains the newly developed methodology used to measure the surface modification mechanism.

Chapter 4

Masked Reference Method

This chapter explains the masked reference method used to study the surface modification mechanisms in vibratory finishing. This chapter first introduces the reader to the general overview of the surface modification mechanisms followed by the methodology, implementation and results.

4.1 Overview

The saturation phenomenon occurring in vibratory finishing is the central concept around which this thesis is written. The wear mechanisms cause the surface modification and hence the saturation is investigated in this part of the thesis. In order to find the individual wear mechanisms, it is essential to find the fundamental type of modification mechanism which modifies the surface. From a tribological point of view, there are only two types of modification mechanisms which can alter the surface:

- Material Removal (MR)
- Plastic Deformation (PD)

As explained in section 2.3, different types of wear mechanisms can result in either material removal (MR) or plastic deformation (PD) or combination of both. For example, ploughing type of wear mechanism results only in PD whereas, cutting

or chipping type of wear mechanism results in both PD and MR. As explained in section 2.4, even though grinding process has three types of wear mechanisms and many types of chips formed, the type of contact occurring between the abrasive and the work surface is only of a single type - two body abrasion. But in vibratory finishing, there are many types of contacts occurring at any point of time. The type of contact can vary depending on the processing conditions such as the type of media and compound used; the shape and material of the workpiece; the machining parameters such as the frequency and amplitude of vibrations; and finally the shape of vibratory bowl used. In addition to this, the continuous intermittent loading due to the vibrations can also cause fatigue or fretting type of wear in addition to the normal adhesive and abrasive type of wear. So it cannot be stated that a single wear mechanism results in the surface modification and hence the saturation. The objective of this part of the thesis is to understand the surface modification mechanism in vibratory finishing and its relationship with the surface characteristics. And this objective is also set based on the industrial need to optimize the vibratory finishing process with respect to achieving one of the modification mechanisms - MR and PD. The following section explains the methodologies available to differentiate the various types of wear mechanisms and surface modification mechanisms.

4.2 Identification of Mechanisms

The different types of modification mechanisms explained in section 2.3 can be identified by one of the following methods:

- Surface topography
- Wear debris (chips) analysis
- Physical measurement of surface properties

When there is a single type of contact occurring on the surface, evaluating the type of wear mechanism is straightforward; it can be ascertained from the surface

topography or the wear debris (chips) formed. The surface topography of the work surface can be used to reveal the type of wear mechanism by observing the surface features such as grooves, ridges, sheared layers which are formed due to different type of wear mechanisms as explained in table4.1. The type of wear debris (chips) such as curled tubular chips, platelets, spheres and striated ribbons can also be used to ascertain the type of surface modification and wear mechanism as explained in table4.1.

Table 4.1: Analysis of Surface topography [Roylance and Hunt (1999)]

Type of wear	Characteristics of worn surface	Wear Debris
Adhesive wear	Tearing and transfer of material	Large irregular particles>10μm
Two body abrasive wear	Presence of scores, grooves, scratches and sometimes embedded hard particles	Swarfs and material lumps
Three body abrasive wear	Less deeper scores, scratches and grooves	Smaller swarfs and material lumps
Fretting wear	Heavily pitted surface, presence of plastically sheared edges	Presence of rust due to oxidation and sometime spherical particles
Erosive wear	Surfaces unevenly worn with matt appearance	Very small particles difficult to measure
Corrosive wear	Signs of oxidation and chemical reactions	Debris in a completely new state usually amorphous

Measurement of sub-surface mechanical properties (like micro-hardness tests) can also reveal the modification mechanism. Micro-hardness tests will reveal the amount of plastic energy stored below the surface of the material. If there is an increased energy, as in case of work-hardened materials, it indicates the occurrence of plastic deformation mechanism as shown in figure 4.1 reported by Bhushan (2000). It shows the hardness distribution beneath the surface during a repeated rolling process. There is a definite increase in hardness at 130μm due to plastic

deformation occurring on the surface.

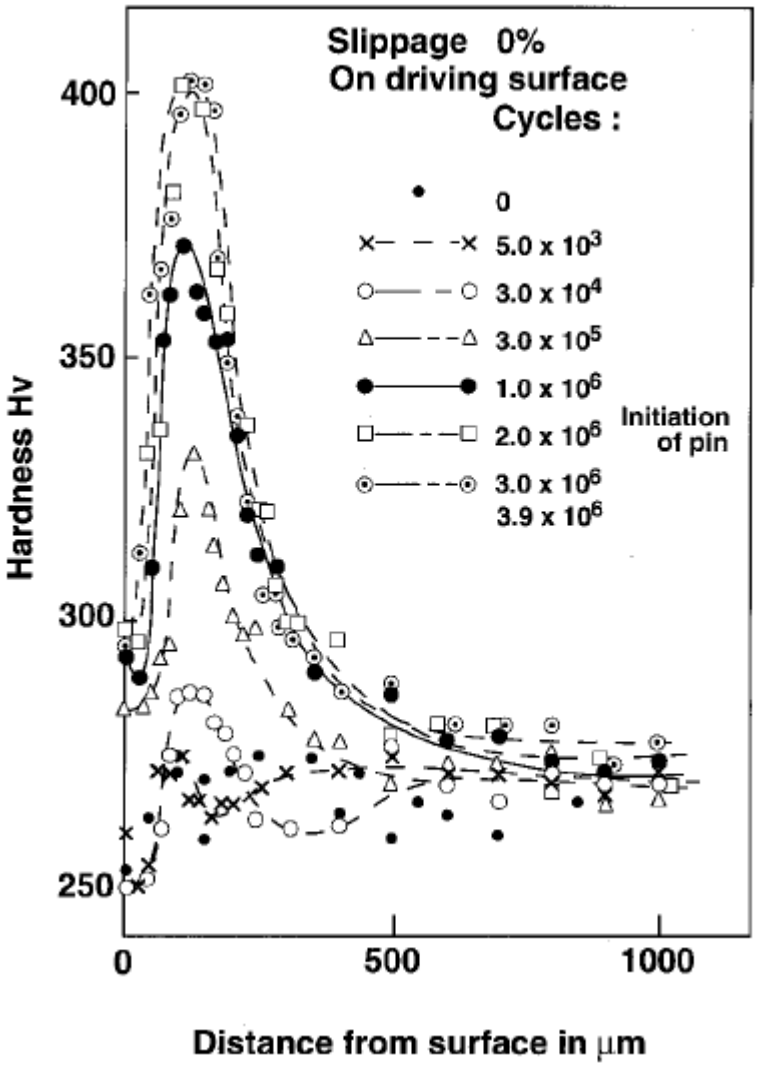

Figure 4.1: Occurrence of Plastic deformation mechanism in work-hardened materials (Hardness vs. Distance from surface) (Bhushan, 2000)

Any single surface modification mechanism can be determined from any of these methods, but in vibratory finishing the modification mechanism is complex involving more than one type of contact and hence more than one type of mechanism. Table 4.2 shows the different types of contacts occurring in vibratory finishing and possible modification mechanism which the contact can cause.

So a single measurement strategy is not sufficient and a novel methodology combining more than one method have to be developed. A detailed analysis of the methods was performed and the methods suitable for vibratory finishing were

Table 4.2: Types of contacts in vibratory finishing and possible mechanisms

Type of contact	Proof from Literature	Possible Mechanism
Impact [Wang et al. (2000)]	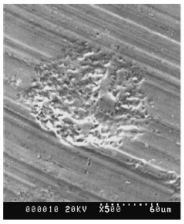	Both PD and MR
Scratching [Wang et al. (2000)]	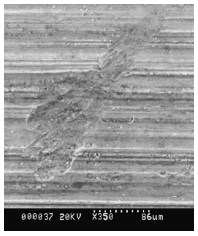	Both PD and MR
Rolling [Yabuki et al. (2002)]	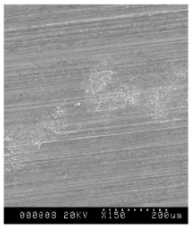	Only PD

selected based on this analysis. Table 4.3 shows the results of the analysis which precedes the description of the analysis.

Table 4.3: Evaluation methods suitable for vibratory finishing

Methodology	Suitability for vibratory finishing
Surface Topography	Suitable
Wear Debris Analysis	Suitable
Measurement of surface physical properties	Not Suitable
Subsurface Microstructure	Not Suitable

Surface topography and wear debris were selected based on the following criteria.

- No disturbance to the process is essential as a small change in process parameters will disturb the mechanism.
  - Surface topography can be measured at specific intervals without disturbing the process. Wear debris generated from the workpiece can also

be collected without disturbing the process.

  - Measurement of sub surface micro-structure requires the cutting of workpiece across its cross section, which requires the process to be stopped and new process to be started at every measurement interval.

- Can measure even a small change in surface. This is essential since the amount of surface deformation resulting from vibratory finishing is very small extending only upto a few micro meters from the surface.

  - The surface topography and wear debris analysis are very sensitive that even a small change in the surface will be reflected in the measurement results.
  - Measurement of surface properties requires the modification mechanism to affect the surface considerably

Hence a novel method combining surface topography and wear debris analysis have been developed. This involves the measurement of surface profile and the wear debris analysis. This chapter explains the methodology involving surface topography, the experiments performed and the results obtained. The wear debris analysis is explained in chapter 5.

4.3 Surface Topography Method

This method involves the analysis of surface topography by measuring the surface profile of the workpiece at different time intervals. There are many methods of measurement of the surface profile and there are numerous surface profile parameters which can be calculated from the measured surface profile. For this investigation, in order to study the saturation of surface in vibratory finishing, the most commonly used roughness parameter - Ra is used. As explained in section 1.3.4, vibratory finishing is evaluated by measuring the Ra of the surface polished by the process.

When the Ra reaches a particular value, the process is stopped and the components are removed from the process. In order to evaluate the surface modification mechanism which causes the change in Ra, an evaluation of the surface profile parameters was performed. From the evaluation, the height of the peaks and depths of the valleys were selected to measure the surface modification mechanism as explained in this section. It will introduce the reader to the methodology developed by depicting the change in height of peaks and valleys qualitatively.

The average height of the peaks and valleys are used to measure the surface modification mechanism as explained below. Assume that the initial surface profile has a set of peaks and valleys as shown in figure 4.3. The peaks and valleys shown in figure 4.3 is a representation of data points measured from the surface as shown in figure 4.2. The average of absolute value of all the points refer to the mean line which is calculated using the formula presented in equation 4.1.

$$h_{mean} = \frac{h_1 + h_2 + h_3 + h_4 + ... + h_n}{n} \tag{4.1}$$

The points which lie above the mean line (h_{mean}) are peaks (points 1 and 2) and those which are below the mean line (h_{mean}) are valleys (points 3 and 4) as shown in figure 4.2.

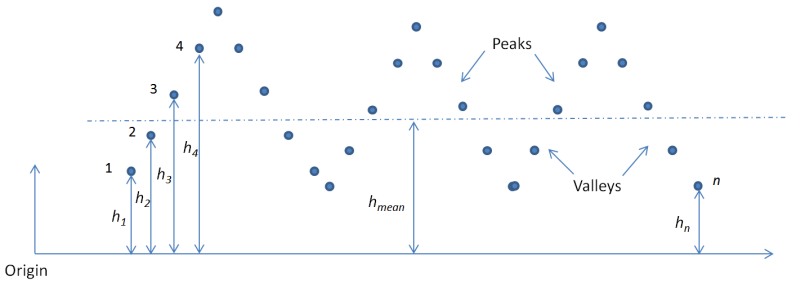

Figure 4.2: Calculation of Peaks and Valleys

The average value of absolute values of points lying above this mean line is represented as average peak height and the average value of points lying below the mean line is represented as average valley height as shown in equation 4.2 and 4.3.

$$h_{peak} = \frac{h_1 + h_2 + ... + h_{n_{peaks}}}{n_{peaks}} \tag{4.2}$$

$$h_{valley} = \frac{h_1 + h_2 + ... + h_{n_{valleys}}}{n_{valleys}} \tag{4.3}$$

Since the reference point for the mean line and the heights are same, the difference in height between the mean line and the average peak (or valley) heights can be represented as the new average peak (and valley) heights as shown in figure 4.3 and represented in equations 4.4 and 4.5.

$$h_{peak} = h_{peak} - h_{mean} \tag{4.4}$$

$$h_{valley} = h_{mean} - h_{valley} \tag{4.5}$$

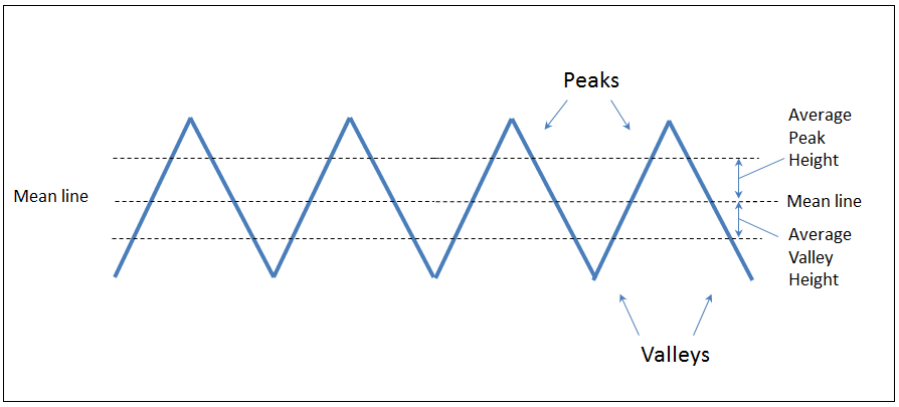

Figure 4.3: Initial Surface Profile showing Peaks and Valleys

The two surface modification mechanisms can be tested by the following methodology, when the modified surface is compared with the initial profile. As shown in figure 4.4, consider the first half of the profile to be the initial profile and the second half of the profile to be the modified profile. The two types of surface modification mechanism can be explained as follows.

- Pure Material Removal: When there is pure material removal (like brittle fracture of peaks) the surface will be modified as shown in figure 4.4. The

peaks are knocked off and the valleys remain unaltered. This causes the peak height to decrease when compared to the original peak height and the valley height to increase when compared to the original valley height.

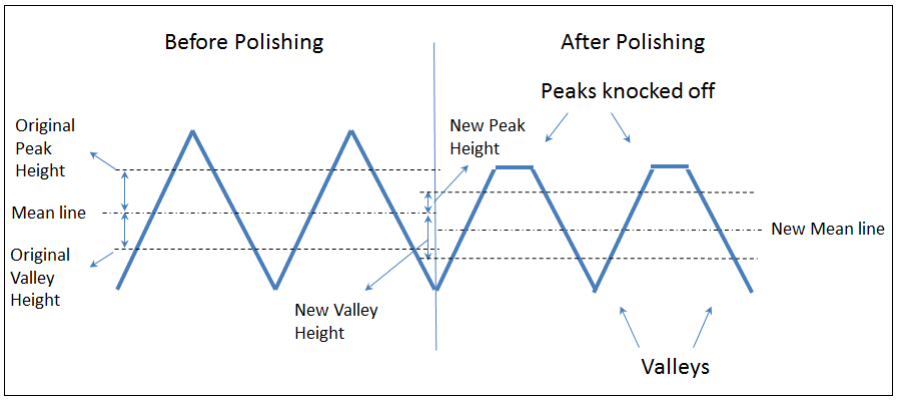

Figure 4.4: Pure Material Removal before and after Polishing

- Plastic Deformation: But when there is a plastic deformation involved, the surface will be modified as shown in figure 4.5. This is assuming that the material does not flow in a direction perpendicular to the view and the peaks broadens and fills the gaps i.e the valleys. Hence both the peaks and valleys will be modified. The average peak height will decrease and the average valley height will also decrease as shown in figure 4.5.

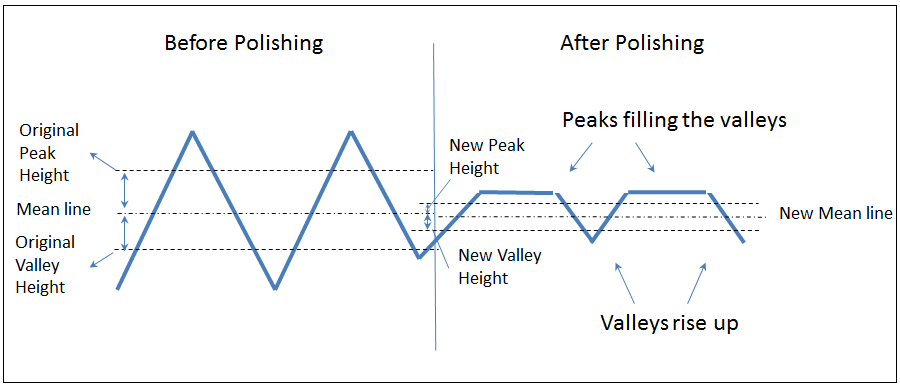

Figure 4.5: Plastic Deformation before and after Polishing

The above analogy can be summarized as follows.

The above analogy can be applied only if the following conditions are satisfied.

Table 4.4: Analogy used for surface modification mechanism

Observation	Reason	Surface Modification Mechanism
Peak height increase	Not possible	Not Possible
Peak height decrease	Peaks being removed	Plastic deformation or Material Removal
Valley height increase	Deeper valleys are formed	Pure Material Removal
Valley height decrease	Valleys are being filled	Pure Plastic Deformation

1. The profile peaks and valleys are uniform throughout the surface: Since the surface modification mechanism depends on the shape and size of the surface peaks and valleys, if the peaks and valleys are not uniform throughout the surface, different mechanisms can be obtained at different points of the surface.

2. The mean line of the original profile is retained. In order to measure the change in peak and valley height, the original mean line must be retained. Without this, the change in peaks and valleys cannot be measured.

The above two conditions are usually not satisfied in a normal component finished by vibratory finishing, as the component usually does not have uniform peaks and valleys. Secondly the surface is completely modified when subjected to this process. There is no trace of original profile when the subsequent traces are performed on the modified surface. Hence to implement the above methodology, a new measurement technique was developed which is explained in the next section.

4.4 Implementation of Methodology

In order to satisfy the first condition - uniform peaks and valleys throughout the surface, the surface is precision milled with a single fly cutting tool. Uniform peaks and valleys are formed on the workpiece as shown in figure 4.6. In addition to this, in order to maintain the original mean line - the second condition, a part of the surface is masked from the finishing action using a masking tape as shown in figure 4.6. This masked region is used each time to calculate the mean line of the original surface, from which the height of the peaks and valleys of the modified surface is calculated.

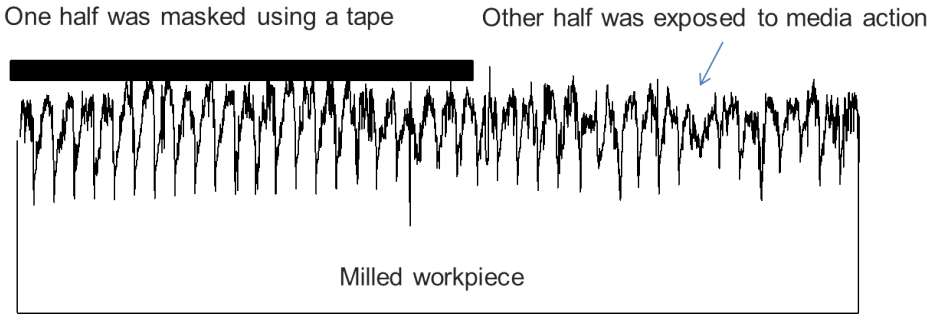

Figure 4.6: Uniform peaks and valleys formed on milled workpiece

4.4.1 Algorithm used

The following section explains in detail the algorithm used to calculate the height of the peaks and valleys and how they are measured with respect to the mean of the masked area. Since this type of measurement was not a standard procedure, the height of the peaks and depth of the valleys were calculated from raw data measured from the profilometer using a custom MATLAB program. The challenge in implementing the methodology was identifying the peaks and valleys since the surface was changing constantly. An adaptive algorithm was used in identifying the peaks and valleys and calculating the difference from the masked reference line. The steps involved are explained as follows.

Step-1: Calculate the mean of **first half** of profile (masked in the experiments) which will act as the height of **masked reference line**

Step-2: Calculate the mean of **second half** of profile which will act as the height of **analysis reference line**

Step-3: Store values **above analysis** reference line as **peaks**

Step-4: Store values **below analysis** reference line as **valleys**

Step-5: Calculate the difference between **masked** reference line and **peaks** and store as peak height; calculate the **average peak height**

Step-6: Calculate the difference between the **masked** reference line and **valleys** and store as valley depth; calculate the **average valley depth**

The surface profile was measured at 5 different points of the surface and the change in peak height and valley height was calculated for every 20 minutes of vibratory finishing. The results obtained are explained after considering the limitations of this measurement technique.

4.4.2 Limitations of this Method

Like any other measurement technique, this measurement technique is also prone to errors. By analyzing the errors and taking them into account during the interpretation of the results, we can make sure that no data is lost or misinterpreted. This section will analyze the possible errors and the limitations of this measurement technique as follows.

As explained in the previous section, by performing precision milling of the surface, uniformly sized peaks and valleys can be fabricated. But there is a tolerance limitation for any type of machining process. Hence our results will depend on the tolerance which can be achieved by the machining process. By using the masked reference method, this problem is eliminated. Since each time the masked reference line is measured, the change in dimensions due to tolerance error will be taken into account each time. Hence the change in dimension of the surface due to waviness, tolerance error will be eliminated by using masked reference method.

As the peaks and valleys are calculated based on the new mean line which varies with respect to time, there is a possibility of some points being misinterpreted. For example, when both the peak and valley positions move together towards the original mean line, the new mean line will go down, but the new valley position might not change. This means that there is a plastic deformation happening, but not reflected in the calculation. This is illustrated in the figure 4.7.

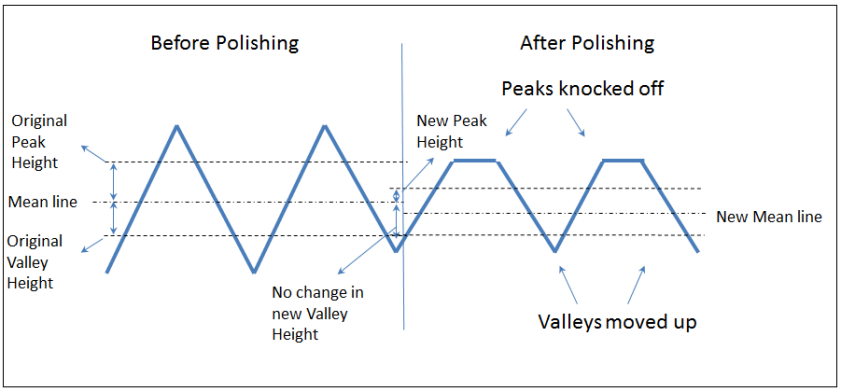

Figure 4.7: Limitations of Masked Reference Method

This is a major limitation of this method. But this does not happen in large deformations as explained previously in figure 4.5. Hence a small change or no change in valley position calculated using this method cannot be treated as a sign of change in surface modification mechanism. Hence the results should be interpreted considering the change in peak and valley position in a general trend and the small changes (<10% change) should not be considered. The limitations and how they are handled are summarized in table 4.5.

This section ends the description of the developed method. A new method is developed based on the literature review and the requirements for current research problem. The method is analyzed in detail - its limitations are identified and possible solutions are also obtained. The next section explains the experimental setup used to conduct experiments to measure the surface modification mechanism using the above method and the following sections present the results obtained from the experiments.

Table 4.5: Limitations and Solutions

Limitations	Solution
The tolerance of the machining affects the calculations	By measuring the masked reference each time, the change in dimension due to tolerance is also taken into account
Small change in peaks and valleys will not be reflected in the calculation	By considering only the overall trend and not the small changes (less than 10% change)

4.5 Experimental Conditions

Structured surface analysis was used to identify the surface modification mechanism in vibratory finishing. The machine used was a typical industrial vibratory finishing machine as shown in figure 4.8a, with three vibratory motors to achieve strong vibratory motions. The frequency and amplitude of vibrations were measured as 50Hz and 2mm respectively. A ceramic abrasive tristar abrasive media of size 10mm x 10mm x 20mm (figure 4.8b) and a detergent based compound were used.

(a) Industrial vibratory finishing machine

(b) Ceramic Tristar Abrasive Media

Figure 4.8: Experimental Conditions Used

The material selected for analysis was Grade 5 Titanium Alloy Ti-6Al-4V, a typical alloy which is used in aerospace applications. Rectangular workpieces of length 20mm, breadth 20mm and 15mm thickness was used.

The surfaces of workpieces were machined using a single-fly cutter in a CNC milling machine to generate uniform structured surfaces of about $10\mu m$ height and $150\mu m$ spacing as shown in the actual trace obtained from the surface profilometer shown in figure 4.9.

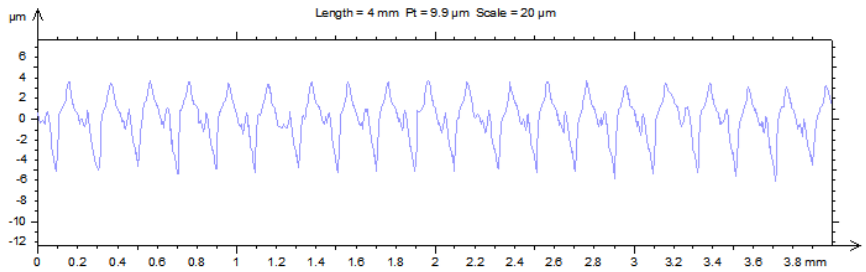

Figure 4.9: Profile of structured surface milled using single-fly cutter

In addition to these, one half of the workpiece was covered with a masking tape as explained in section 3.4 to conduct masked reference analysis explained in the previous section. These surfaces were suitable for measurement using surface profilometer. Hence a Taylor Hobson Formtracer was used to measure the surface profiles. The workpiece was taken out every 20 minutes for the measurement of surface profile and SEM (scanning electron microscope) analysis after a thorough cleaning with chemical solvent - Acetone, so that no debris accumulation is present on the surface. This is also confirmed from the SEM pictures obtained which shows no signs of debris accumulation on the surface.

4.6 Results and Discussion

Experiments were conducted in Ti-6Al-4V titanium alloy to measure the surface modification mechanism. This section presents the results obtained from Ti-6Al-4V alloy.

4.6.1 Surface Profile Results

Figure 4.10 shows the variation of difference calculated between peak height and masked reference along with valley height and masked reference line. The peaks are

higher compared to the masked reference line and hence they are positive, whereas the valley height is less than the masked reference line giving negative difference values. As the time progresses, both peaks-masked reference and valley-masked reference difference decreases gradually approaching zero. This indicates that the analysis surface slowly reaches and tend to move towards the center as its reaches saturation.

For example, when the peak height reduces from 1.9 µm from initial level to 1.1 µm at 20 minutes, it means that the peak difference between the average peak line and mean reference line reduces by 0.8 µm and hence there is a reduction of peaks. Whereas, the valley height is increasing from -1.5µm to -1.3µm. This represents that there is an increase of 0.2µm height in valley height with reference to the mean reference line.

As explained in the limitations, a change in peaks and valleys less than 10% cannot be interpreted as the indicators for surface modification mechanism. But the general trend of peak height difference and valley height difference with respect to the original mean line (masked reference line) is taken into consideration along with the analogy explained in table 4.4. The peak height decrease (due to peaks going down) can be due to either plastic deformation or material removal, but the valley height decrease (due to valleys moving up) is due to only plastic deformation.

It is evident from the Figure 4.10 that there is a change in peak height and valley height behavior at 60 minutes. The rate of change of peak height decreases for the first 60 minutes is higher compared to the next 40 minutes. The reverse is observed for the valley height, the rate of change of valley height for the first 60 minutes is lower than the next 40 minutes.

Since the overall valley height trend directly represents the plastic deformation, it can be interpreted that at the initial 60 minutes there is less plastic deformation which increases after that time. This can be attributed to the fact that initially the peaks are sharp and favors brittle fracture and material removal. When the peaks gets shortened and smaller, their strength increases which cause the material

removal to decrease, resulting in the plastic deformation of the weak portions of the structured surface which are the edges. This hypothesis is made only based on the behavior of peaks and valleys. In order to test this, the surfaces were also analyzed under SEM (scanning electron microscope) which is explained in the next section.

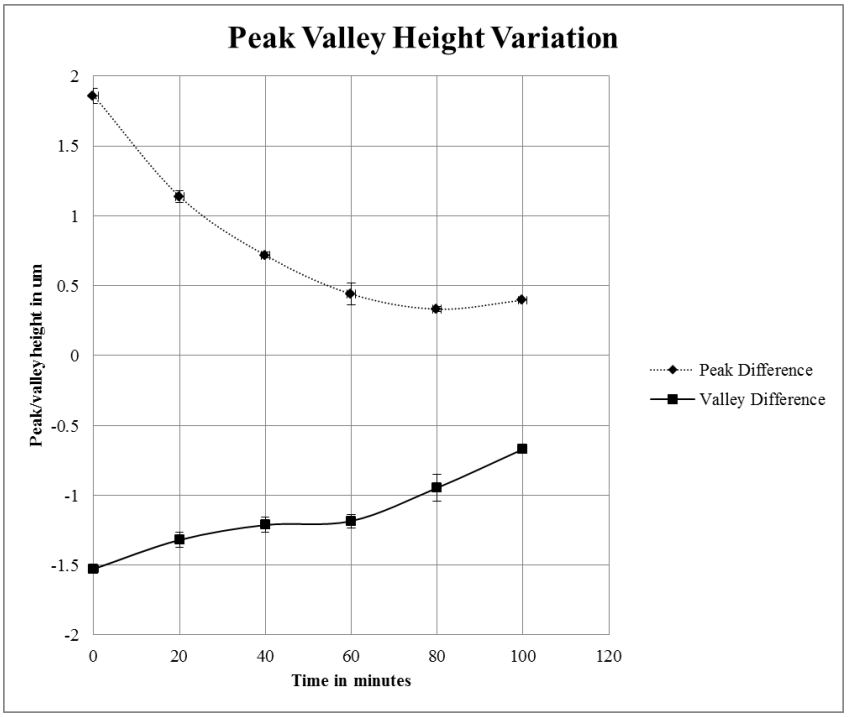

Figure 4.10: Peak and Valley height variation with time for Ti-6Al-4V

4.6.2 SEM Analysis of surfaces

This section explains the SEM analysis of surfaces which were analyzed using the masked reference method in the previous section. Figure 4.11 shows the surface morphology of initial surface before finishing and after 20 minutes of finishing. It can be noted that the patches of surfaces have been modified by the finishing process, leaving behind traces of unchanged surfaces. The presence of scratches indicates that the type of wear mechanism is abrasive wear. These patches indicate the peak region of the milled surface. The peaks are modified initially, leaving the valley unaltered. This is also reflected in the peak and valley height change as shown in figure 4.10 for 20 minutes time interval. The presence of scratches on

the surface indicates that there is an abrasive wear mechanism happening which contributes towards the material removal.

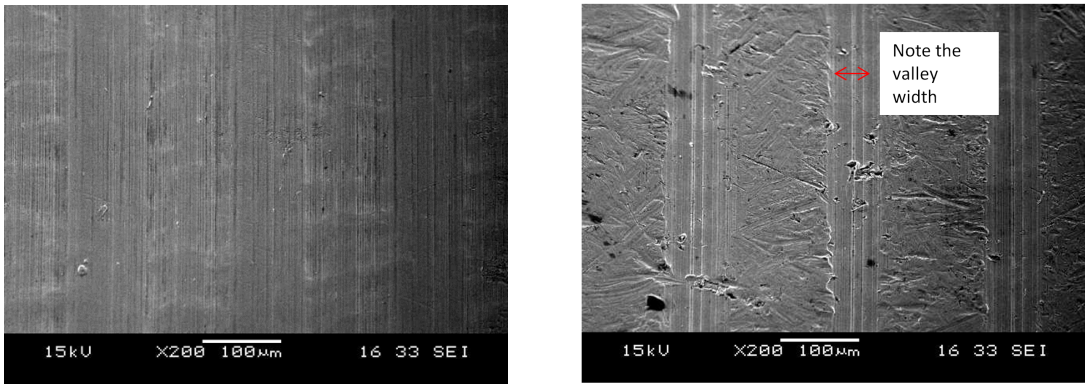

(a) Initial surface before finishing (b) Surface after 20 mins of finishing

Figure 4.11: SEM images of surface formed

Figure 4.12 shows the SEM pictures of surfaces formed after 40 minutes and 60 minutes. It can be noted that after 40 minutes, the valleys start getting affected by the media action. This behavior is similar to that of fretting wear as shown in figure 2.35. At this stage, due to a number of repeated contacts, fretting wear occurs. There are also presence of scratch marks on the surface, indicating the scratching behavior which causes more material removal than plastic deformation. After 60 minutes, it can be noted that the width of the valleys slowly reduces. If this change in surface morphology is due to material removal, the depth of the valleys will increase. However, measurement of surface profile shows that the valley depth decreases, indicating that the peaks are being plastically deformed and pushed into the valleys.

After 80 minutes, it can be noted that the valleys are almost deformed, and after 100 minutes there is no clear separation between peaks and valleys. Also there are more number of plastically deformed edges indicating an increase in plastic deformation. This change in mechanism results in saturation of surface roughness which is explained in the next section.

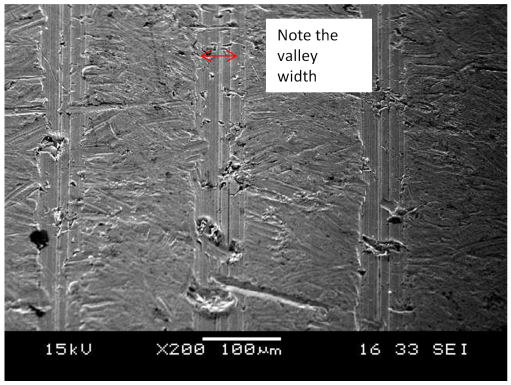

(a) After 40 mins

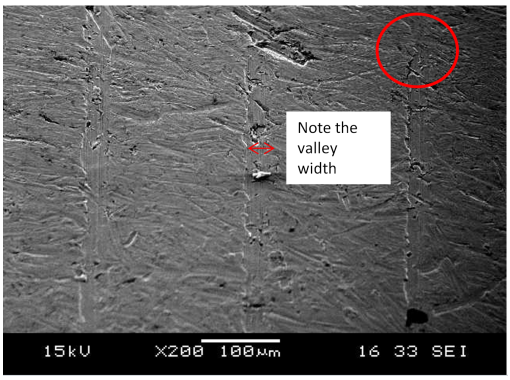

(b) After 60 mins

Figure 4.12: SEM images of surfaces formed after polishing

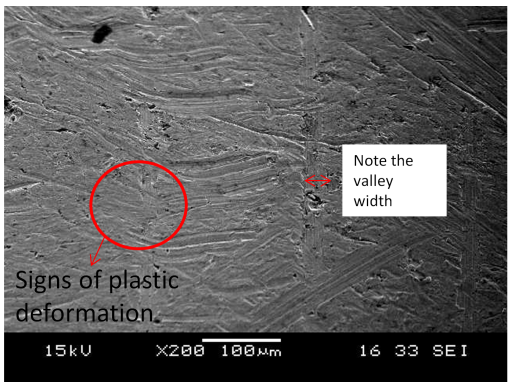

(a) After 80 mins

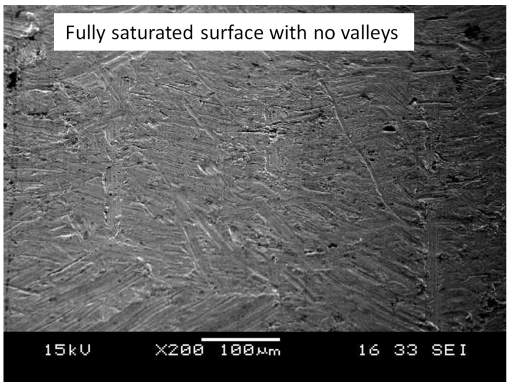

(b) After 100 mins

Figure 4.13: SEM images of surfaces formed

4.6.3 Comparison with surface evolution

The surface roughness is represented by the roughness parameter, Ra which is the average value of peaks and heights with respect to the mean reference line. Ra is the evaluation parameter used to check the process. The process is stopped after the roughness reaches the required value. It can be seen from figure 4.14, that as the process progresses the roughness value decreases constantly and reaches a minimum value after 100 minutes of processing. Figure 4.15 shows the percentage change of Ra between time intervals. It can be noted that during the initial phase of the process, the percentage change of Ra is less and after 60 minutes it reaches a maximum and starts reducing afterward. This can be related to the surface modification mechanism as explained in the previous sections. Figure 4.16 shows the rate of change of valley height between various time intervals. It can be assumed

that, when the valley height decreases, plastic deformation occurs. Hence the rate of change of valley height is assumed to be the amount of plastic deformation. As shown in figure 4.16, when there is less plastic deformation, the change in Ra is less (20 and 40 mins). But when plastic deformation increases, the Ra value starts decreasing rapidly (80 mins) reaching a minimum value. This was the same mechanism which was reported in the SEM pictures as well. Hence it is evident that the surface modification mechanism plays a major role in the rate of change of surface roughness which is obtained. This information can be used to optimize the process further, so that a particular mechanism can be achieved to obtain better surface roughness.

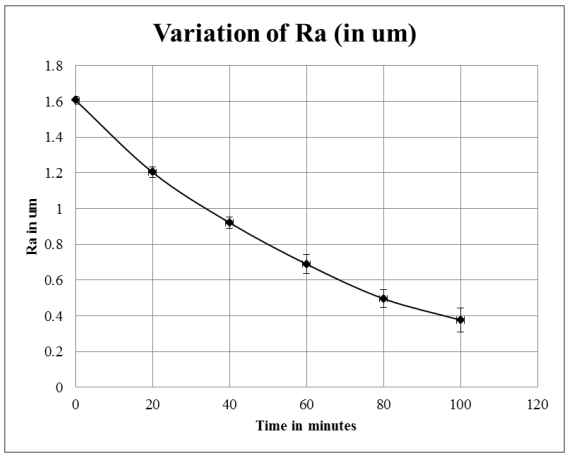

Figure 4.14: Variation of Ra Variation of Ra with time

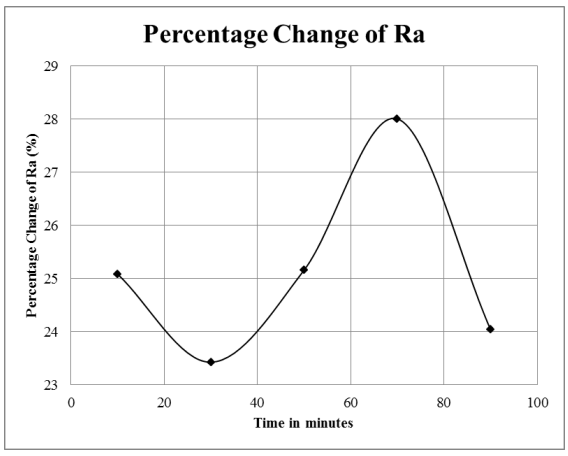

Figure 4.15: Percentage change of Ra with time

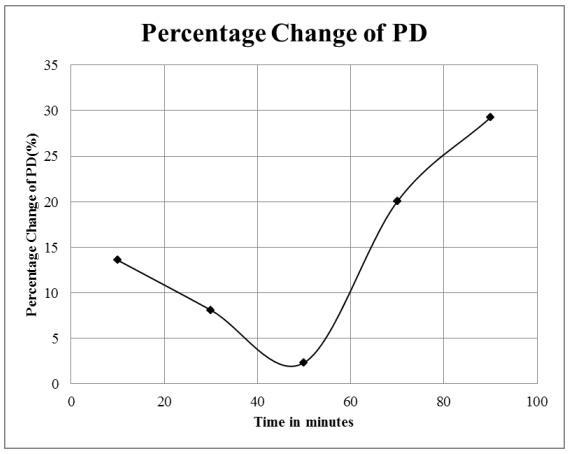

Figure 4.16: Percentage change of Valley Height wih time representing Plastic Deformation

4.7 Saturation Study

Hence the developed methodology has been used to measure the surface modification mechanism which results in change in surface roughness of the parts in vibratory finishing and the method was validated using SEM pictures of the surface. Further experiments were conducted to study the behavior of this surface modification mechanism during the saturation of surface roughness explained earlier in section 1.3.4. The results of the previous experiments show no saturation of the surface. Hence experiments were repeated with the same conditions, but this time until reaching a saturated surface roughness only for Ti-6Al-4V titanium alloys. The previous experiments were conducted to validate the developed methodology. The experiment in this section will be used to analyze the saturation occurring in vibratory finishing process using the validated methodology.

Figure 4.17 and 4.18 shows the variation of Ra with respect to time and the percentage change of Ra with respect to time respectively. It can be seen that as the surface reaches the saturation level, the percentage change of Ra increases initially as seen in figure 4.16 and gradually reduces and reaches zero.

Comparing this with the previous results (figure 4.15), it is clear that even though the initial condition and the process parameters are constant, the rate of change of Ra varies. This can be attributed to the stochastic nature of the process. Ev-

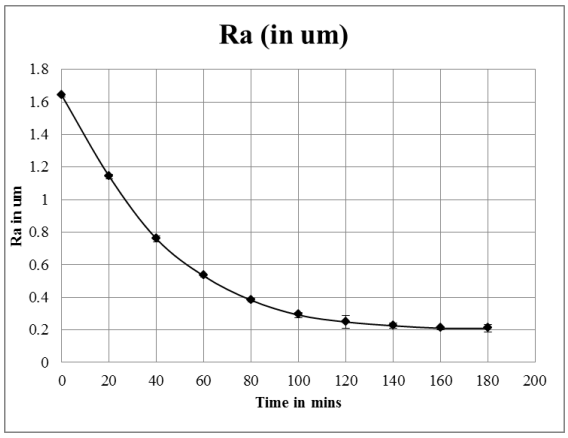

Figure 4.17: Saturation Study - Variation of Ra with time

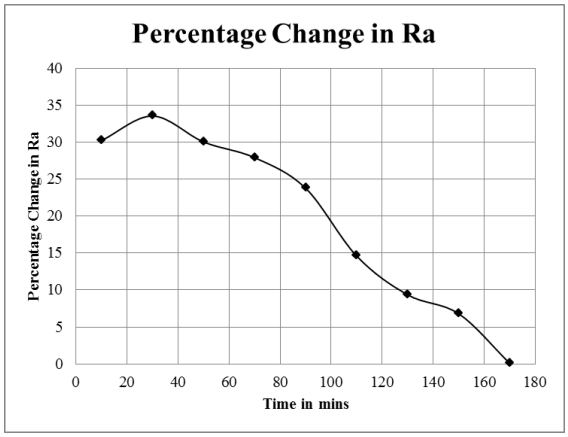

Figure 4.18: Saturation Study - Percentage change of Ra with time

ery time the surface is polished, many types of contacts occur, which cannot be controlled. Hence the surface modification mechanism may not be constant every time. But the overall trend of the mechanism should be the same. This hypothesis was proved by repeating the same experiment more than few times. Every time the behavior of the peaks and valleys followed the same trend as shown in figure 4.19.

The peak and valley height values initially decreased sharply and saturated after the surface roughness reached a saturation level as shown in figures 4.19 and4.17. This trend is also observed in the rate of change of valley height (i.e. plastic deformation) as shown in figure 4.20. This rate of plastic deformation was compared with the rate of change of surface roughness. It was observed that they followed the same trend. The rate of plastic deformation and rate of change of surface roughness (Ra) were compared with the correlation formula explained in equation 4.6.

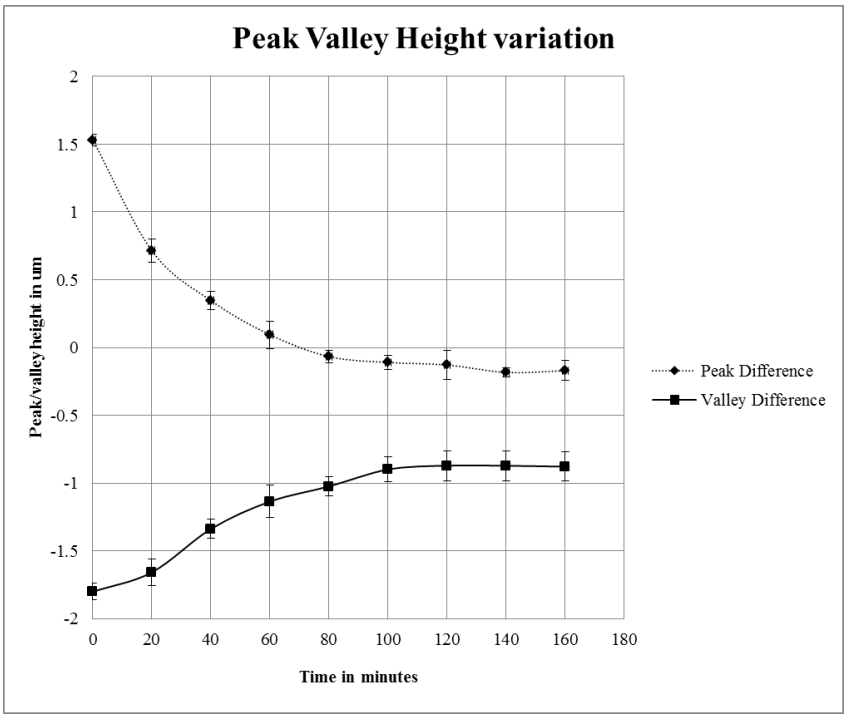

Figure 4.19: Variation of Peak & Valley Height with time

$$Corr = \frac{\sum(x-\bar{x})(y-\bar{y})}{\sqrt{\sum(x-\bar{x})^2(y-\bar{y})^2}} \tag{4.6}$$

where x is the value of the variable 1, y is the value of variable 2, $\bar{x}$ is the average value of the variable 1 and $\bar{y}$ is the average value of variable 2. It was found that the correlation coefficient between the rate of change of Ra and the amount of plastic deformation was 0.94.

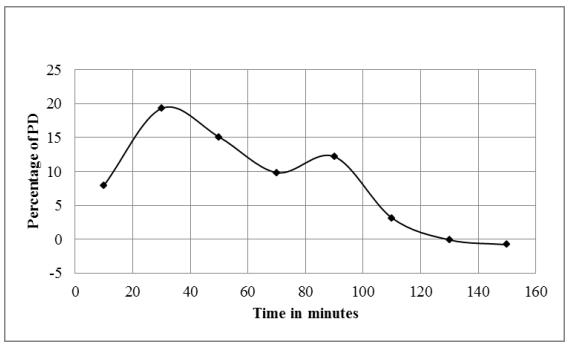

Figure 4.20: Variation of Percentage Change of Valley Height with time representing PD

4.8 Summary

Hence the surface modification mechanism which resulted in the saturation of surface in vibratory finishing process is determined by using the newly developed surface topography method. This method was developed after a detailed review and analysis of all the methods available from the literature and also considering the conditions suitable for vibratory finishing and for industrial application. The amount of plastic deformation and material removal calculated from the newly developed technique correlates well with that of the SEM pictures obtained. Hence this method was used to find the surface modification mechanism during saturation. The results obtained indicated a presence of correlation between the amount of plastic deformation evaluated by this method and the rate of change of Ra.

This newly developed method will be used to find the surface modification mechanisms in various other processing conditions which are explained in different parts of this thesis. The next chapter will explain the method of wear debris analysis used for identifying the surface modification mechanism.

Chapter 5

Wear Debris Analysis

This chapter explains in detail the wear debris analysis work conducted to analyze the surface modification mechanism in vibratory finishing. This chapter starts with a general overview of the wear debris analysis, followed by the methodology used, its implementation in the experiments and concludes with the results obtained.

5.1 Overview

The debris particles generated by the wear mechanism is termed as wear debris. The analysis of wear debris is another method of identification of the surface modification mechanism. Different types of wear mechanisms result in different types of wear debris. The wear debris particles are generated by vibratory finishing process due to the action of media on the workpiece surface. Both media and workpiece surface wears and will result in considerable wear debris. When the wear debris particles generated by the work surface is analyzed, the type of wear mechanism, amount of surface modification can be obtained.

In addition to this, wear debris particles generated by vibratory finishing have not been studied previously by any of the researchers. So an attempt to understand the type of wear debris particles generated by vibratory finishing has been made in this thesis, so that the surface modification mechanism of this process can be better understood. In addition to this, the relationship between the wear debris

particles and surface roughness is also studied. The findings are presented in the following sections.

5.2 Methodology

Wear debris analysis is carried out in three stages:

1. Sampling
2. Analysis
3. Reporting

The wear debris particles have to be first identified and collected properly in order to analyze them. So the first step in the process is to identify and sample the wear debris particles. As discussed in section 2.5, there are many methods of wear debris identification and collection. A detailed analysis was performed on the methods available and their suitability for analyzing the wear debris particles generated by vibratory finishing process which is explained in the following section.

5.2.1 Sampling

There are four components of vibratory finishing - part, machine, compound and media. The finishing action on the part is due to the action of media excited by the machine and compound is used to aid the process. There are two major sources of wear debris particles in vibratory finishing,

1. Media
2. Part

The media particles are usually bonded abrasives with ceramic or a synthetic binder bonded with abrasive grits. When these media particles contact each other under considerable force due to the vibratory action of the bowl, a large amount of wear

particles are generated. The amount of wear debris generated by the media is very high compared to the other wear debris particles generated in this process.

Since the material is being removed from the part, a small amount of wear debris particles is generated from the material as well. In addition to this, there may be other minor sources of wear debris such as the fixture and screws used inside the bowl and also the polyurethane lining from the wall of the bowl.

The wear debris which is of interest to characterize the surface modification mechanism of the work surface is the wear debris generated from the work surface. Since the amount of wear debris generated by the part is very less compared to the wear debris from the media, selecting a proper foolproof collection method will be a challenging process. Table 5.1 shows the list of wear debris methods as explained in the literature review. They are analyzed based on their suitability for the specific application and the results are shown in the same table (Table 5.1). As shown in table 5.1, all methods except for the analytical ferrography or magnetic seperation method will remove the characteristics of the debris particles such as shape, size, texture etc. which are essential to ascertain the surface modification mechanism. Hence the analytical ferrography or magnetic separation method is used to detect the wear debris particles in this thesis. The basic requirement for this method is that the wear debris particles must be magnetic. Hence a 2025 duplex stainless steel workpiece is used. The mechanism obtained by this steel workpiece will not be the same as obtained by Ti6Al4V and T6061-Al Alloy workpieces, but an understanding of wear debris particles generated by the vibratory finishing process can be obtained from these results. After collection, the next step is analysis which is the core of this part of this thesis. This is explained in the following section.

5.2.2 Analysis

Analysis of wear debris particles can be performed using a normal optical microscope or Scanning Electron Microscope (described in section 3.6.1) depending on the resolution of the measurement required. Even though the wear debris particles

Table 5.1: Wear Debris Collection Methods [Fitch (2013)]

Collection Method	Analysis Type	Results available	Suitability for Vibratory Finishing
Spectrometric Analysis	High heat vaporization of metals	Parts per million of elements	Not suitable, as the high heat causes the change in texture and form the particles
Particle Counting	Laser light scatter or pore blockage	Number and size of particles	Not suitable, as it will not give information about the texture and form
Direct image particle counting	Shadow casting from laser	Number and size of particles	Not suitable, same as above
Ferrous density analysis	Magnetic flux	Number and size of particles	Not suitable, same as above
Analytical ferrography or Magnetic Separation	Microscopic analysis	Size, shape, texture, color, orientation, chemical composition	Suitable

generated from the work surface are separated by magnetic separation method, there will be a considerable amount of wear debris particles from the media and other sources present in the collected sample. In order to differentiate between the two, the EDX analysis tool (described in section 3.6.1) available in SEM is used. EDX is used to find the chemical composition of each wear debris particle and this composition is used to differentiate between the two types of wear debris particles. Hence from hundreds of particles obtained using the magnetic separation, the wear debris particles of interest are differentiated and analyzed using SEM and EDX manually. The subsequent section on the implementation, explains clearly how this process is carried out.

5.2.3 Reporting

After the wear debris particles are collected by magnetic separation and analyzed using SEM, the size and shape of the particles are measured from the SEM pictures. This operation is performed manually by observing the scale obtained in the SEM pictures and comparing the size of the particle with the scale. This is explained clearly in the implementation section. Hence a manual method of reporting is performed for the reporting of size and shape of the wear debris particles.

5.3 Implementation

This section will explain how the methodology developed from the literature for sampling, analysis and reporting of wear debris particles is implemented in the experimental conditions. This section will explain in detail how the materials and fixtures presented in chapter 3 are used to implement the methodology explained in the previous section.

The wear debris analysis was performed in a step-by-step procedure every time so that the results are repeatable as explained below. The first six steps are performed online - during the process. The next four steps are performed after the process in an analysis laboratory. So the steps are divided into two parts - online and offline.

5.3.1 Online Part of Analysis

These steps are performed during the process except for the first step which is a sample preparation. The rest of the steps are repeated for every wear debris experiment.

Step 1: Fabrication of Steel Workpiece

The first step involved the fabrication of a structured surface similar to the ones used in the previous chapter on a duplex stainless steel workpiece of size 50mm x 50mm x 10mm (*lxbxh*). A standard milling cutter was used to fabricate the uniform

peaks and valleys as shown in figure 5.1

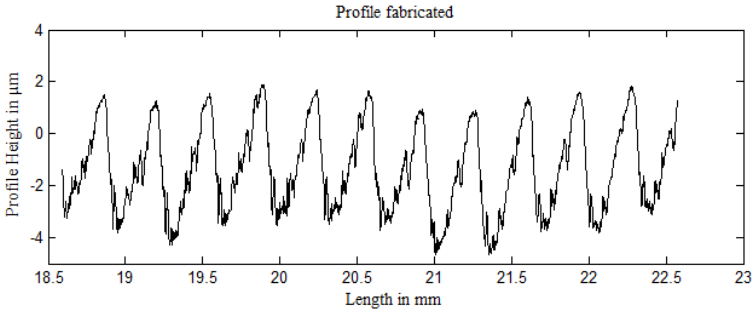

Figure 5.1: Profile fabricated for wear debris analysis

Step 2: Fix the workpiece in AV75 Bowl

The fabricated workpiece is fixed either in a small chamber attached to the AV75 bowl or directly inside the bowl using the fixture as shown in figure 5.2. When a workpiece is fixed with respect to media motion, there are more number of contacts between the workpiece and the media. Also, the energy imparted by the media particles on the workpiece surface is much higher when compared to freely moving workpiece. This creates a more aggressive polishing and surface modification mechanism on the workpiece surface.

The workpiece which is freely moving along with the media experiences a relatively lower energy contacts from the media motion, thus resulting in a less aggressive polishing and surface modification.

In addition to the above, polishing of the fixed workpiece depends on the direction of orientation of the surface with respect to the media motion. Surfaces which are fixture parallel to the media motion are more polished and has a finer surface roughness than those fixture perpendicular to the media motion. This has been explained in detail in section 6.2.1.

Step 3: Swipe the wear debris from workpiece surface

The wear debris particles are collected directly from the workpiece surface by swiping the surface physically with a glove. This method was chosen based on trial and error. Initially the entire debris particles were collected by washing the media

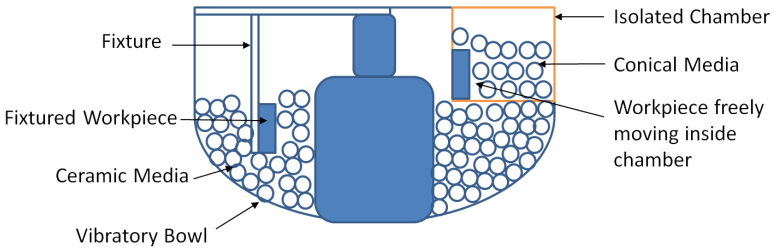

Figure 5.2: Schematic of Fixture Setup for Wear Debris Analysis

with water and locating the debris from the collected water. But the presence of wear debris particles from the workpiece was very less. This was due to the presence of more media debris than part debris. It was later found that the debris particles directly sticking to the workpiece had more part debris and hence this swiping method was adopted. This is shown in figure 5.3.

Figure 5.3: Step 3 - Collection of wear debris particles

Step 4: Use a magnet to attract the magnetic wear debris particles

In addition to this, to eliminate the media debris particles from the collected debris, a magnet was used to attract the magnetic part debris particles as shown in figure 5.4. This method significantly reduced the number of non part debris particles from entering the analysis part of the process.

Step 5: Transfer the particles collected to a carbon tape

This step was important to transfer and store the collected wear debris particles

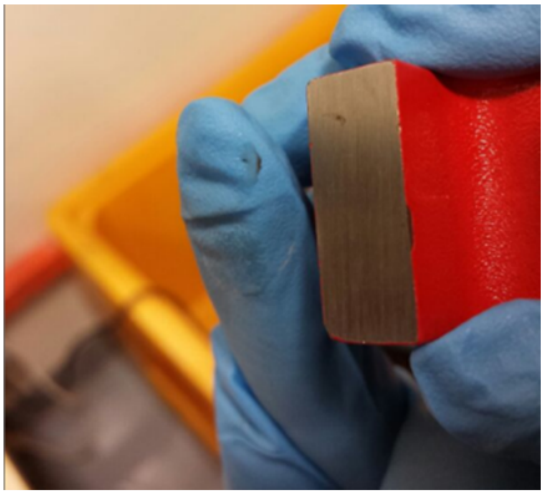

Figure 5.4: Step 4 - Magnetic Separation of wear debris particles

for further SEM and EDX analysis from which its physical and chemical characteristics were analyzed and recorded. So a carbon tape was stuck on the magnet and particles were transferred as shown in figure 5.5. Due to the adhesive present in the carbon tape, the particles were transferred from the magnet to the tape. 4 samples of carbon tape were taken for each time interval.

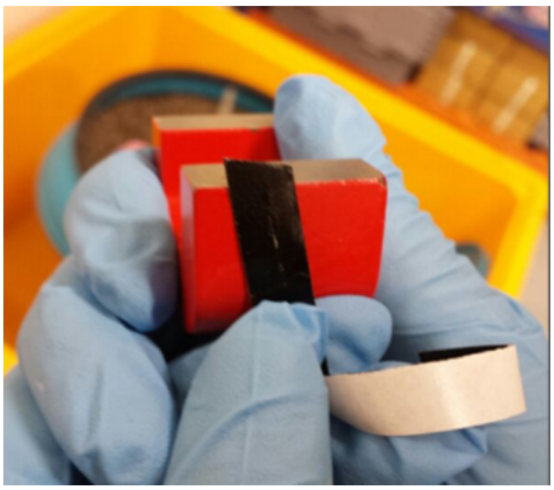

Figure 5.5: Step 5 - Collection in carbon tape

Step 6: Measure the average surface roughness Ra of workpiece

The Ra of the workpiece is measured using a surface profilometer. The Ra value is measured at five different points and an average value is calculated and recorded for analysis.

All these steps are repeated every 30 minutes of finishing. After each collection,

entire system including the media, workpiece and the bowl is thoroughly washed, so that the old wear debris particles do not remain in the system. This is to avoid the old debris particles being collected again during further analysis.

5.3.2 Offline Part of Analysis

After collection of wear debris particles in the carbon tape, the tape is transferred to an analysis laboratory, where the following steps are carried out.

Step 7: Locate the wear debris particles in SEM

SEM analysis covers only an area of about 500μm by 500μm. But the size of each carbon tape was around 10mm by 30mm. Hence locating the wear debris particles from the carbon tape was a laborious process. This process was repeated for each sample collected at every time interval to locate the wear debris particles and analyze them.

Step 8: Analyze the particles using EDX

In spite of the magnetic separation method to eliminate the non-steel wear debris, there was a significant amount of other wear debris particles which were present in the carbon tape. To avoid analyzing them, each and every particle was subjected to EDX analysis and its chemical composition was compared to that of the part used. Only those particles which were confirmed as steel particles were analyzed and reported.

Step 9: Measure the size and shape of wear debris particles

The next step was to analyze the steel particles. Two factors were measured - shape and size to correlate with the wear debris mechanism. The size was measured by comparing the size of the particle obtained and the SEM scale visually using a digital ruler as shown in figure 5.6. The figure shows that a digital ruler is placed on the bottom of the screen to measure the scale of SEM picture. It shows that 10mm in ruler corresponds to 10μm in the SEM picture. So the size of the particle is recorded as 32μm length and 31μm breadth.

Step 10: Correlate the wear debris with Ra and wear debris literature

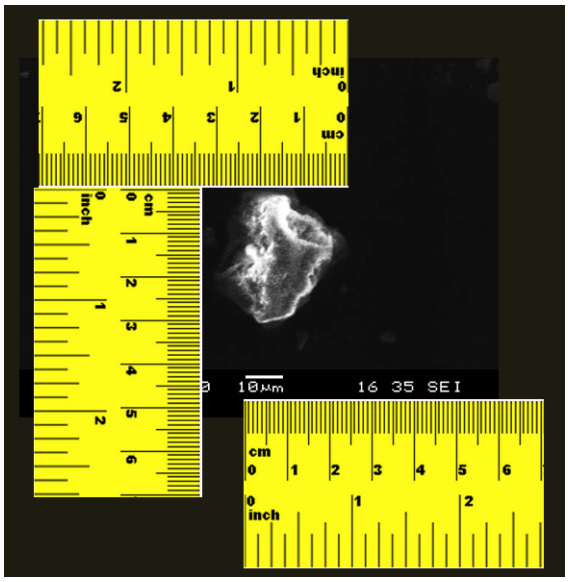

Figure 5.6: Step 9 - Measurement of shape and size of wear debris particle by digital ruler

Finally the measured size values and shape characteristics are correlated with the Ra variation and wear debris mechanism as explained in the following section. All the above steps are summarized in figure 5.7.

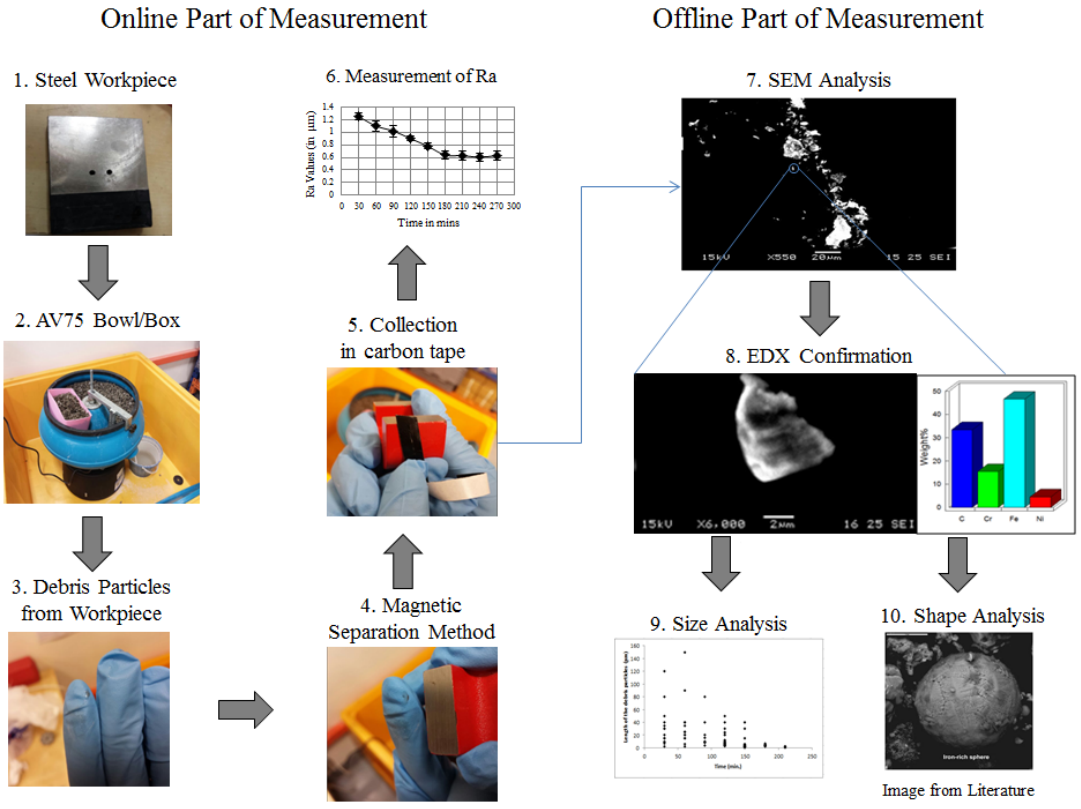

Figure 5.7: Steps involved in Wear Debris Analysis

5.4 Experiments Performed

A standard methodology is developed and the experiments are performed to analyze and characterize the wear debris particles. Two sets of experiments are performed. The first experiment is performed in a controlled setup which accelerates the process of wear debris formation and facilitates easy collection of wear debris. The next experiment is performed to test and validate the methodology in the actual vibratory finishing process.

5.4.1 Accelerated Experiment

This experiment is performed in a small chamber attached to the bowl as shown in figure 5.2. In addition to this, the plastic cone media is used. This is to increase the chances of wear debris particles being generated from the part as the amount of debris resulting from this plastic media is very less. This is due to the nature of the media which does not abrade in contact with each other, but has the same abrasive nature as the ceramic media as explained in section 3.3.3. The objective of this experiment is to validate the developed methodology and find the wear debris particles.

5.4.2 Analysis Experiment

This experiment is performed in the AV75 bowl by fixturing the workpiece inside the bowl using the fixture as shown in figure 5.2. This experiment is performed with the ceramic media. Because of this, the chances of finding the wear debris particles for this experiment is very less compared to the accelerated experiment. This experiment was performed to test if the methodology developed can be used to find and characterize the wear debris particles in the actual vibratory finishing process.

5.5 Results Analysis

The results obtained from the above experiments are described in this section. As explained in the methodology, the size and shape of wear debris particles were measured and compared with the average surface roughness and the wear mechanism data available from literature. From this analysis, an understanding of the surface modification mechanism is obtained which is described at the end of this section. These results and analysis are categorized under different sub-sections as follows.

5.5.1 Size of Wear Debris Particles

The length and breadth of the wear debris particles were measured as explained in figure 5.6 and the average of the values were calculated. Figure 5.8 shows a sample (10 nos.) of SEM pictures obtained from the metallic wear debris particles obtained at various time intervals for the accelerated experiment and Figure 5.9 shows the SEM pictures obtained from the analysis experiment. These figures shows only the metallic wear debris particles resulting from the surface of the workpiece. As explained earlier, this sorting of particles was done by analyzing the chemical composition from the EDX. A complete record of all the images obtained is presented in section A.2 of Appendix A. As expected the amount of wear debris particles obtained during the accelerated experiments was more than the analysis experiment. On an average, a minimum of 10 wear debris particles were collected at each time interval for the accelerated experiment, whereas for analysis experiment this number reduced to 5.

Figure 5.10 shows the length and breadth of the wear debris particles obtained from the accelerated experiment. Both the data points and average value is shown in figure. It can be observed that the average size of the particles gradually reduces from 30μm at 30 minutes to less than 5μm at 210 minutes of polishing. This shows that the size of the wear debris particles considerably reduces as the surface reaches saturation. The average length and breadth of all the particles obtained during this experiment were calculated as 14.15μm and 7.39μm respectively.

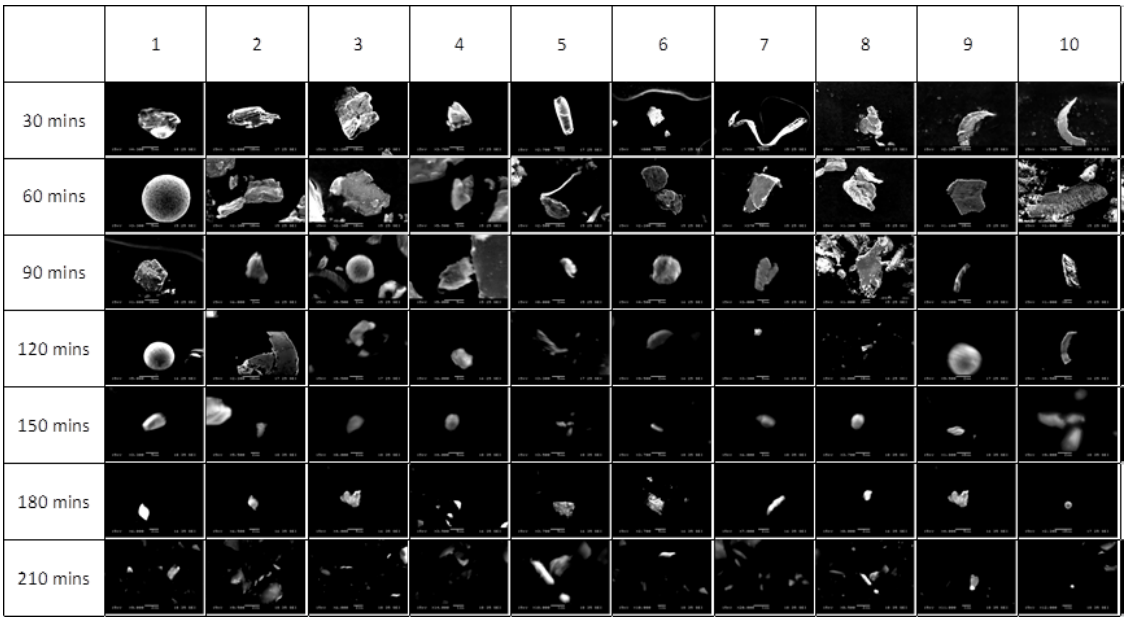

Figure 5.8: SEM pictures of Wear Debris Samples for Accelerated Experiment

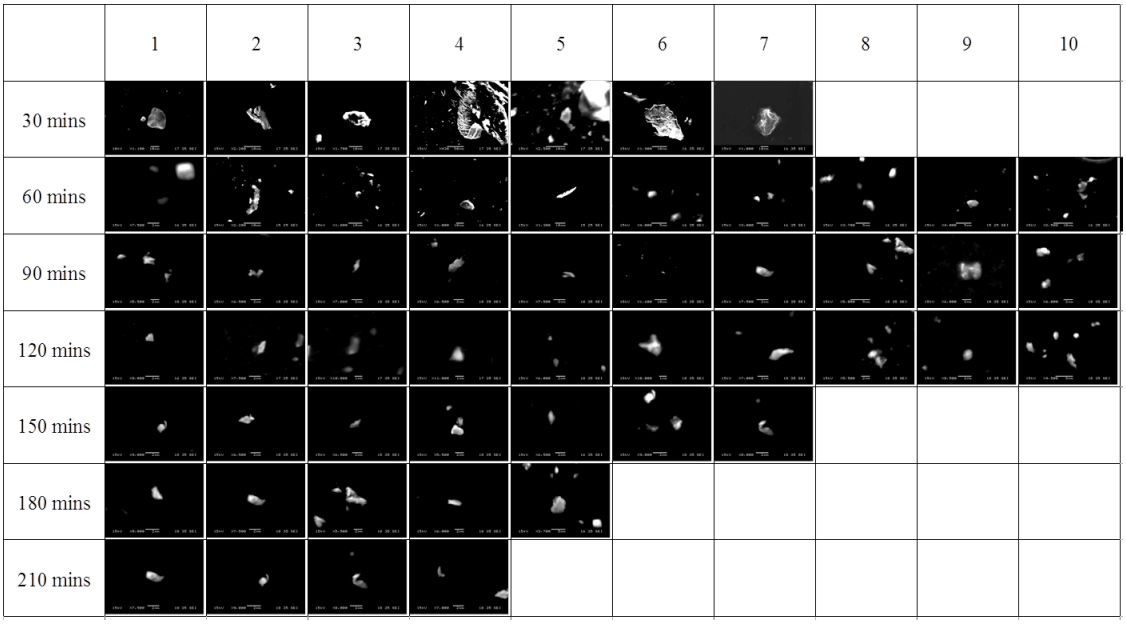

Figure 5.9: SEM pictures of Wear Debris Samples for Analysis Experiment

Figure 5.11 shows the length and breadth of the wear debris particles obtained from the analysis experiment - which is from the actual bowl. Both the data points and the average value are presented in the figure. It can be observed that the average size of the wear debris particles gradually reduces from 20μm at 30 minutes to less than 5μm after 210 minutes of polishing. The average length and breadth of the wear debris particles was calculated as 6.05μm and 4.29μm respectively. This is considerably less than that of the accelerated experiment which was 14μm and

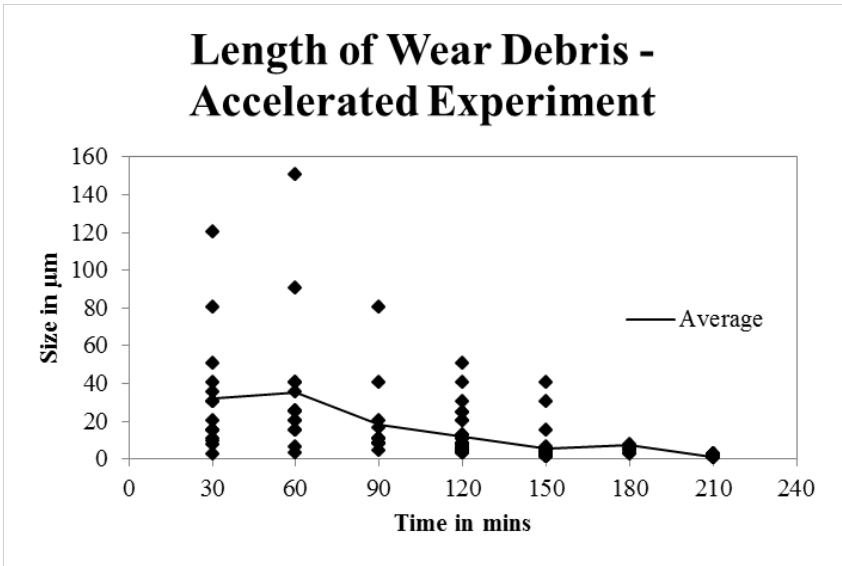

(a) Length of Wear Debris Particles

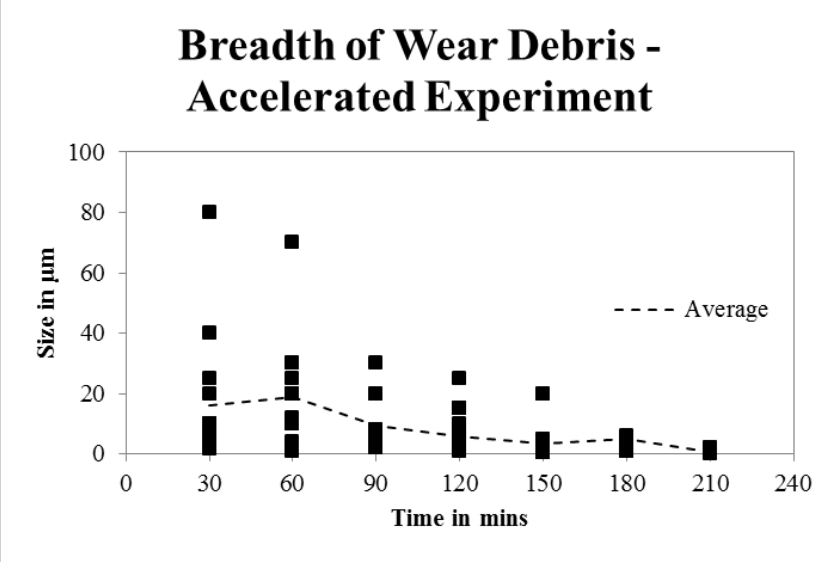

(b) Breadth of Wear Debris Particles

Figure 5.10: Length and Breadth of Wear Debris for Accelerated Experiment

7μm. Also it can be noted that after 90 minutes the size of the wear debris particles reaches saturation. This can be due to the fact that the smaller wear debris particles not being detected by the developed methodology. Hence this shows that the wear debris particles less than 1 microns in size cannot be detected by this method.

Figure 5.12 shows the average dimensions of the wear debris particles collected from the accelerated experiment. The reduction in size can be attributed to the

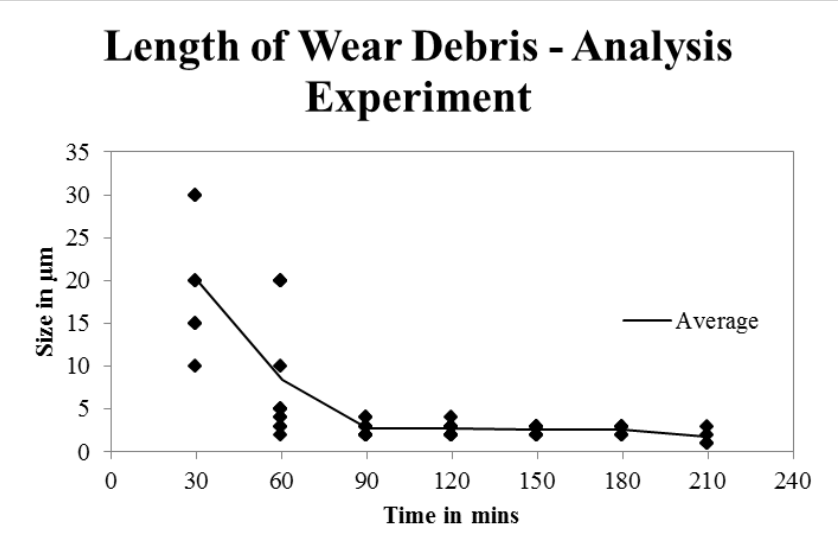

(a) Length of Wear Debris Particles

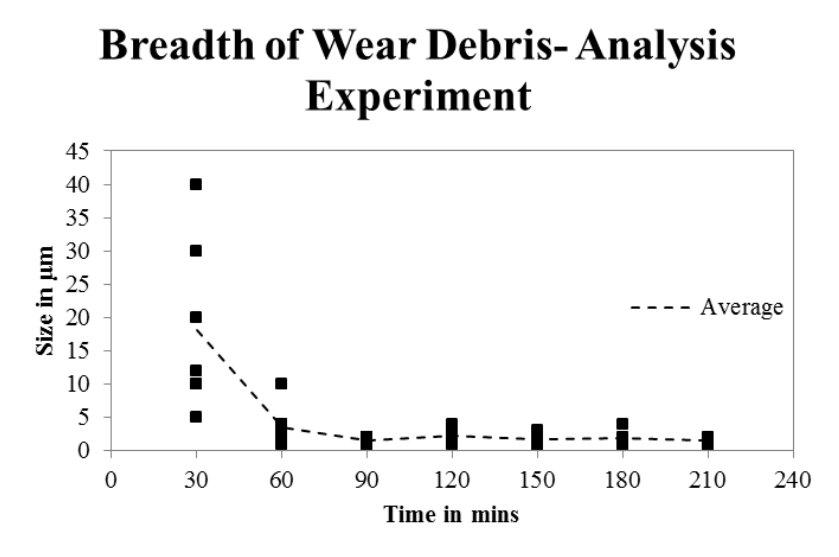

(b) Breadth of Wear Debris Particles

Figure 5.11: Length and Breadth of Wear Debris Particles for Analysis Experiment

size of the peaks on the surface. When the peaks are initially sharp, they are susceptible to more material removal and as the peaks are removed, the broader portion of the profile is exposed. This makes the peaks considerably stronger giving only smaller wear debris particles. This can also be related to surface modification mechanism. It was seen (in section 4.7) that initially the plastic deformation is less and it increases and eventually saturates to a value closer to zero when the surface reaches saturation as shown in figure 4.17.

The same trend is seen in analysis experiment as well (as shown in figure 5.13).

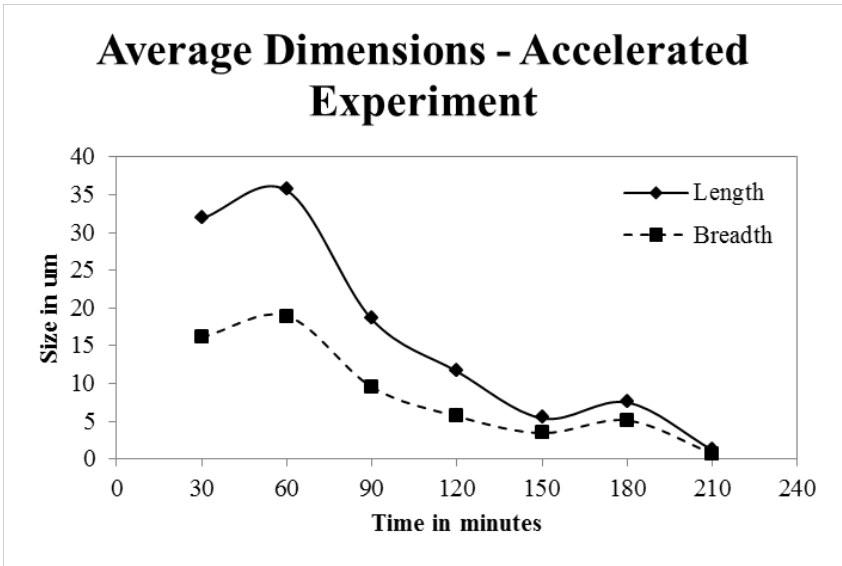

Figure 5.12: Average Size of Wear Debris for the Accelerated Experiment

But for the analysis experiment, the size of the wear debris particles reduces and reaches a minimum saturation value of around $2\mu m$ around 90 mins. This saturation in the size of wear debris particles is predicted due to the failure of the methodology to capture wear debris particles which are less than 1 micron in size as the resolution of the SEM equipment used is 1 micrometer.

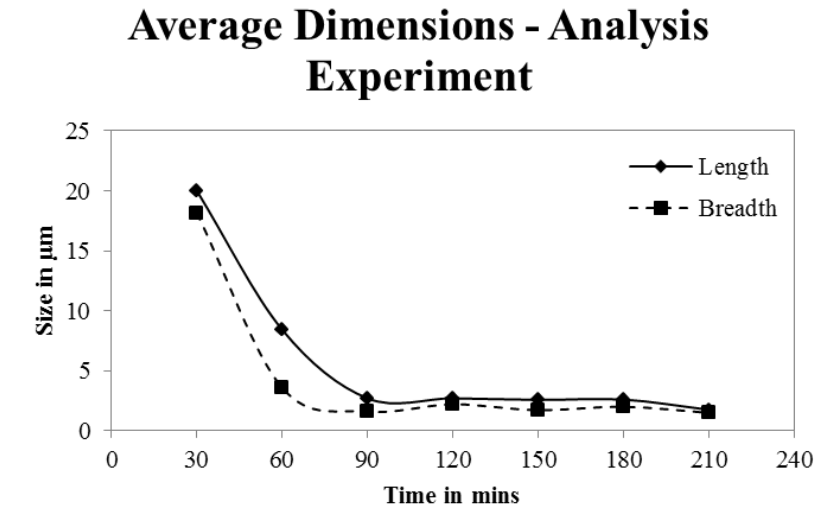

Figure 5.13: Average size of Wear Debris for Analysis Experiment

5.5.2 Analysis of surface roughness measured

When the dimensions of the wear debris particles are compared with the surface roughness obtained, the size of wear debris particles reduces as the surface roughness decreases and after the surface reaches saturation, the size of the wear debris particles reduces to almost zero. This is evident in figures 5.14 and 5.15. In both accelerated and analysis experiments, the Ra value reaches a saturation, but at different time intervals. Accelerated experiment sample reaches a saturated value of 0.6μm Ra at 180 mins and analysis sample reaches a saturated value of 1.2μm Ra at 120 mins. This is due to the different types of media used for both the experiments. In addition to that, the accelerated experiment has more impact velocity than the actual media motion, causing the lower saturation value. But since the objective of this study is to investigate the different types of wear debris generated by vibratory finishing process, the saturation is not of importance in this study and only the wear debris particles formed and the correlation of its characteristics with the obtained surface roughness is analyzed and studied in detail. From comparing the size of the wear debris particles (figures 5.12 and 5.13) with surface roughness (figures 5.14 and 5.15), it is clear there is a positive correlation between the two of them.

5.5.3 Analysis of Shape of Wear Debris Particles

This section analyzes the shape of the wear debris particles obtained at various time intervals. The shape analysis is performed only on the size of particles greater than 1μm in size. This is due to the incompatibility of the current SEM setup to focus and obtain pictures less than 1μm as the resolution of the equipment is less. As seen in the length data, the wear debris particles obtained upto 150 minutes for the accelerated experiment and upto 60 minutes for the analysis experiments falls above this range and they are analyzed in this section. It is to be noted that on an

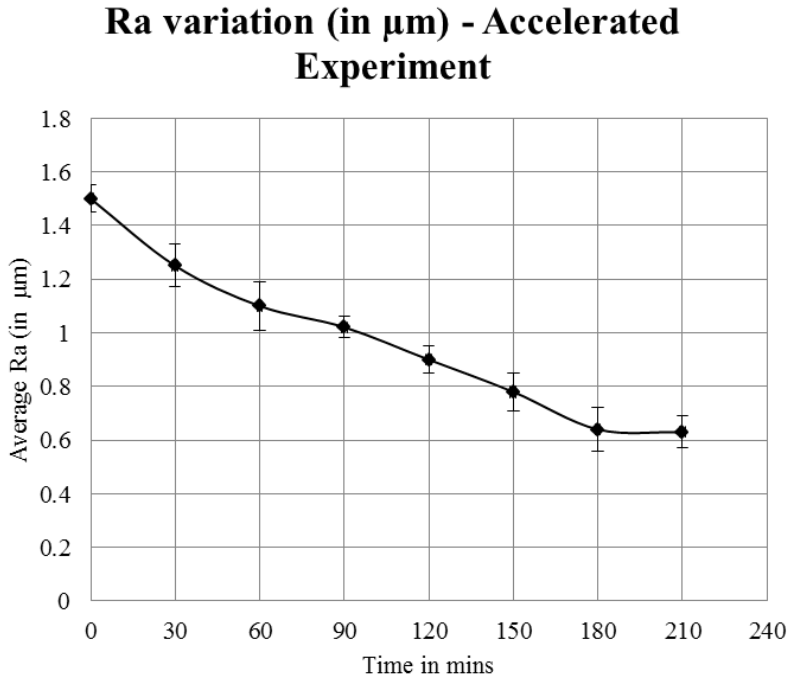

Figure 5.14: Ra Variation with time for Accelerated Experiments

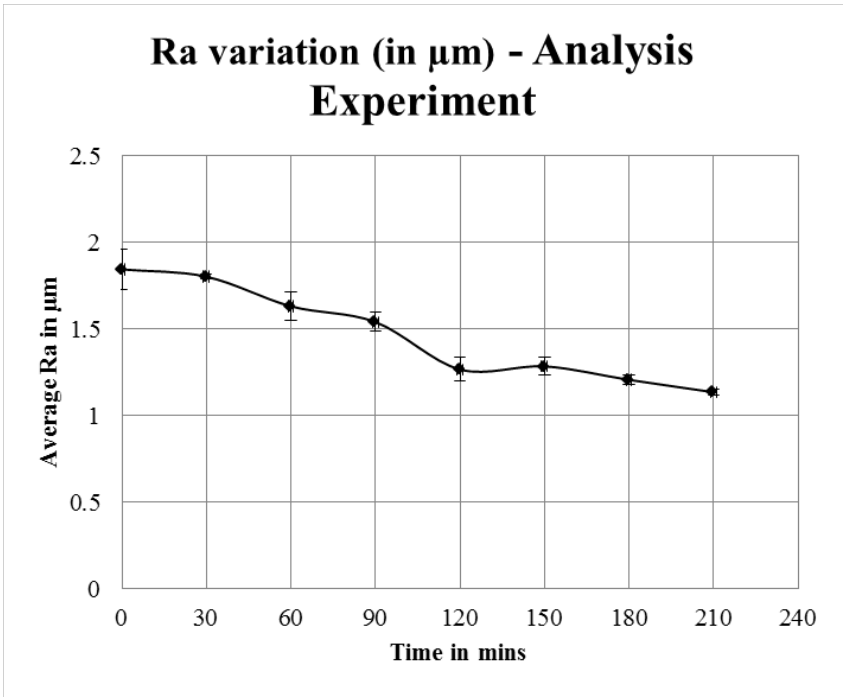

Figure 5.15: Ra Variation with time for Analysis Experiments

average, about 90% of the particles were irregularly shaped wear debris particles. But the remaining 10% consisted of the following wear debris particles.

5.5.4 Chip Shaped Wear Debris Particle

Chip shaped wear debris particles represent the presence of material removal mechanism by cutting behavior. Figure 5.16 shows a chip shaped wear debris particle obtained after 30 minutes of polishing using the accelerated setup. Only 2 such particles were obtained. The presence of this wear debris particle shows that the abrasives present in the media attack the surface and cause them to break and forms the chips. These kind of chips are usually observed in cutting operations like turning, milling and also in the case of grinding as explained in section 2.4.

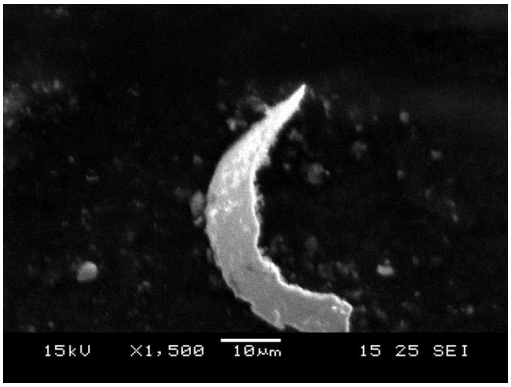

Figure 5.16: Chip shaped wear debris obtained at 30 mins

5.5.5 Ribbon Shaped Wear Debris Particle

Ribbon shaped wear debris particles are also usually found in the cutting operations. The shear forces involved in cutting cause a rectangular particle to bend and form a ribbon shaped structure as shown in figure 5.17. This ribbon shaped wear debris particle also refers to the same material removal operation which causes the chip shaped wear debris particle explained in the previous section. This particular particle is obtained at 30 mins of polishing in accelerated experiment and two such particles were obtained. These two particles indicate that there is a presence of cutting type of material removal occurring in vibratory finishing process.

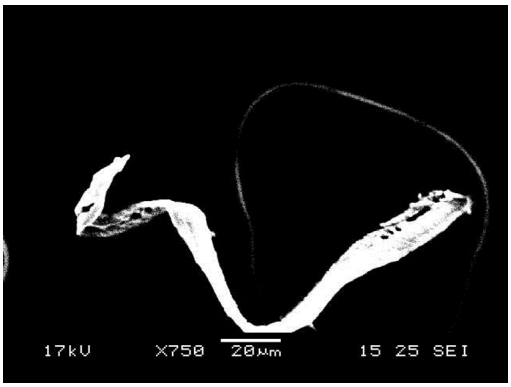

Figure 5.17: Ribbon Shaped Wear Debris obtained at 30 mins

5.5.6 Adhesive Wear Debris with Striations

Figure 5.18 shows the presence of striations in the wear debris particle obtained. This shows that there is also a presence of adhesive wear in the vibratory finishing in addition to the cutting process as explained earlier. These striations are formed due to the adhesive force being greater than the friction force as explained in section 2.3. Adhesive wear occurs when there is a presence of strong forces between the mating surfaces due to the chemical compatibility of the surfaces. This particle shows that adhesive wear is also present in this complex process. This particle was obtained at 30 mins of polishing and 60 mins of polishing.

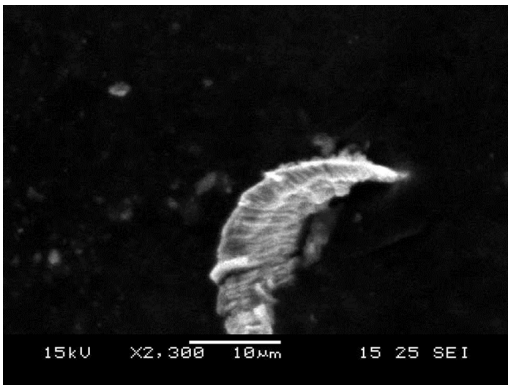

Figure 5.18: Striations in wear debris obtained at 30 mins

5.5.7 Platelet Shaped Particle

Platelet shaped particles like the one obtained as shown in figure 5.19 are usually formed due to the rolling type of motion causing plastic deformation which eventually leads to the failure of the material causing the wear. More than 5 particles of this shape were obtained in total and one particle was obtained in the first 30 minutes of polishing. Hence all the above types of wear - cutting type of abrasive wear, adhesive wear, rolling type of wear occurs simultaneously during the first 30 minutes of polishing. Hence it cannot be stated that a single mechanism results in the surface modification during the first 30 minutes of polishing.

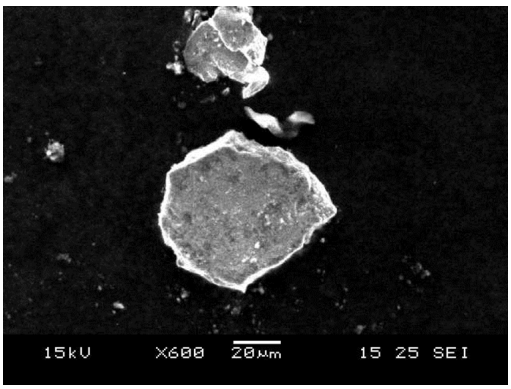

Figure 5.19: Platelet shaped Wear Debris obtained at 30 mins

After 30 minutes, the wear debris particles generated previously are discarded by washing the media particles and the process is repeated for another 30 minutes. During the next time interval some new shapes are obtained as explained below.

5.5.8 Spherical Shaped Particle

Spherical shaped particles as shown in figure 5.20 are also obtained from the accelerated vibratory finishing process. This kind of wear debris particles indicates that there is a presence of high temperature contact region causing the local melting of metal. This kind of particle usually occurs in grinding process where there is a high temperature between the contact region. But this particle is not present initially or the later stages. It indicates that the shape of the profile has a major

role in determining the type of mechanism which causes the surface modification. This kind of particles are generated upto 120 minutes of polishing and more than 5 such particles were obtained.

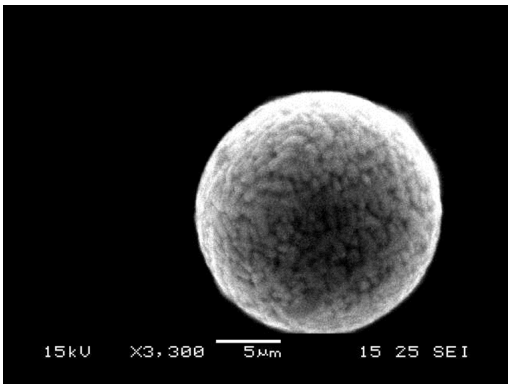

Figure 5.20: Sphere shaped Wear Debris Particle obtained at 60 mins

5.5.9 Irregularly shaped particles

After 120 minutes, in addition to the spherical particle, there are numerous irregularly shaped particles found in the wear debris collection. As mentioned earlier, these particles constitute 90% of the wear debris particles obtained. These are shown in figures 5.21, 5.22, 5.23, 5.24. Figures 5.21 and 5.22 can be termed under chips or platelets obtained due to cutting or plastic deformation. But the surface morphology is not clear due to the inability of the SEM to focus the small area. These represents particles which are about 5μm in size. This is the minimum size, whose features can be identified by the currently available SEM setup. Figures 5.23 and 5.24 shows the irregularly shaped particles generated after 180 and 210 minutes of polishing. But the size of these particles are less than 1μm due to which both the shape and size are not clear, which is again due to the limitation of the system used.

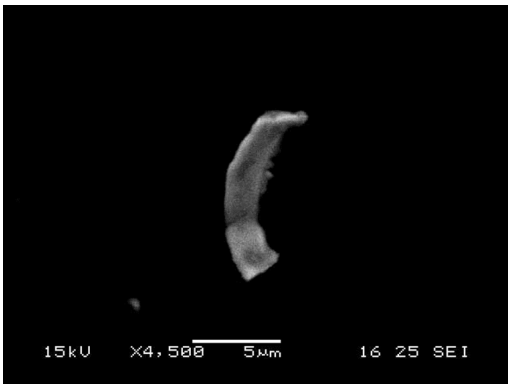

Figure 5.21: Irregularly Shaped Wear Debris obtained at 120 mins

Figure 5.22: Irregularly shaped Wear Debris obtained at 150 mins

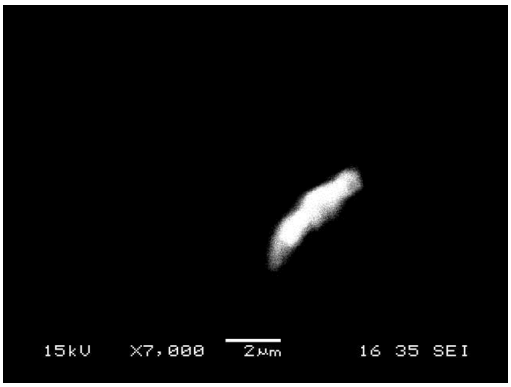

Figure 5.23: Irregularly shaped Wear Debris obtained at 180 mins

The different types of wear debris particles which are present in the accelerated experimental process were reported above. In the analysis experiment the initial particles collected after 30 minutes also show the presence of cutting and plastic deformation, but the particles collected after 90 minutes reduce in size less than 1μm, due to which the shape and features are not identifiable. The same mechanism is predicted to occur, but the wear debris particles are smaller due to change in type of media and the forces imparted by each media.

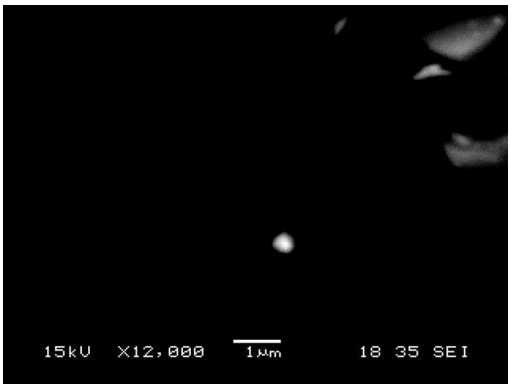

Figure 5.24: Irregularly Shaped Wear Debris obtained at 210 mins

5.6 Summary

The wear debris particles are collected using a novel technique developed specifically for this process. The developed technique is able to detect the particles and the size and shape of the wear debris particles, at different time intervals are analyzed and recorded. Two types of experiments are conducted - one in an accelerated environment, which facilitates the generation of wear debris particles, and another one in the actual AV75 bowl. It is seen that the experiment conducted in bowl generates a very small amount of wear debris particles and in addition to this the size of the particles formed in this process is smaller when compared to the accelerated process. But the accelerated process can be compared to some of the conditions of the vibratory bowl, since the type of media and the input motion is the same as used in other processes. The plastic media is used for polishing purpose and the controlled chamber was directly attached to the AV75 bowl.

The conditions for analysis experiment was selected based on the other experiments performed in this thesis. But since the size of the wear debris particles was too small (less than 1μm), only the particles generated by the accelerated experiment are analyzed.

The results show that the size (length & breadth) of the wear debris particles gradually reduces from 20μm to 30μm and reaches zero. This is in accordance with the surface modification mechanism which stated that significant plastic deformation occurs initially, but it gradually reduces to zero. In addition to the size, the

shape analysis performed on the wear debris particles obtained from the accelerated experiment shows that all types of wear mechanisms such as abrasive wear, adhesive wear and plastic deformation occurs in vibratory finishing. This chapter concludes here with the basic understanding on the different types of wear debris particles generated by vibratory finishing process for a duplex stainless steel alloy. Even though, these findings cannot represent other materials (such as Ti6Al4V and T6061-Al Alloy) used in this thesis, the technique to use the magnetic separation method to find that the size of the wear debris particles reduces with time is significant for further research.

Thus these findings have some limitations as the results obtained are applicable only for the stainless steel alloy in a controlled setup. The various ways of improving have been analyzed in detail and are discussed in section 8.4.

A detailed understanding of the surface modification process which causes the saturation in vibratory finishing have been analyzed using masked reference method and wear debris particles which are generated by the process have been studied. The next chapter will present the work where the effect of process parameters are tested on this surface modification mechanism.

Chapter 6

Effect of Process Parameters on Surface Modification

6.1 Overview

The previous chapters discussed in detail the methods developed to understand surface modification mechanisms which cause the saturation in vibratory finishing. The objective of this chapter is to study the effect of changing the process parameters of vibratory finishing such as the frequency and amplitude of vibration on the surface modification mechanisms and process time. This study was performed basically to understand the capability of decreasing the process time in vibratory finishing process.

In order to achieve this objective, it is essential to precisely control the parameters such as the vibratory frequency and amplitude. In conventional vibratory finishing, it is not possible to achieve this since the vibratory frequency and amplitude are inter-related. As explained in the introductory chapter, the frequency and amplitude of vibrations depend on the speed of rotation and weight of the eccentric masses attached to the vibratory motor. The load of the vibratory finishing machine (which is the combined mass of the media and workpiece) will also control the amplitude of vibrations. Sangid et al. (2011a) have studied the effect

of frequency and amplitude, but an attempt to increase the frequency beyond the conventional ranges have not been made previously. The hydrodynamic shaker presented in section 3.7.1 was used to build a custom vibratory finishing setup for the precise control of frequency and amplitude. In addition to this, it is also possible to increase the frequency precisely, in the range of few kHz, which is more than 10 times the conventional frequency ranges used currently in industries, which ranges from 25Hz to 60Hz. Frequency ranges of upto 1000Hz and amplitudes of range of upto 5mm were tested. From these studies, an ideal frequency and amplitude was selected and the effect of varying the frequency, amplitude (from conventional range to the ideal range) and vibratory direction on surface modification mechanism was studied. The following section compares the custom 2D setup with a conventional vibratory finishing machine.

6.2 2D vs 3D Vibratory Finishing

The 2D vibratory finishing setup specifically developed for this thesis is presented in section 3.7.1. As explained previously (in section 3.7.1) even though the input vibratory motion is single dimensional the media moves in two directions across the length and breadth of the chamber. Only the movement in the third direction perpendicular to the direction of view is negligible and hence the term 2D vibratory finishing which is a controlled form of the conventional vibratory finishing. The components are fixed to the side walls of the chamber. So the components fixed in the direction parallel to vibration experiences more of rolling and scratching action, whereas the components fixed to the direction perpendicular to the vibrations experiences more of impact action. Thus, in addition to the control of frequency and amplitude, the type of contact occurring between the media and the workpiece (impact vs scratching) can also be controlled using this setup. This section will compare the 2D vibratory finishing with that of the conventional vibratory finishing in terms of surface morphology obtained after finishing and also the media motion which influences the surface morphology.

6.2.1 Surface Morphology

The surface morphology obtained between 2D and 3D vibratory finishing is compared in this section. As explained earlier, the 2D vibratory finishing has two distinct types of media motions depending on the direction of clamping of the workpiece, whereas the conventional 3D vibratory finishing has both the types of media motions occurring simultaneously irrespective of the clamping direction. Preliminary experiments were conducted and the resulting surface morphology and surface roughness obtained after the same time of polishing were calculated and the results are shown in figures 6.1 and 6.2 respectively.

Figure 6.1 shows the SEM pictures of the surface obtained at different time intervals for the same material (T6061-Al Alloy) and processing conditions in the MV32 vibratory machining setup and 2D vibratory finishing setup described in chapter 3.

Conventional 3D Vibratory Finishing: It can be seen that initially after 20 minutes of processing (Figure 6.1a) there is a rough surface which is formed due to plastically deformed region and after subsequent polishing after 60 minutes (Figure 6.1b), these plastically deformed layers are removed. So there are both plastically deformed and material removal areas occurring in conventional vibratory finishing but at various time intervals.

2D Vibratory Finishing: For 2D vibratory finishing, these kind of plastically deformed and material removal layers occur by changing the clamping directions. As shown in figure 6.1c surface scratches which correspond to material removal mechanism is formed in the parallel side of clamping. And as shown in figure 6.1d, plastically deformed rough layers are obtained when clamping the workpiece in a perpendicular direction to the media motion.

In addition to this, the surface roughness obtained for the same material and processing conditions are compared between a conventional 3D vibratory finishing machine and the 2D vibratory bowl. Figure 6.2 shows the Ra values of T6061 Al-Alloy workpiece polished using a conventional 3D vibratory finishing machine

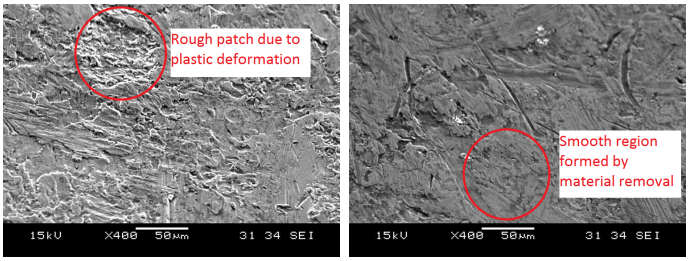

(a) Conventional vibratory finishing after 20 mins

(b) Conventional vibratory finishing after 60 mins

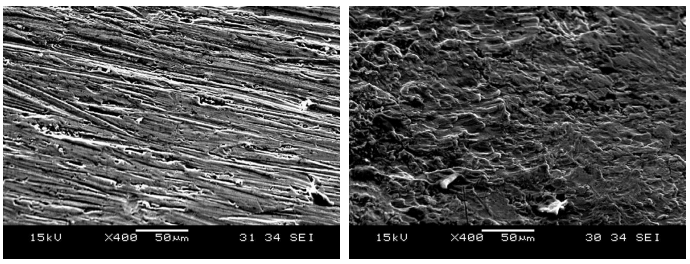

(c) Parallel 2D vibratory finishing after 25 mins

(d) Perpendicular 2D vibratory finishing after 25 mins

Figure 6.1: Comparison of surface morphology for 2D vs 3D vibratory finishing

and the 2D vibratory finishing. It can be seen that the Ra value of 0.40μm is achieved at the same time of around 35 minutes for the conventional and parallel 2D vibratory finishing machine. The perpendicular side does not seem to polish the material due to the excessive impact action on the surface of the workpiece.

6.2.2 Media Motion

This section compares the media motion between the conventional 3D and 2D vibratory finishing machines. Figure 6.3a shows the media motion in a conventional vibratory finishing where the media motion has two types of movements viz. Roll and Feed and the media moves in a form of spiral helix. The components to be polished are usually fixed in the center using a fixture or freely floating. At any point of time, the components to be polished experience impact, rolling and scratching types of contact with the media. Whereas the 2D vibratory finishing developed, has a media motion which flows from the center towards the walls as shown in figure 6.3b. This motion was recorded using an high speed camera apparatus discussed in section 3.7.4 of chapter 3.

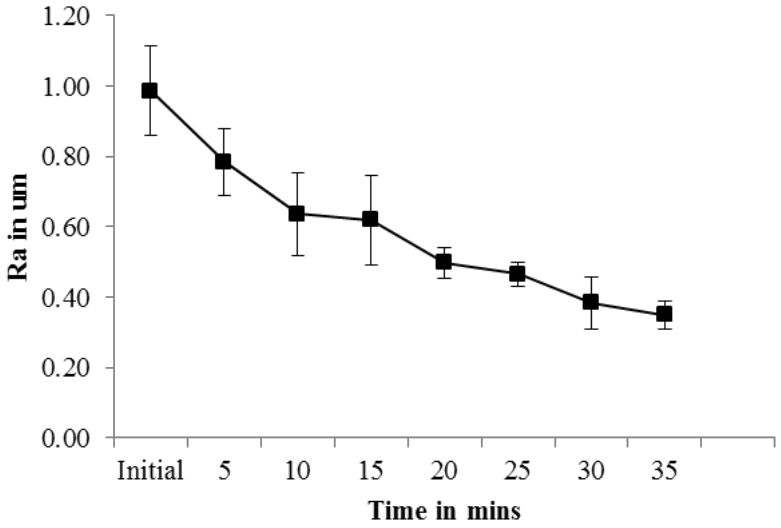

(a) Conventional vibratory finishing

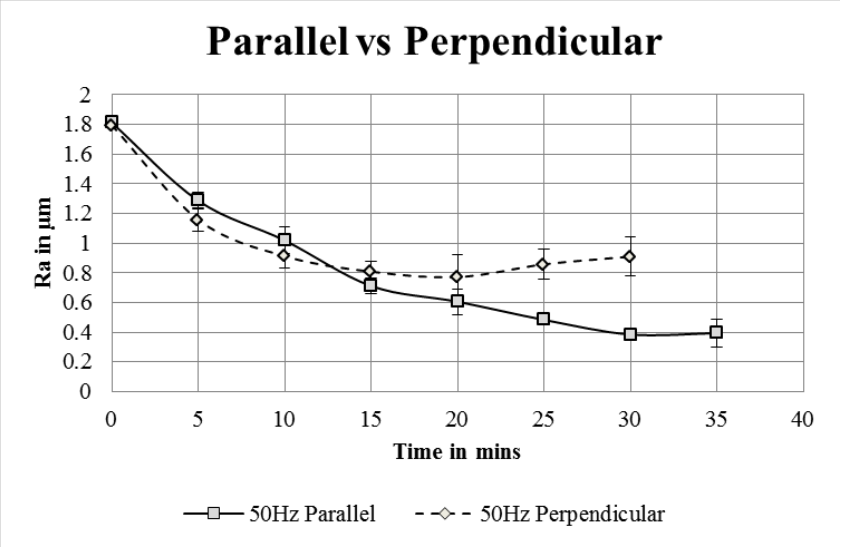

(b) Parallel and Perpendicular 2D vibratory finishing

Figure 6.2: Comparison of surface roughness for 2D vs 3D vibratory finishing

Figure 6.3b shows the overall media motion in the 2D bowl obtained from a high speed camera setup described in section 3.7.4 . But when a single media particle is tracked, the motion will follow a zig-zag path as shown in figure 6.4. The surface modification mechanism which was discussed in chapter 4 mainly depends on these small motions. So as the frequency and amplitude varies the size of the zig-zag motion also varies thus changing the surface modification mechanism. The objective of this part of the thesis is to investigate the effect of these parameters on the surface modification mechanism.

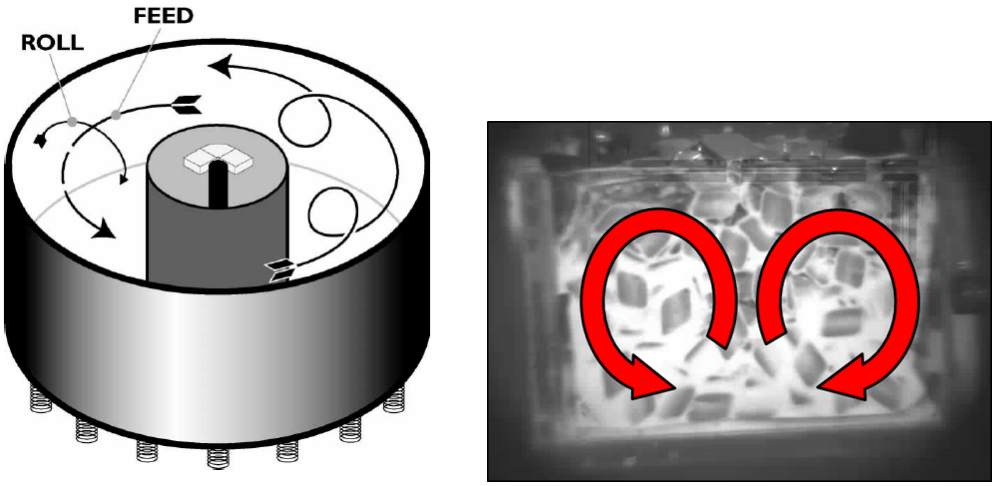

(a) Conventional vibratory finishing (b) 2D vibratory finishing

Figure 6.3: Comparison of Media Motion

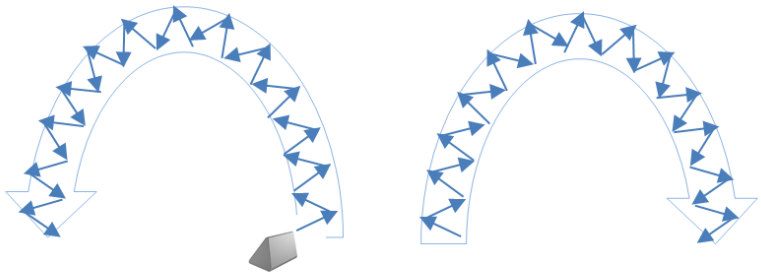

Figure 6.4: Zig-zag media motion in 2D vibratory bowl

6.3 Parameters of 2D Vibratory Finishing

6.3.1 Frequency

The frequency of vibrations refers to the total number of to and fro motions achieved by the vibratory machines per unit time. This is represented in Hz which is the number of cycles per unit time. The typical frequency range of conventional vibratory finishing machines are from 25Hz for general purpose bowl type vibratory finishing machines to 60Hz for industrial grade high intensity bowl or tub type vibratory finishing machines. The frequency of vibrations are transferred from machine to the media which in-turn contacts the workpiece. Changing the frequency changes the overall velocity of media motion around the bowl and also the to-and-fro motion of the media, depending on the efficiency of transfer between

the machine and media and among the media particles.

6.3.2 Amplitude

The amplitude of vibration is fundamentally the distance traveled by the media because of the to and fro motions of the vibrations. This distance traveled by the media can affect the surface modification mechanism in many ways as compared to the frequency which only decreases the process time by increasing the number of to and fro media motions. This effect is studied by conducting experiments which is described later in this chapter.

The following section explains the experimental methodology used for testing the effect of the above parameters of 2D vibratory finishing.

6.4 Experiments and Results

The objective of these experiments were to test the effect of 2D vibratory finishing parameters such as frequency and amplitude on the surface roughness and modification mechanism. Preliminary tests were conducted to determine the ideal set of parameters in which the polishing occurred. The following section explains the preliminary experiments and results obtained.

6.4.1 Preliminary Experiments

The hydrodynamic shaker can be excited to frequency ranges of upto 3kHz, but increasing the frequency also decreases the amplitude of vibrations to about 0.01mm. This is measured by using an in-built acclerator in the shaker. Alternatively the amplitude can be increased upto 5mm when the frequency is reduced to 10Hz. Some initial tests were conducted increasing the frequency and amplitude to 1000Hz and 5mm. Both these settings reduced the effective media motion with respect to the bowl. Tests were conducted with different types of media particles such as,

- Ceramic media of three shapes

  - Angle cut cylinder
  - Tristar
  - Spherical

- Plastic media of conical shape
- Raw aluminium oxide abrasives

The size of these media particles were also different. The size of the media particles are listed in the table 6.1.

Table 6.1: Size of media particles

Media	Length (mm)	Breadth (mm)
Angle cut cylinder	3	3
Tristar	20	10
Spherical	10	10
Conical	30	30
Raw Aluminium Oxide	1	1

It was hypothesized that for high frequencies, the smaller media particles will be more efficient as the energy required to excite each media particle is lesser when compared to larger media particles. Nevertheless, for all types of media particles tested, as the frequency was increased to 1000Hz, the amplitude decreased to 0.05mm which greatly reduced the velocity of media motion. There was no considerable change in roughness as the process progressed. Further, as the amplitude was increased to 5mm, the frequency was reduced to 10Hz which caused the media to move along with the bowl causing no effective motion between the media and workpiece. Tests were conducted with different levels of frequencies and amplitudes and an ideal range of frequency and amplitude was obtained. Figure 6.5 shows the graph of range of frequencies tested and the selection of ideal frequency range.

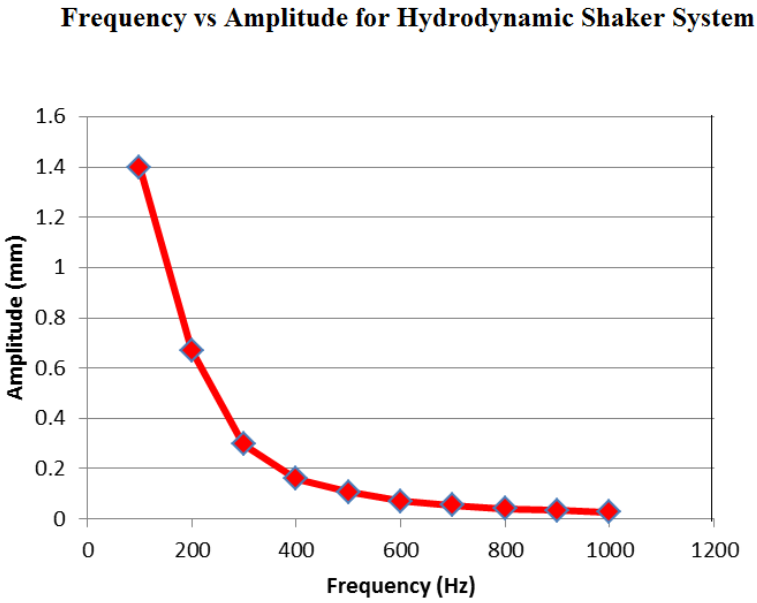

Figure 6.5: Maximum operating amplitude at different frequency levels of the hydrodynamic shaker

6.4.2 Design of Experiments for testing the effect of process parameters

A frequency range from 50Hz to 75Hz with a corresponding amplitude of 2mm to 3mm was obtained as the ideal range where the polishing occurred. This range was selected based on the experiments described in the previous section. This range is only about twice the frequency range used in typical vibratory finishing machines. This effect may also be due to the fact that the media particles which were used for testing were originally designed to be used in the frequency ranges of typical vibratory finishing machines. Hence, to study the effect of increasing the frequency beyond the conventional range a new type of media particle should also be designed which is out of scope of this thesis. A two level full factorial experimental design was used to test the effect of frequency and amplitude as listed in table 6.2.

Table 6.2: Two factor full factorial DOE

Frequency (Hz)	Amplitude (mm)
50	2
75	3

6.4.3 Variation of Ra

The experiments were conducted according to the design of experiments. The surface roughness was measured and surface modification mechanism was evaluated using the masked reference method as explained in chapter 4. Figure 6.6 shows the variation of Ra with respect to time for various levels of the DOE. It can be seen that the high frequency and high amplitude setting of 75Hz-3mm reaches the saturation first followed by 50Hz-3mm, 75Hz-2mm and finally 50Hz-2mm. It is clear that the combination of high frequency and high amplitude is better for achieving faster saturation. But the reason for this change can be explained only by studying the surface modification mechanism for all these conditions using masked reference method which is explained in the next section.

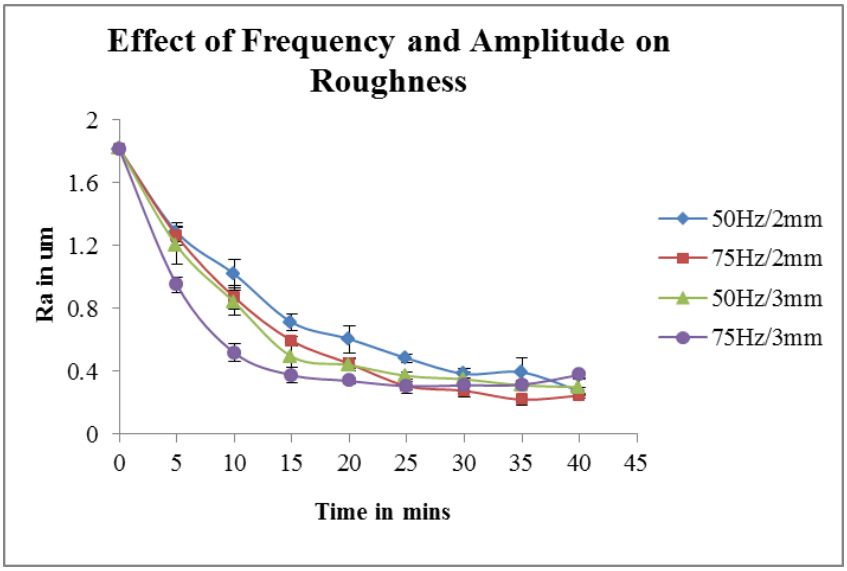

Figure 6.6: Variation of Ra with time for different processing conditions

6.4.4 Surface Modification Mechanism

The surface modification mechanism was studied by measuring the peak height and valley height with respect to a constant masked reference with the same technique as explained in section 4.3. The height of the peaks and valleys measured with respect to a constant reference line for various levels of DOE is shown in figure 6.7. It can be seen that the overall curve and trend for all the settings of DOE are same

except for the rate at which the trend is occurring. All the curves represent an initial sharp decrease in valley height representing plastic deformation and followed by gradual decrease in the rate.

But the high frequency and high amplitude setting of 75Hz and 3mm has the least valley height and the rate at which it is attained is also very less compared to the other curves. There is not much difference between the 50Hz-3mm and 75Hz-2mm settings. But the 50Hz-2mm is significantly lower than the other curves.

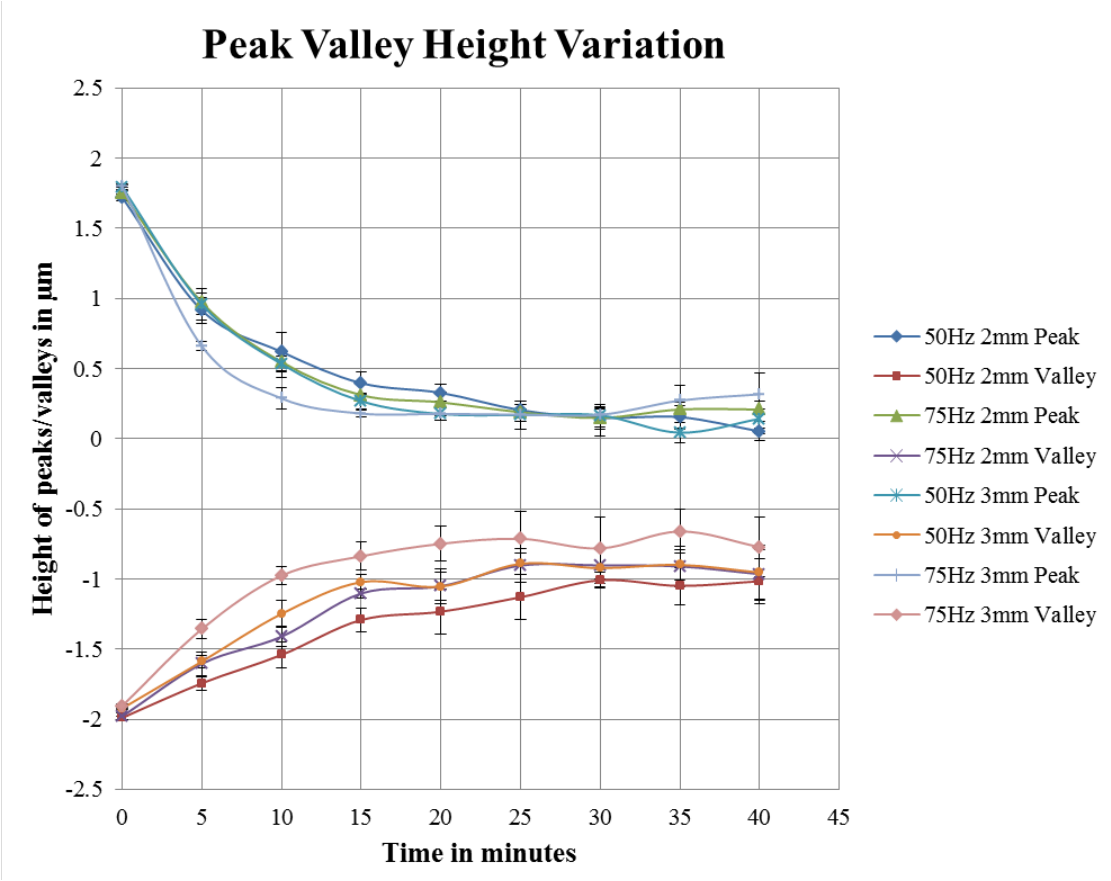

Figure 6.7: Peak Valley Height Variation with time for various levels of DOE

As discussed previously (in chapter 4), only the valley height is considered to calculate the surface modification mechanism, since the valley height increase can result only from plastic deformation, whereas peak height decrease can be due to both plastic deformation and material removal. Figure 6.8 shows the amount of plastic deformation calculated from the rate of change of valley height. As the process progresses, it can be seen from figure 6.7 that the rate of valley height change decreases. This decrease is represented in figure 6.8 as the amount of

plastic deformation. This illustration also has a line fitted linearly to the plastic deformation curve with the equation shown above the graph.

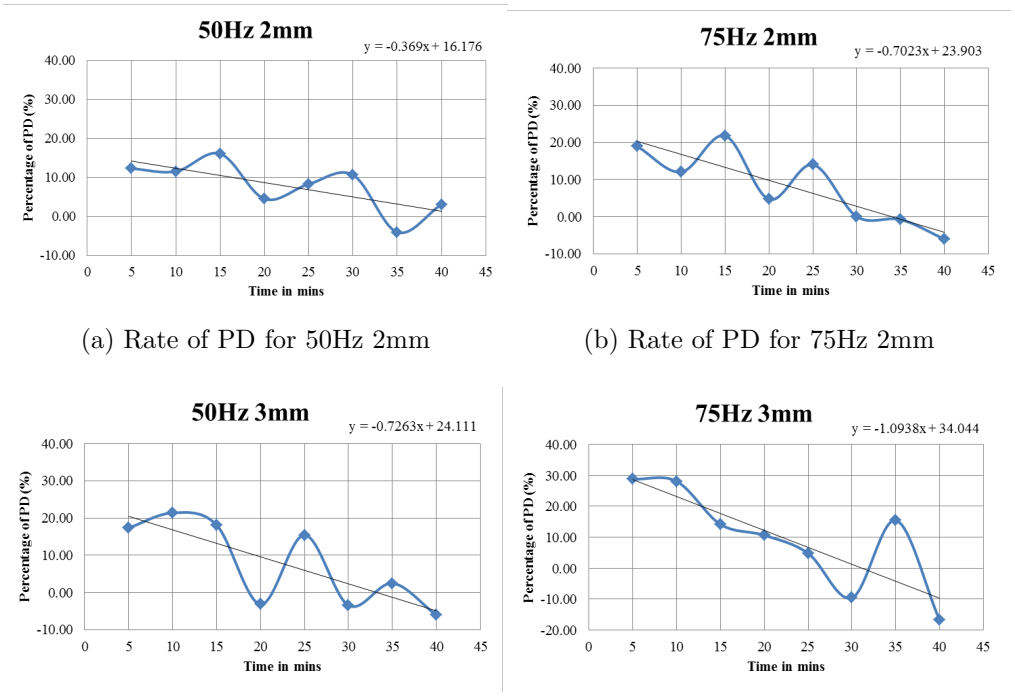

(a) Rate of PD for 50Hz 2mm

(b) Rate of PD for 75Hz 2mm

(c) Rate of PD for 50Hz 3mm

(d) Rate of PD for 75Hz 3mm

Figure 6.8: Rate of Change of PD for various parameters

The slope of the fitted lines is listed in table 6.3.

Table 6.3: Slope of Plastic Deformation (PD) Curves for different conditions

Condition	Slope of best line fit of PD curve
50Hz 2mm	0.369
75Hz 2mm	0.702
50Hz 3mm	0.726
75Hz 3mm	1.094

It can be seen that the slope of the plastic deformation significantly increases as the frequency and amplitude settings are increased from 0.369 for 50Hz-2mm to 1.094 for the 75Hz-3mm condition. But the overall trend of plastic deformation curve, remain the same. This can be seen from the shape of the curve, which are similar for all the four conditions. Hence, this shows clearly that the trend and

surface modification mechanism does not change with frequency and amplitude, but only the rate at which it occurs changes. High frequency and high amplitude setting has the most rapid surface modification mechanism with a slope of 1.094.

The next step is to analyze which factor has more significant effect - frequency or amplitude. This study is conducted in the next section, where the Ra data obtained is used for the statistical analysis of the process parameters - frequency and amplitude.

6.4.5 Analysis of DOE

6.4.5.1 Interaction Plot

This section explains the statistical analysis of the DOE by comparing the different values of Ra obtained for various experiments performed. This analysis is performed using a statistical analysis software, Minitab. Figure 6.9 shows the interaction plot for Ra. It shows the combined effect of frequency and amplitude on the Ra obtained at various time intervals.

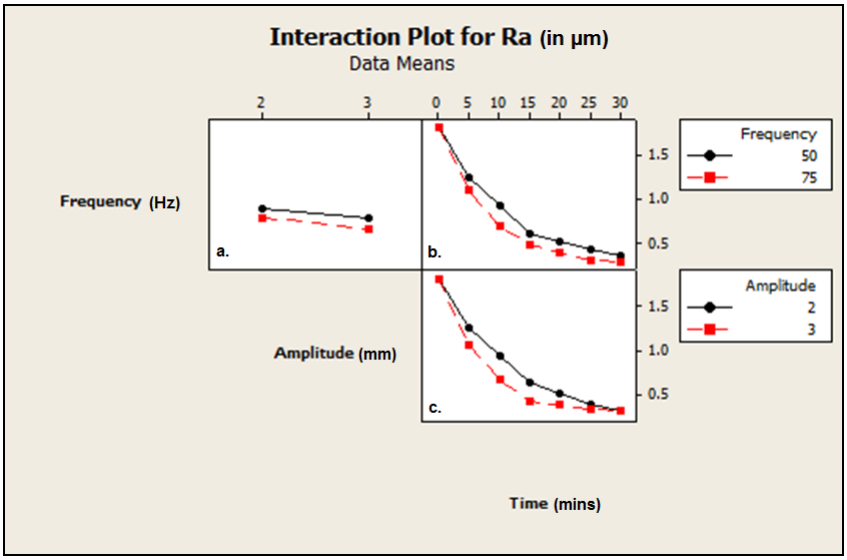

Figure 6.9: Interaction plot for Ra

- Figure 6.9a shows that the effect of frequency and amplitude with time as constant factor. It shows that higher amplitude has lower Ra when frequency is constant, with higher frequency giving better Ra of 0.7μm.

- Figure 6.9b shows the effect of frequency at constant amplitude. It shows that higher frequency reaches a faster saturation as the slope of the red curve (75Hz) is more than that of the black curve (50Hz).
- Figure 6.9 c shows the effect of amplitude at constant frequency. It shows that the higher amplitude reaches a faster saturation as the slope of red curve (3mm) is more that that of black curve (2mm)

The above analysis clearly shows that high frequency and high amplitude are essential for the Ra to be minimum. And with respect to time, the high amplitude shows to achieve a faster saturation than the high frequency. This is analyzed in detail for each time interval in the following section.

6.4.5.2 Pareto Analysis

Figure 6.10 shows the effect of frequency and amplitude on the surface roughness values obtained at various time intervals for the various levels of DOE. Figure 6.10 shows the pareto chart of the standardized effects calculated with a confidence level of 95%. All these pareto charts show that amplitude has an higher effect than the frequency at all the time intervals (figures6.10a, b, c, d) except for 25 mins (Fig. 6.10e) and 30 mins (Fig. 6.10f). This is the period where the saturation occurs. This is mainly because of the lower saturation value achieved by the higher frequency experiments. This shows that for achieving faster saturation, increasing amplitude is the better way and for achieving a lower saturation increasing the frequency is better. So an adaptive machining technology can be developed which can excite the bowl with high amplitude vibrations until the saturation value and change to high frequency vibrations after reaching the saturation point. This way both a faster as well as a lower saturation value can be obtained.

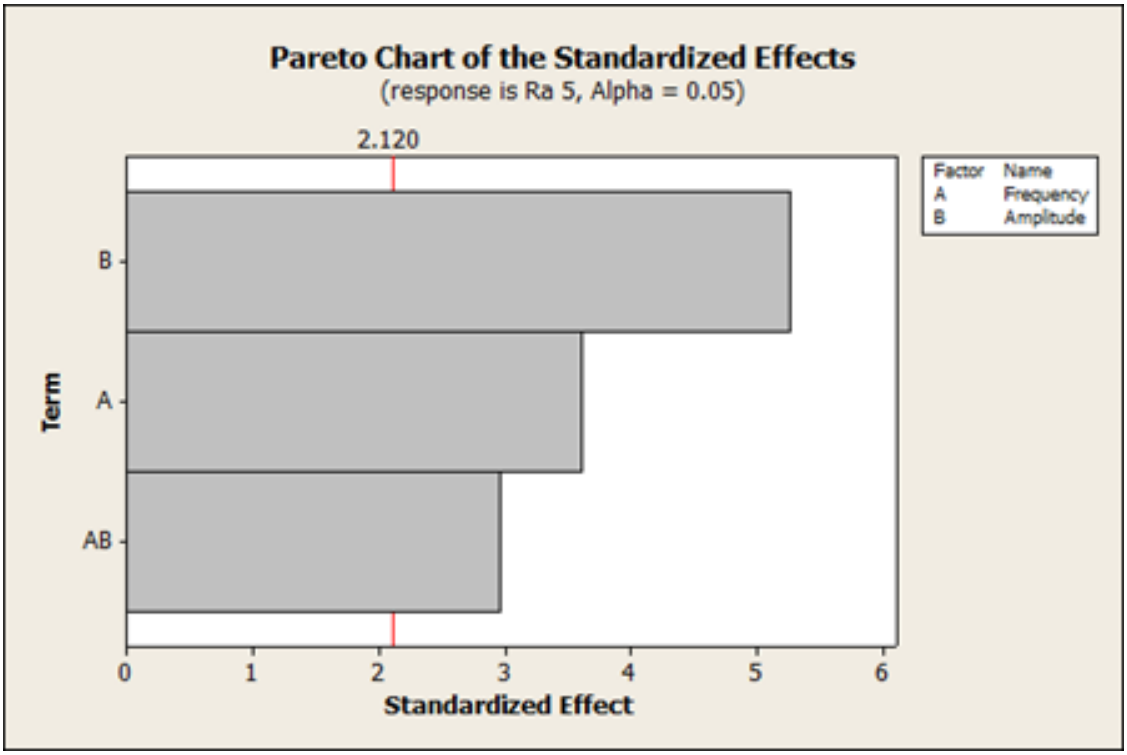

(a) After 5 mins

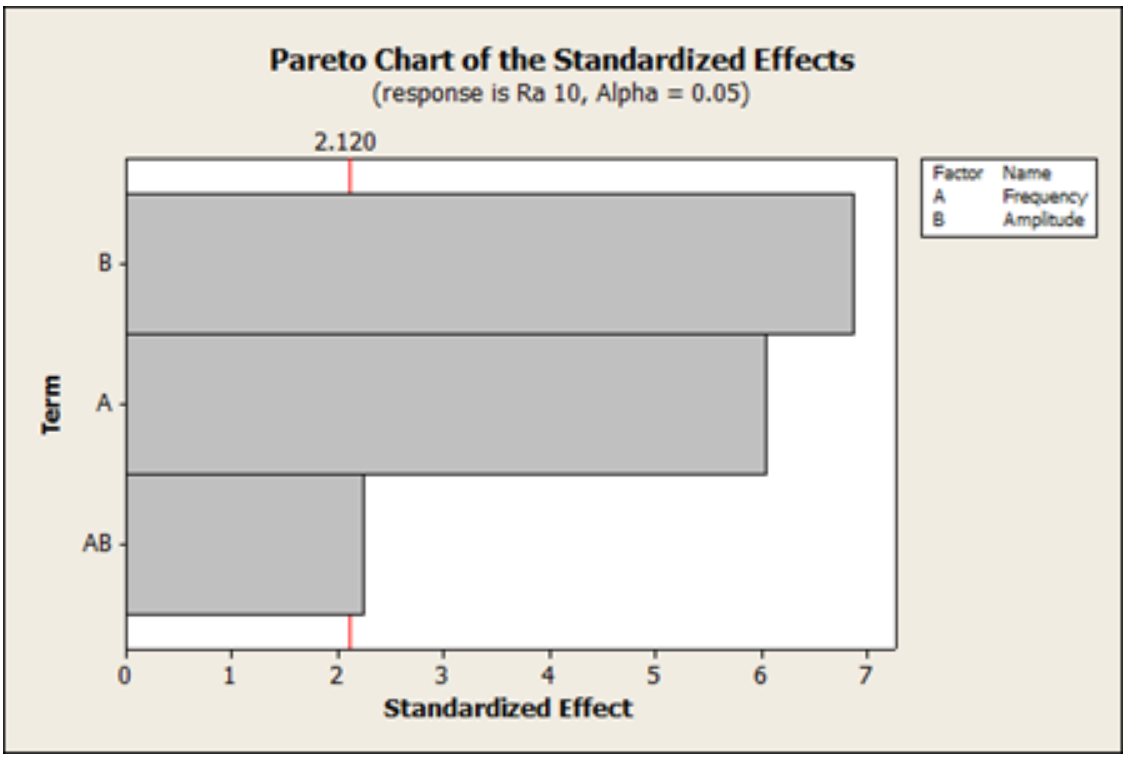

(b) After 10 mins

Figure 6.10: Effect of Frequency and Amplitude at different time intervals

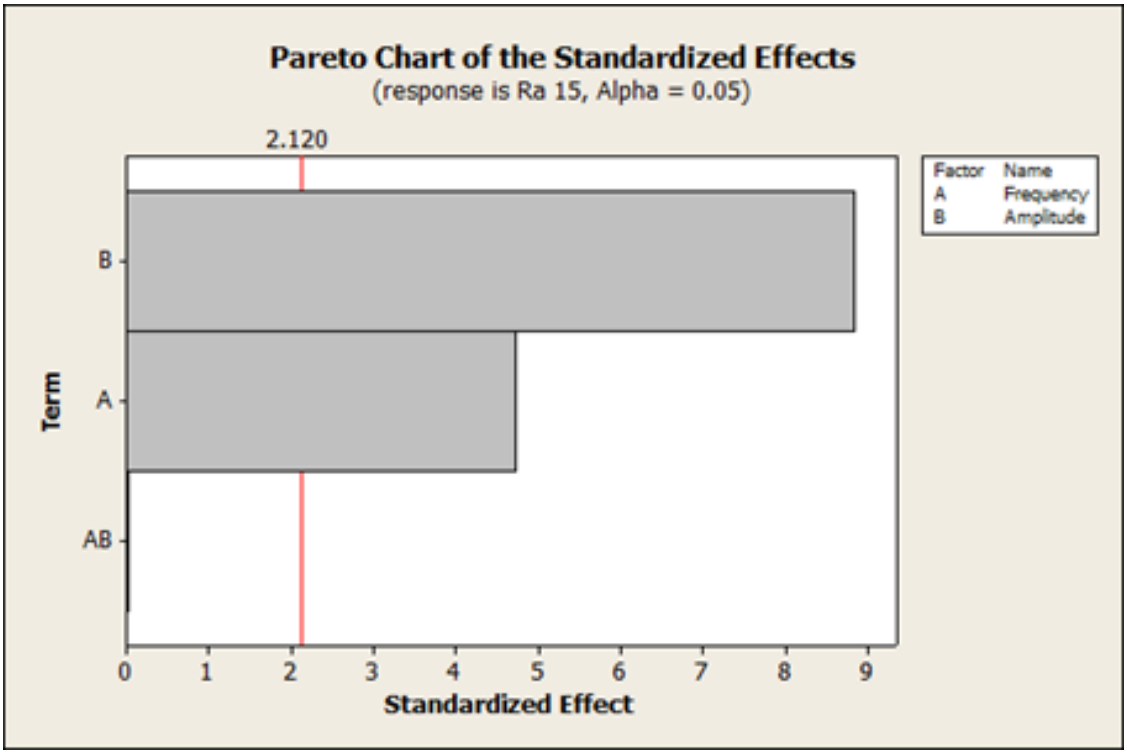

(a) After 15 mins

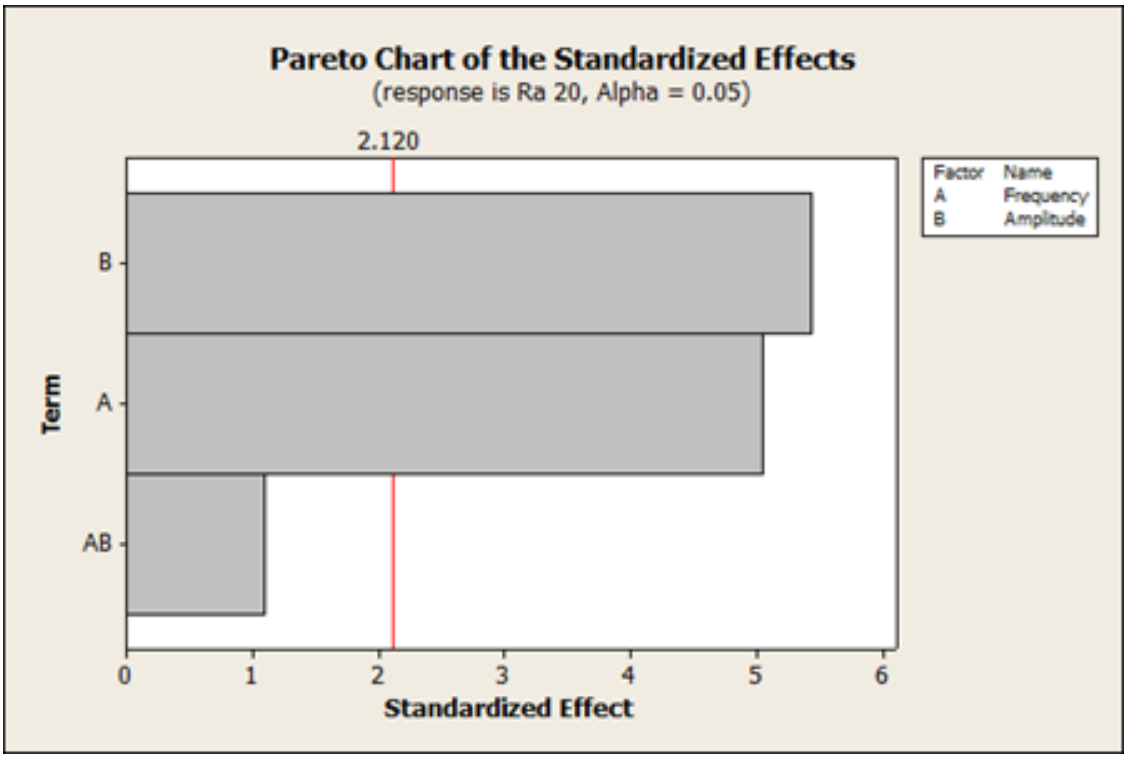

(b) After 20 mins

Figure 6.11: Effect of Frequency and Amplitude at different time intervals

6.5 Summary

The effect of frequency and amplitude of vibrations are tested on the surface modification mechanism and the surface roughness of the workpiece surface. Results

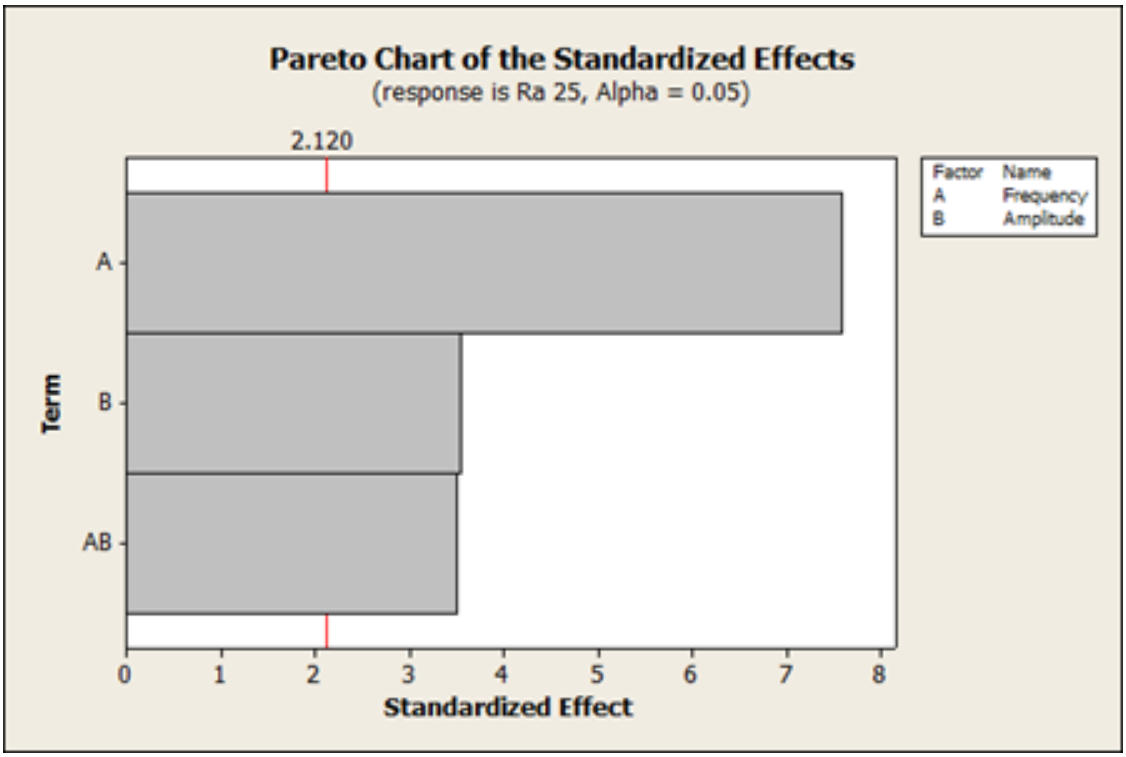

(a) After 25 mins

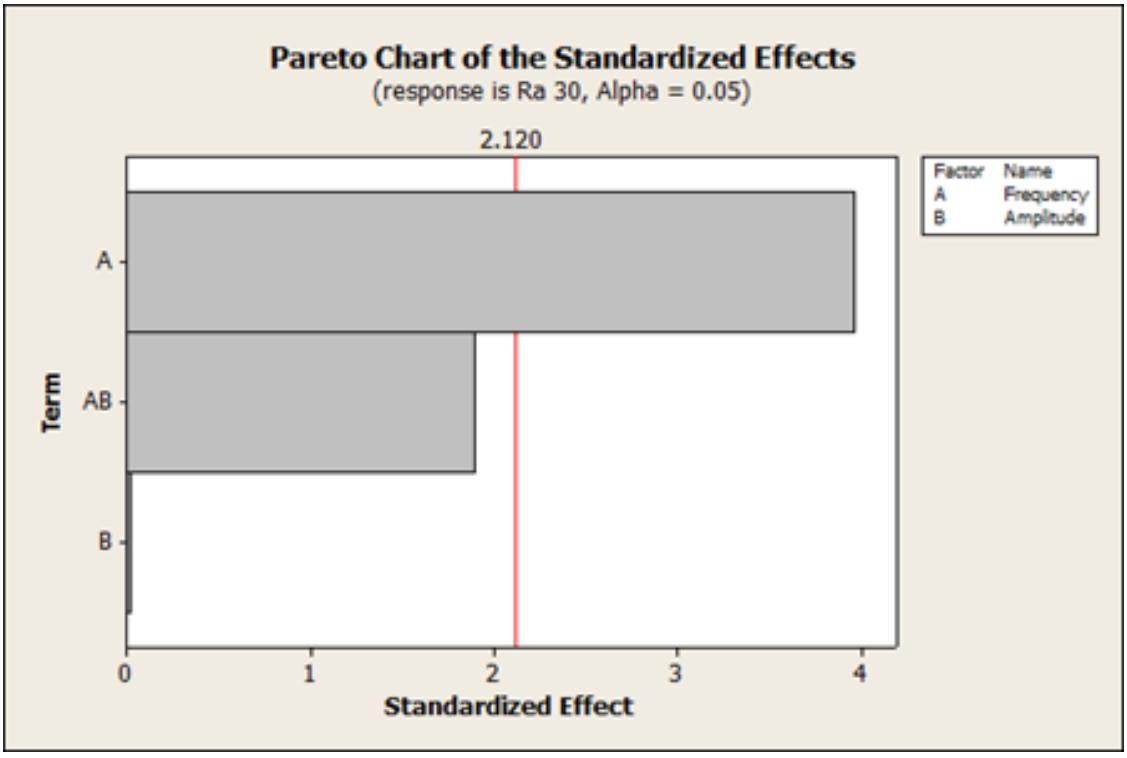

(b) After 30 mins

Figure 6.12: Effect of Frequency and Amplitude at different time intervals

indicate that the increasing amplitude has an higher effect on the surface than increasing the frequency upto the saturation. But after reaching the saturation point,

it is better to increase the frequency. Based on this an adaptive high frequency vibratory finishing process is proposed which employs high amplitude in the initial phase upto saturation followed by high frequency vibrations after saturation.

These results are obtained after a series of preliminary experiments, where all the frequency and amplitude ranges are tested with various types of media. An optimal level of frequency (50Hz to 75Hz) and amplitude (2mm to 3mm) are selected for the tristar ceramic media and the effect of frequency and amplitude are tested by following a full factorial DOE.

Thus a detailed analysis of the surface modification mechanism has been performed for vibratory finishing process in three stages - development of a method to identify the surface modification mechanism (chapter 4), wear debris analysis (chapter 5) and testing the effect of process parameters (chapter 6) on the surface modification mechanism. The next chapter deals with studying this surface modification mechanism from a different perspective - by using a sensor.

Chapter 7

Online Monitoring of Surface Modification

7.1 Overview

The surface of the workpiece being finished using vibratory finishing is usually measured by taking out the workpiece out of the bowl after stopping the process. There is no method currently available to measure or monitor the surface in-situ or online without stopping the process. The objective of this part of the thesis is to investigate the possibility of developing a surface monitoring technique for vibratory finishing process.

This chapter deals with studying the surface modification mechanism of vibratory finishing using the novel technique of surface profile measurement explained in chapter 4 along with the measurement of sensory signals captured from the process with a suitable sensor. The surface modification and the signals are analyzed and the feasibility of using the sensory signal as a method of vibratory finishing process monitoring is investigated.

A detailed literature review was performed (as explained in chapter 2) in order to short list the available sensing parameters and their suitability to vibratory finishing process. This is explained in the following section.

7.2 Sense Parameter Shortlisting

From the detailed literature study of works related to vibratory finishing and related processes and monitoring techniques, the sense parameters have been selected based on the following criteria.

- Relationship with surface roughness
- Feasibility of implementation in vibratory finishing process

Table 7.1 evaluates the suitability of the sense parameters discussed in section 2.7. A ☆ rating is used to represent the correlation with surface roughness and ease of implementation of measurement setup in vibratory finishing process.

The findings of literature review (section 2.7) proved that force and Acoustic Emission (AE) were the most significant parameters which showed a positive correlation with the surface roughness and hence the surface modification mechanism. Also their ease of measurement for vibratory finishing played a major role in their selection. Contact force measurement was initially selected for measurement, but the dynamics of the vibrations were disturbing the force values measured by the sensor. In fact, the noise generated due to vibrations were higher than the actual contact force occurring between the media and workpiece. Hence they were not selected for measurement in the experiments performed for this thesis.

Ultrasonic signals are similar to surface profile measurement using a surface profilometer. Instead of using the stylus, the ultrasonic signals are used to measure the surface characteristics. As explained in section 2.7.8, it does not take the amount of energy imparted by the media or the surface modification mechanism which happens during the process. Hence it has not been selected as a sense parameter in this thesis. Impact velocity was not selected as it required a completely new setup and the use of high speed cameras installed inside the vibratory bowl to monitor and measure the velocity of media motion. Temperature measurement will not work due to the presence of compound which acts as coolant and eddy current cannot be used in an environment involving multiple material properties change

Table 7.1: Evaluation of Sense Parameters

Sense Parameter	Relationship with Surface Modification	Ease of Measurement	Selected	Reason for rejection
Force	☆☆☆☆☆	☆☆☆☆☆	No	Dynamic force of vibrations are more than the contact force
Velocity	☆☆☆	☆☆	No	Measurement require a complex setup of high speed cameras and transparent bowl
Contact Pressure	☆☆☆	☆☆☆☆☆	No	Can be estimated from contact force measurement
Strain Rate	☆☆	☆☆☆☆☆	No	Same as contact force measurement
Temperature	☆☆☆☆	☆☆	No	Difficult to implement and not suitable for vibratory finishing
Eddy Current	☆☆	☆☆	No	Not suitable for vibratory finishing
Radiography	☆	☆	No	Not feasible for vibratory finishing
Ultrasonic Signals	☆☆☆☆	☆☆☆	No	Cannot be implemented for in-situ measurement
Acoustic Emission	☆☆☆☆☆	☆☆☆☆☆	Yes	-

at same time. But the AE signals have been proved by researchers to correlate with the surface roughness. The small size of the AE sensors makes them possible to be easily mount on the workpiece surface. In addition to all these the acoustic emissions are highly sensitive to even small deformations. As explained earlier in chapter 4, the change in surface profile of even a few micro meters can be detected

by AE sensors. the Hence Acoustic Emission was selected as a sense parameter to be used for developing an online monitoring technique for vibratory finishing process. The following section describes the selection criteria used for the selection of Acoustic Emission sensors.

7.3 Selection of Acoustic Emission Sensors

Acoustic Emission (AE) was selected as the sensory parameter to be measured. In order to implement the AE measurement in the vibratory finishing setup, a suitable sensor was selected based on the operating frequency range of the sensor. The frequency range in which the signals caused by different kinds of wear mechanisms occurs has been consolidated by Hase et al. (2012). This is illustrated in figure 7.1. It is clear that the frequency range of abrasive wear falls between 250kHz to 1MHz. Hence the AE sensor which had it's operating frequency in this range was selected.

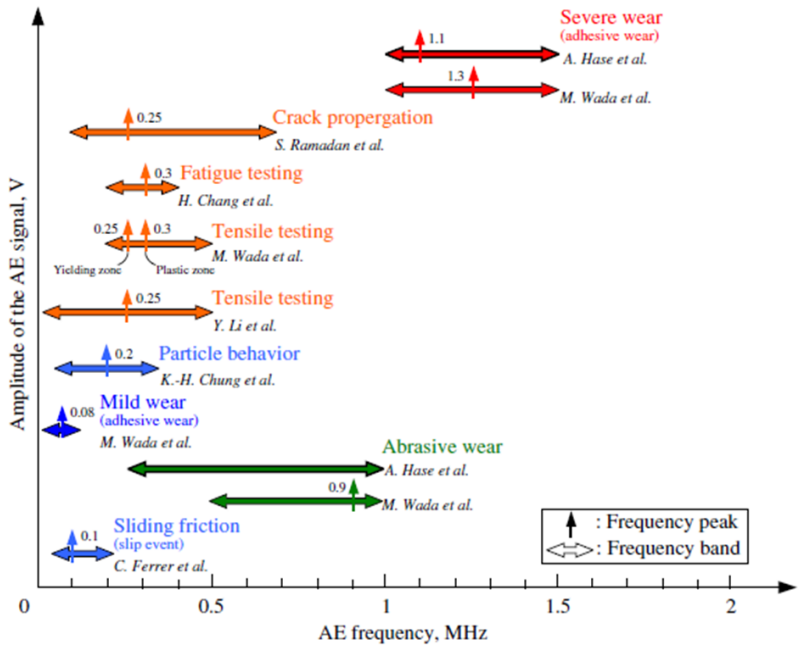

Figure 7.1: Frequency Ranges of different Wear Mechanisms (Hase et al., 2012)

ISWD sensor used for this thesis has it's operating frequency in the range of 150KHz to 850KHz which falls in this region. In addition to this, the hard case

protection in ISWD played a major role in the selection of these sensors for this thesis.

7.4 Acoustic Emission Measurement Setup

Acoustic Emission measurement is performed using the two types of Acoustic Emission (AE) sensors as explained in section 3.8.1. The measurement setup for both these sensors is the same which is explained in the following section. The measurement setup comprises of a physical noise isolation part which isolates the measurement area from the rest of the vibratory finishing setup. A CAD schematic of this setup is shown in figure 7.2. There is a central part of the workpiece which is wire-cut and isolated from the rest of the fixture. There is a small gap of about 1mm between the central part and the rest of the workpiece. This central part is directly attached to the sensor by an epoxy adhesive which also acts as a coupling agent between the sensor and the workpiece. The sensor is then mounted on the anti-vibration pad which is in-turn mounted on to the fixture. The only connection between this isolated part and the rest of the machine is the anti-vibration pad. A MISUMI anti-vibration pad of 3mm thickness was used and it protects the vibrations and shocks from the rest of the machine being passed on to the sensor and affecting the data. This setup is mounted on a fixture as explained previously in section 3.3.1.

Figure 7.3a shows the closed fixture having the isolated part of the workpiece and 7.3b shows how the workpiece is mounted on to the sensor which is in turn fixed on a dynamometer. This setup was initially used to measure the force signals along with acoustic emission. However, force signals were not used since the noise due to dynamics was higher than the actual force signals, but the setup remained the same.

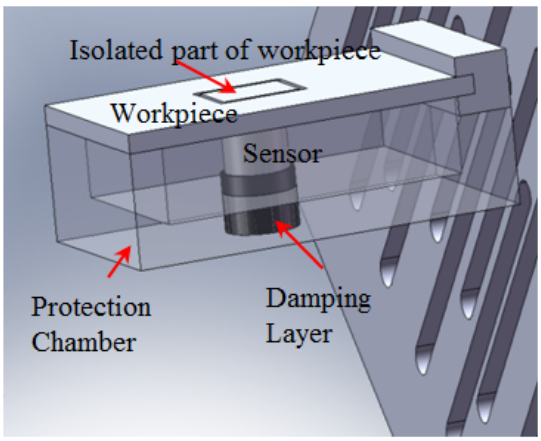

Figure 7.2: Schematic of Acoustic Emission Measurement

(a) Closed with cover plate

(b) Cover plate opened showing workpiece and sensor

Figure 7.3: Actual Fixture Used

7.5 Acoustic Emission Parameters

As explained in section 2.7.9, acoustic emission is the shock wave generated either by the contact between the media and workpiece or it can be due to movement of dislocations inside the workpiece. These shock waves are transferred to a piezo-electric transducer which converts the shock waves into electrical signals. These signals are then converted into digital form by a Data Acquisition System (DAQ) and stored in a computer for further analysis. The raw data represents the output which comes directly from the sensor after passing through the analog filters. The raw data obtained from one of the measurements is shown in figure 7.4.

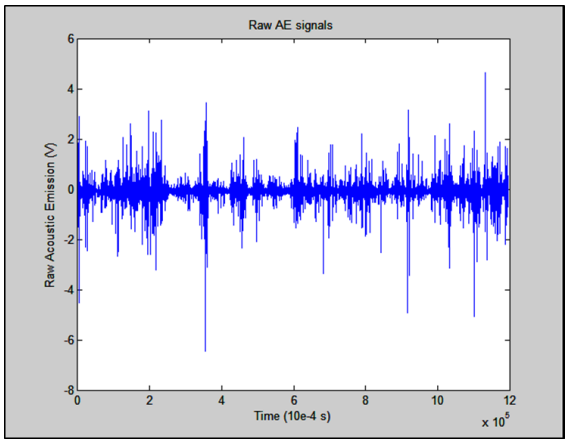

Figure 7.4: Raw AE signal obtained

This raw data is composed of many small features called "Hits". Each Hit is considered to be a set of definite waveforms. The parameters which are used to define a Hit are explained in the next section. Figure 7.5 shows a single Hit from which a set of parameters can be calculated from the raw signal. They are as follows.

- Amplitude
- Rise time
- Energy
- Peak Count

Amplitude is the maximum value (positive or negative) of the signal obtained at the particular time interval. The amplitude is represented in dB (decibel) using the relationship in equation 7.1.

$$dB = 20\log(V_{max}/1\mu - volt) - (Preamplifier\,Gain\,in\,dB) \tag{7.1}$$

where V_{max} is the maximum voltage level obtained. For example if the preamplifier gain is 40dB and maximum voltage detected is 1volt, the amplitude is 40dB.

Rise time is the time required to reach the maximum amplitude.

Energy is the value of the area covered by the AE signals above a certain threshold level. It is the integral of the voltage signal over the duration of AE Hit. It

is represented in microvolt-seconds (voltage integrated over time represented in microseconds).

Peak counts are calculated by counting the number of peaks which crosses a certain threshold value as shown in figure 7.5. Figure shows there are 17 peak counts.

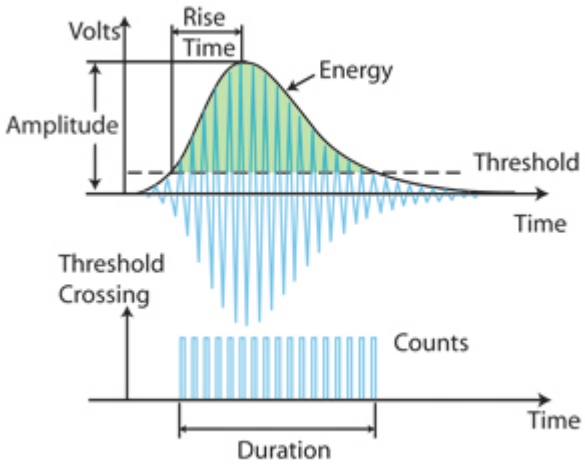

Figure 7.5: AE Parameters calculated from a single 'Hit'

In addition to this, there are also time driven parameters like,

- Root Mean Square (RMS)
- Average Signal Level (ASL)

RMS (Root Mean Square) is calculated using the formula presented in equation 7.2.

$$RMS = \sqrt{\sum \frac{x_n^2}{n}} \tag{7.2}$$

where x_n is the value of the signal occurring at certain time interval and n is number of signals measured at the same time interval.

ASL (Average Signal Level) is the value of amplitude averaged over a particular time interval.

For this thesis, the parameters which will be used are Energy and the Peak count. These parameters are chosen based on their correlation with the surface

roughness as explained in section 2.7. The selection of parameters was also based on several preliminary experiments, ranging from scratch tests performed in a tribometer to AE measurements in 2D bowl discussed in chapter 6.

In short, energy directly represents the amount of energy provided by the contact between the media and workpiece. Peak count represents the duration or the number of contacts. For example, if a high energy impact contact occurs, it will have a high energy. This high energy contact can cause sufficient material deformation only when it occurs for a certain time interval which is represented by the peak counts. Hence for material deformation to occur, both these parameters should be high. Hence a correlation has been developed between the amount of surface deformation and these parameters using the results obtained. It is to be noted that only the plastic deformation type of surface modification mechanism has been used for the correlation.

7.6 Signal Processing

The raw signals which are converted into digital form are computed by a software suite called AEWin^{TM} provided by Physical Acoustic Corporation. This software computes the various characteristics of the acoustic emission signals as explained in the previous section with three user defined inputs such as,

- Peak Definition Time (PDT)
- Hit Definition Time (HDT)
- Hit Lockout Time (HLT)

Peak Definition Time (PDT) is the amount of time required to record the peak value. Hit Definition Time (HDT) is the amount of time required to record a Hit, which is defined as the one complete acoustic emission signal waveform. The Hit Lockout Time (HLT) is the time required to complete the Hit recognition and start the next peak definition time. The standard method of determining these three parameters are explained in section A.3.1 of Appendix A.

The PDT, HDT and HLT is determined by observing the raw signals obtained from the vibratory finishing process. Figure 7.6 shows a magnified single Hit obtained from the AE raw signals with time (in μs) in x-axis and voltage (in mV) in y-axis obtained from a MV32 vibratory finishing machine with tristar ceramic media explained in chapter 4. It can be seen that the duration of single pulse is 21823000μs to 21828000μs which is equal to 5000μs. The peak occurs between the first half of the pulse and hence the PDT is chosen as 3000μs and HDT is chosen as 3000μs and HLT as 2000μs. So the software will calculate the peak in the first 3000μs and complete the hit recognition in the next 3000μs and will start the next PDT after 2000μs. This calculation was performed after several trial and errors so that no acoustic emission signals are characterized as multiple or erroneous signals.

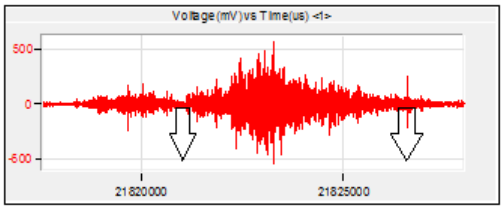

Figure 7.6: Single Hit obtained from Raw Signal

7.7 Experiments Conducted

Using the above setup and methodology, AE measurement was performed along with the saturation experiments conducted using the measurement technique for surface modification mechanism as explained in section 4.7. A Ti6Al4V structured surface has been used so that the surface modification mechanism can be correlated to the change in surface characteristics as well the change in acoustic emission parameters. The AE signals were measured using an ISWD sensor with PAC-PCI2 DAQ at a sampling frequency of 2MHz as explained in section 3.8. This sensor and DAQ system was specifically selected and acquired for this thesis based on its operating frequency range and suitability for the process. The parameters such as Energy and Peak count were calculated as discussed in the previous section. The

results are explained in the following section.

7.8 Analysis of Results

7.8.1 Evolution of Surface Roughness

From figure 4.17 from section 4.7 of Chapter 4, it can be seen that the surface roughness reaches a saturation value of 0.2μm around 160 mins. The acoustic emission values measured during these experiments are explained in the next section.

7.8.2 Evolution of Acoustic Emission Peak Count

The AE signals were measured for a duration of around 5 minutes for each time interval and the parameters were normalized by dividing them with the number of seconds, so that a comparison can be made. The first AE parameter calculated was the peak count. The threshold level for the peak count was selected by conducting trial experiments where the signals from other parts of the machine other than the central isolated workpiece are not being detected by the sensor. In other words, this threshold was the minimum value which the media workpiece contact generated and it was 40dB. Figure 7.7 represents the mean value of the peak count calculated by AEWin^{TM} software for a set of three saturation experiments. The average value of standard error was 4.3%. It can be seen that the number of peaks starts at 10000 and gradually reduces as it reaches 160 minutes. It was mentioned in the previous section that the saturation for these experiments happens around 160 mins.

7.8.3 Evolution of Acoustic Emission Energy

Another AE parameter which have been calculated from the raw AE signals was the Energy of the acoustic emission signals. As explained earlier, the energy is the integral of the acoustic emission signals obtained and is represented in microvolt-seconds. Since the parameters are normalized by dividing it by the number of

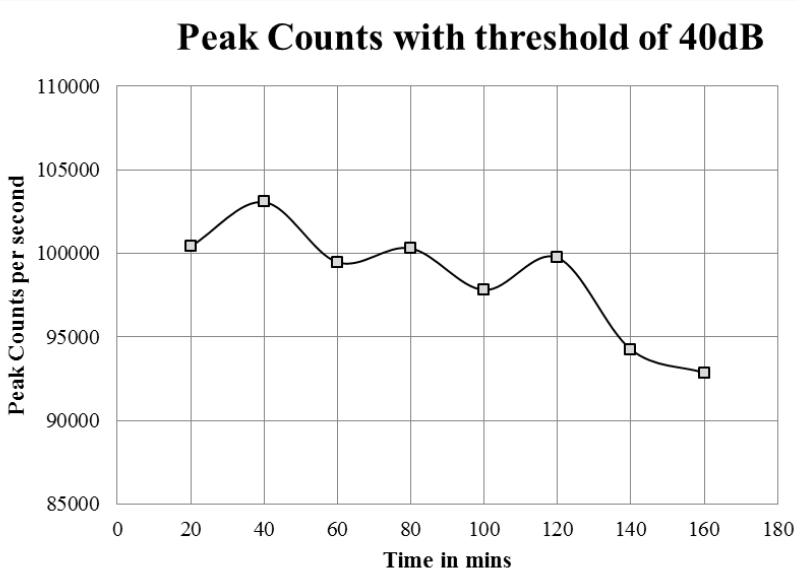

Figure 7.7: Evolution of Peak Counts from three saturation experiments

seconds, the energy is represented in micro-volts. Figure 7.8 shows the energy of the acoustic emission signals obtained during the three saturation experiments. The average value of standard error was 13.5%. This energy curve also follows the same trend as the peak count, that is, it starts with an initial value of around 65000 μvolts and gradually reduces as it reaches saturation point of 160 minutes. These two curves are compared with the amount of plastic deformation calculated from the measurement technique discussed in chapter 4 in the next section.

7.8.4 Correlation with Surface Modification Mechanism

Figure 7.9 shows the comparison of amount of plastic deformation calculated from the masked reference method (explained in chapter 4) and the Peak Counts explained in the previous section. Figure 7.10 shows the comparison of amount of plastic deformation with the AE Energy discussed in the previous section. It shows that the mean values of both the AE energy and AE peak count follows the same trend as the amount of plastic deformation. This represents that the amount of physical energy supplied by the vibratory finishing reduces as the time progresses. But in vibratory finishing, the amount of energy supplied at various time intervals

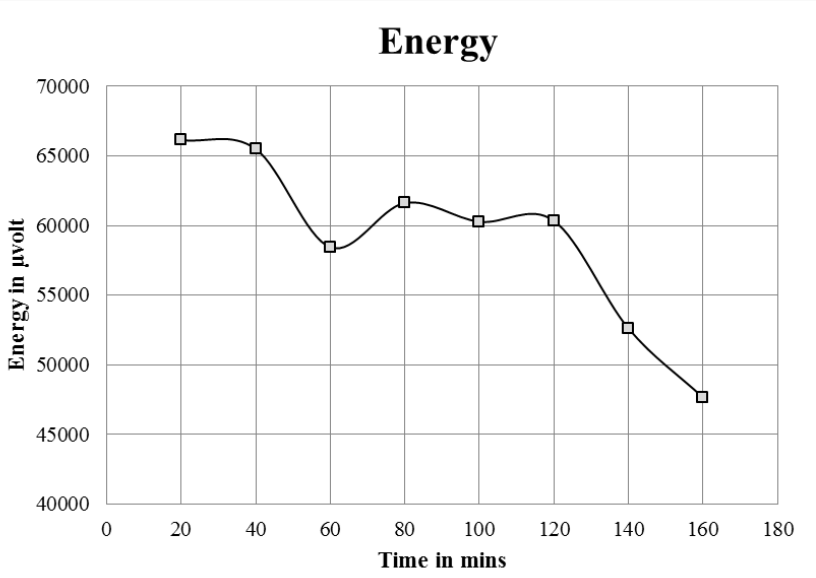

Figure 7.8: Evolution of Energy from three saturation experiments

is almost constant (as the operating conditions are constant neglecting the media wear). The only change which occurs in the process is the profile of the surface being polished. This is explained in this section.

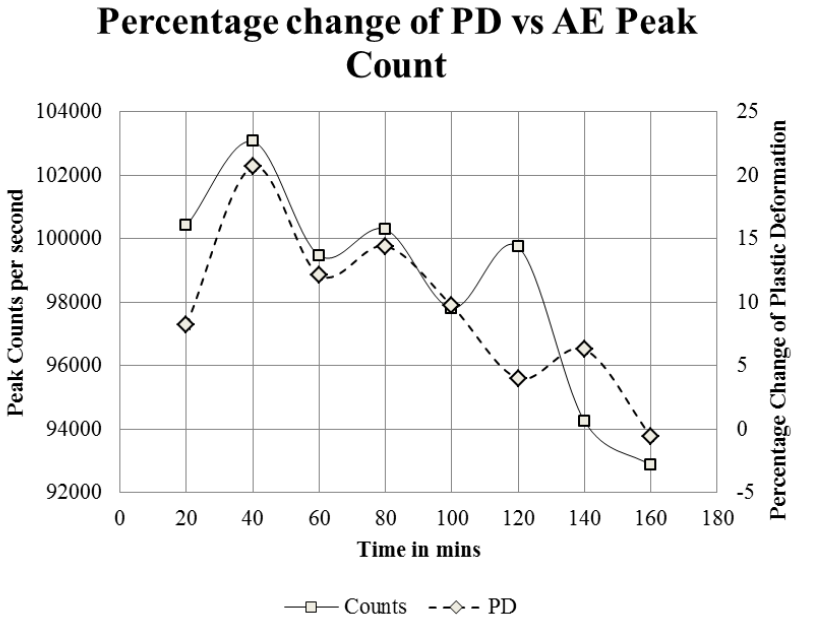

Figure 7.9: Comparison of Peak Count and Percentage of Plastic Deformation with time

Figure 7.11 shows a schematic of profile evolution occurring in vibratory finishing process. It is hypothesized that the amount of deformation depends on the

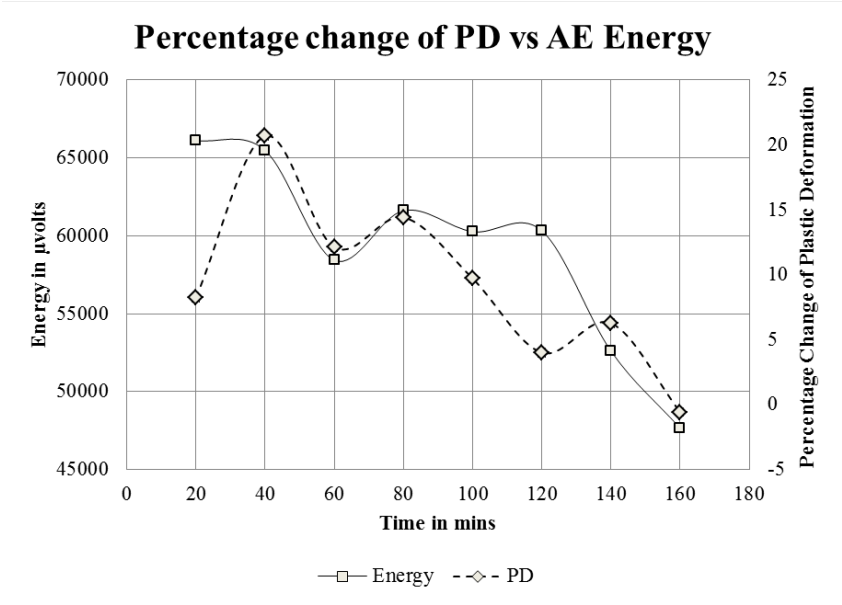

Figure 7.10: Comparison of Energy and Percentage of Plastic Deformation with time

amount of valleys present in the surface. When an initial structured surface gets polished by the media, the amount of valleys available for deformation is quite large. As the surface is getting polished, the peaks and valleys are modified and the amount of valley available for deformation reduces. When the surface reaches saturation, the valleys are completely filled forming an almost smooth surface. The surface roughness value, amount of plastic deformation and the acoustic emission signals follows the same trend which is explained as follows.

Acoustic Emission (AE) peak count can be correlated to the number of contacs of the media particles on the surface of the workpiece. It is to be noted that in vibratory finishing there are three types of contacts viz. impact, scratching and rolling. Peak count takes all these types of contacts into consideration. When the peak count reduces, it means that there is a reduction in number of contacts of media on the surface of the workpiece. This can be attributed to the change in surface roughness of the workpiece. As the surface becomes smoother, there are less number of peaks and valleys (as shown in figure 7.11) which are available for the media particles to contact and hence there is a reduction in peak count.

Similarly AE energy can be correlated to the intensity of the contact. As the

number of contacts decreases, the intensity also decreases since there are absence of contacts and surface peaks/valleys resulting in an energy transmission. This analogy is in accordance with the results obtained by Ivantsiv et al. (2009).

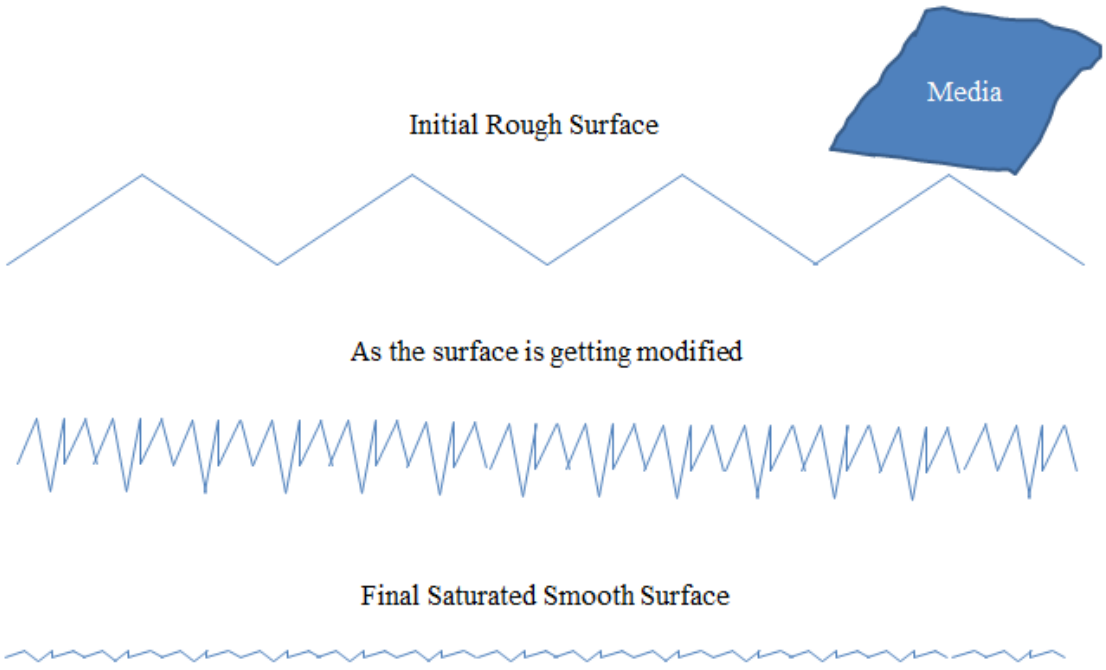

Figure 7.11: Analogy for explaining peak count behavior

The AE Energy, Peak Counts, the percentage of plastic deformation and Ra were compared with the correlation formula explained in equation7.3.

$$Corr = \frac{\sum(x-\bar{x})(y-\bar{y})}{\sqrt{\sum(x-\bar{x})^2(y-\bar{y})^2}} \tag{7.3}$$

where x is the value of the variable 1, y is the value of variable 2, $\bar{x}$ is the average value of the variable 1 and $\bar{y}$ is the average value of variable 2. Table 7.2 tabulates the value of correlation coefficients calculated between Energy, Peak Counts, amount of change in plastic deformation (PD) and change in Ra.

It can be seen that the AE Peak Counts offers a better correlation of 0.88 with Ra and 0.80 with the amount of plastic deformation, whereas the AE Energy offers a lesser correlation coefficient of 0.86 with Ra and 0.71 with the amount of plastic deformation. Acoustic Emission parameters have been correlated with the

Table 7.2: Correlation between AE Energy, Peak Count, PD and Ra

	Counts	Ra	PD	Energy
Counts	1			
Ra	0.88	1		
PD	0.80	0.81	1	
Energy	0.94	0.86	0.71	1

change in surface roughness and the amount of plastic deformation. The maximum percentage of correlation obtained at this stage is about 88% for AE Peak Count vs Surface Roughness. Even though this number is significantly high, this represents only the correlation values obtained for the average values obtained from the experiments performed. There was an average standard error of 4.3% for Peak Counts and 13.5% for Energy. Hence these results have to be analyzed taking these limitations into consideration. Since there is no other online monitoring technique (for vibratory finishing) currently available to compare this result numerically, this study can be concluded as the first step in developing a monitoring technique for the surface roughness and plastic deformation using acoustic emission. A detailed recommendations for improving this work is presented along with the conclusions in chapter 8.

7.9 Summary

Acoustic Emission (AE) was selected from a list of sense parameters shortlisted from the literature review for developing an online monitoring technique for vibratory finishing process. A specialized measurement setup and methodology were developed to measure the acoustic emission resulting from the workpiece media contact in vibratory finishing. AE Parameters such as peak counts and energy were calculated from the recorded signals. They were correlated with the change in amount of Ra and the plastic deformation (calculated using the measurement technique developed in chapter 4) occurring on the surface. Even though the correlation was prone to errors, there was a significant correlation obtained between the AE parameters and surface roughness obtained. Hence Acoustic Emission is

proposed as a new online monitoring technique for vibratory finishing. But as the results indicate, this technique is still prone to errors and it is still far from being implemented on an industrial scale to predict the end-point of surface roughness or the type of modification mechanism in vibratory finishing.

Thus a detailed study about the surface modification mechanism in vibratory finishing is performed in four stages as mentioned in the introduction - masked reference method, wear debris analysis, effect of process parameters and online monitoring. The following chapter summarizes all the results and concludes the thesis along with some recommendations for future work.

Chapter 8

Conclusion and Future Works

8.1 Conclusion

An experimental investigation of vibratory finishing process has been performed and the surface modification mechanism is studied experimentally. The investigations can be summarized as follows.

- The surface modification mechanism in vibratory finishing has been identified, analyzed by using a novel measurement technique involving the measurement of peaks and valleys. It was found that material removal and plastic deformation together causes the saturation. But amount of material removed cannot be calculated accurately, only plastic deformation was calcuated. A correlation coefficient of 0.94 was obtained between the amount of plastic deformation calculated by this method and the rate of change of Ra.
- Wear debris analysis was introduced to vibratory finishing using magnetic separation method. Various shapes and sizes of wear debris particles were identified and analyzed. The size of wear debris particles reduced as the surface was polished, but the different types of shapes were obtained indicating the presence of various types of contacts and wear mechanisms in vibratory finishing.
- The effect of process parameters such as the frequency and amplitude on the

surface modification was tested. The results show that the surface modification mechanism do no change but the rate at which the surface modification happens increases with increase in frequency and amplitude.

- Acoustic Emission signals emitted due to the media-workpiece have been measured, analyzed and related to the surface modification mechanism and surface roughness. Parameters such as peak count and energy was correlated with surface parameters. A correlation coefficient of 0.88 was obtained between the rate of change of Ra and peak count. Hence this method is proposed as an online monitoring technique for surface roughness in vibratory finishing.

This chapter concludes this thesis by summarizing in detail the results obtained in each chapter. This is followed by presenting the significant contribution from the works presented in this thesis and recommendations for future work.

8.2 Summary

8.2.1 Surface Modification Mechanism

As mentioned earlier, an initial surface can be modified basically by two mechanisms - material removal and plastic deformation. The challenge lies in differentiating and measuring this mechanism and identifying which mechanism results in the surface modification. This thesis studied the surface modification mechanism using a novel method of surface profile measurement.

The peaks and valleys were measured at certain time intervals with respect to a constant reference line. In order to achieve this, a novel method of masking was developed. A part of the surface being finished was masked from the action of media using a masking tape. This masked part of the surface acted as a reference line for the surface being polished. The change in position of peaks and valleys were compared with respect to this masked reference and the mechanism was identified by the behavior of these peak and valley positions as follows.

When average peak position comes down with respect to a constant reference, it indicates that the peaks are being removed. This removal can be due to either material removal or plastic deformation. When the average valley position comes down with respect to a constant reference it indicates that more valleys are being created. This can also happen due to either material removal or plastic deformation.

But when the average valley position move up with respect to a constant reference line it indicates that the valleys are being filled with material. This filling can occur due to the local melting of peaks and material flowing to the valleys or plastic flow of peaks inside the valleys due to plastic deformation. The possibility of the melting is not considered due to the nature of contact and only the valley filling is assumed to be only due to plastic deformation.

Conclusion: Only the valley height increase have been related to the plastic deformation as the peak height reduction can be due to both material removal and plastic deformation.The valley behavior for a Ti-6Al-4V work surface (for the specified media and vibratory conditions) showed that there is an initial removal of material which is followed by the plastic deformation which results in the surface saturation. These results have also been validated by observing the physical features developed on the surface such as scratches and plastically deformed layers. A correlation coefficient of 0.94 was obtained between the amount of plastic deformation calculated by this method and rate of change of Ra.

8.2.2 Wear Debris Analysis

Wear debris analysis is another way of determining the surface modification mechanism, as it is the direct byproduct of the surface modification. But there are challenges involved in the collection and analysis of wear debris particles, particularly for vibratory finishing. This was mainly due to presence of wear debris particles resulting from the media which is very high when compared to the parts. As mentioned, in a typical vibratory bowl, the ratio of part to media volume will be more than 1:1000. So finding and locating the wear debris of the parts is extremely

difficult. But a novel method of collecting the wear debris from the surface of the part is presented in this thesis.

The wear debris particles which were still lying on the surface of the workpiece were removed physically and the particles from the part were separated using a magnet. These particles were then analyzed in a SEM from which the size and shape characteristics were recorded and analyzed manually. In order to do this, the debris resulting from the part had to be magnetic. A non-magnetic material was also tested, but the presence of wear debris particles from the part was very small and the results were not repeatable. Hence a duplex stainless steel part has been used to perform the wear debris analysis and the results show that there is a definite trend in the size of the wear debris particles analyzed. Two types of experiments were performed - one in a controlled setup and another in an actual bowl. A controlled setup was used with a plastic media in a small chamber attached to the bowl. This was performed in order to facilitate and accelerate the process of wear debris formation, since the plastic media does not generate debris and the wear debris particles cannot escape the chamber. The next experiment was performed in a small bench type vibratory bowl in order to reduce the amount of media particles. This size and shape recorded were compared with the surface roughness and the surface modification mechanism.

Conclusion: The results show that the average size of the particles decreases with respect to time and the analysis of surface topography in SEM showed that there is a mixture of both material removal and plastic deformation occurring in the process. But this is just an overall observation and an in-depth analysis have to performed to understand the surface modification mechanism more clearly.

8.2.3 Effect of Process Parameters

Effect of process parameters such as the frequency and amplitude of vibrations on the surface modification mechanism were studied using a custom built 2D vibratory finishing setup. This custom setup was built since the frequency and amplitude

cannot be controlled accurately in traditional vibratory finishing process. A hydrodynamic shaker usually used for structural testing was modified to replicate the vibratory finishing process. A rectangular chamber was fabricated and attached to the shaker head. The 1D vibrations from the shaker was transferred to the bowl and in turn to the media particles. This caused the media to rotate inside the bowl as explained in chapter 6 and hence the name 2D vibratory finishing. Experiments were performed on this new setup to test the effect of frequency and amplitude since the frequency and amplitude are the principal parameters which decides the type of contact between the media and workpiece, for a particular media-workpiece combination.

Prior to this, a detailed comparison was made between the newly developed process and the traditional process. Even though the power supplied in terms of frequency and amplitude are same, the net energy supplied is not same since only a small portion of media is used in this newly developed process. But when a very soft material like aluminum was used, it was observed that the polishing achieved was similar and comparable to the traditional process. Hence a DOE and experiments were performed on this setup to test the effect of frequency and amplitude.

The frequency and amplitude used in traditional vibratory finishing was 50Hz and 2mm. These values were increased 1.5 times and a frequency and amplitude of 75Hz and 3mm were tested. A simple full factorial DOE with 2 levels for frequency and 2 levels for amplitude was performed.

Conclusion: The results showed that the increase in frequency and amplitude does not change the surface modification mechanism, but only changes the rate at which the surface modification occurs. The effect of frequency and amplitude was also studied and it was found that amplitude has an higher effect than the frequency upto saturation and after saturation, frequency has an higher effect. These results have been used to propose a new kind of vibratory finishing called adaptive high frequency-amplitude vibratory finishing which employs high amplitude in the initial phase upto saturation followed by high frequency vibrations after saturation. This

process can attain a faster saturation with low polishing times.

8.2.4 Online Monitoring using Acoustic Emission

Vibratory finishing has been in use for more than a few decades now and still the process is run based on a trial and error basis. In this world of modern innovations, it is essential to make the process more efficient and smarter. Using the understanding of the surface modification mechanism from the previous works, it was analyzed how to make the process more efficient by using smart sensors. From a detailed literature review, acoustic emission was selected to monitor the surface modification online during the polishing, without disturbing the process. The acoustic emission is just the shock waves generated by the workpiece-media contact which can be recorded by using a sensor which has a piezo-electric crystal which converts the shock waves into electric pulses. These electric pulses were analyzed and correlated with the surface modification mechanism. So mounting a sensor with the workpiece for the measurement of the shock waves can record the signals. And as the surface gets modified different shock waves will be generated, which when analyzed can give the change in surface modification mechanism.

There were a lot of challenges faced in measuring the correct acoustic signals and filtering the noise generated by the process. In addition to the workpiece-media contact there are numerous other contacts and mechanisms occurring in vibratory finishing which can disturb the acoustic emission signals from the workpiece media contact. Hence it is essential to measure the signals originating only from this kind of contact.

In order to achieve this, a combination of physical noise filtering techniques were designed and used. A small portion of workpiece was wire-cut from the rest of the workpiece and it was physically isolated from the rest of the process. An acoustic emission sensor was attached to this isolated workpiece. By doing this, the noise generated from the rest of the machine was restricted from being passed on to the sensor. But as any physical mechanism is prone to errors and since this a

dynamic process, the mechanism was not fully efficient. There was a small amount of noise being transmitted to the sensor. In addition to this, there electrical noise was an in-built noise being generated from the sensor.

The signals obtained using the above measurement method was analyzed, and it was found to be in accordance with the plastic deformation mechanism and surface roughness. As the plastic deformation mechanism and surface roughness reduces, the amount of acoustic emission parameters such as energy and peak counts also decreases. A correlation coefficient of 0.88 was obtained between the peak count and rate of change of surface roughness.

8.3 Significant Contribution of this research

The significant contributions of this thesis work can be stated as follows.

As explained, the thesis has four parts and each of these four parts has a significant contribution to the research community.

- The knowledge of surface modification mechanism in vibratory finishing was not known initially, but now using the methods presented in this thesis it is possible to study the surface modification mechanism of vibratory finishing process.
- This can be stated both in terms of wear debris analysis as well the measurement technique developed since the wear debris analysis have not been performed for vibratory finishing process yet.
- This work also makes its contribution in terms of acoustic emission monitoring for the vibratory finishing process. The understanding obtained from the surface modification mechanism and acoustic emission analysis can be combined to develop a new online monitoring technique for vibratory finishing process.
- In addition to this, the effects of parameters of vibratory finishing such as frequency and amplitude on surface modification mechanism have been re-

ported. A new method of controlled 2D vibratory finishing has been developed specifically for this. This setup and understanding obtained can be used to develop a new type of adaptive high frequency vibratory finishing.

8.4 Future Works

Each of the works presented in this thesis can be continued to be a new study in each category as follows.

- The masked reference method can be developed further by considering the masked line as a reference to calculate the peaks and valleys. But this requires the surface to have no waviness component.
- In addition to this, different types of media (ranging from smooth steel media to raw abrasives) can be used to test different types of surface modification mechanisms and this algorithm can be used to develop a comprehensive relationship between the media type and surface modification mechanism.
- The wear debris analysis work presented here utilizes the basic magnetic separation method. In addition to this method there are other methods listed in the literature review section such as spectrometric analysis, particle counting technique and ferrous density analysis. These methods were not selected as they will change the form and shape of the wear debris particles which was required to study the wear mechanism.
- The SEM analysis was performed manually to analyze the size and shape of the particles. But there are software tools available which can automatically scan the selected area and measure the shape and size of particles using a specialized algorithm. These resources were not available at the time of research.
- Acoustic emission measurement have been performed without any digital signal processing. One of the methods which have been tried is the wavelet analysis. This can be used to remove the noise digitally.

Hence this research has opened many new paths in the industrial research of vibratory finishing process. The findings of these works can be directly used to understand and optimize the vibratory finishing process.

The results obtained, their significance and future recommendations are summarized in the table

Table 8.1 Summary of Thesis

Thesis Part	Results Obtained	Description	Significance	Limitations	Recommendation for future work
Surface Modification Mechanism	Novel Method to measure surface modification mechanism	Measure peak and valley height change with respect to constant reference	Novel technique; fast, non-destructive method to find surface modification mechanism	Small changes (<10% changes) cannot be predicted	The masked reference can be used as a new mean line
	Percentage of Plastic Deformation	Correlated well with rate of change of surface roughness (Ra) with correlation coefficient of 0.94	Ra vs PD correlation can be used to modify the process to obtain better Ra	Amount of material removal cannot be calculated	

Thesis Part	Results Obtained	Description	Significance	Limitations	Recommendation for future work
Wear Debris Analysis	Size of Wear Debris	Correlated with decrease in Ra	Can be developed into online monitoring for Ra	Results are obtained in an optimized setup; cannot be used for normal process	Other methods of wear debris analysis can be used
	Shape of Wear Debris	Understanding of different wear mechanisms	Understanding of wear mechanism in vibratory finishing filling the gap in literature	The resolution of SEM equipment used is 1μm	SEM equipment with higher resolution have to be used

Thesis Part	Results Obtained	Description	Significance	Limitations	Recommendation for future work
Effect of Process Parameters	Effect of Frequency and amplitude	Decreases process time	Can be used to develop a new type of high frequency and high amplitude vibratory finishing process	Cannot be increased beyond a certain limit (75Hz-3mm) as the media is not designed for this purpose	New type of media have to be used for testing in high frequency and amplitude settings

Thesis Part	Results Obtained	Description	Significance	Limitations	Recommendation for future work
Online Monitoring using Acoustic Emission	AE Peak Count	Correlation with Ra - 0.88; Correlation with PD - 0.80	Correlation can be used to develop online monitoring technique for vibratory finishing	Error percentage - 4.3%	Perform Key Process Variable Study on the factors affecting the different AE Signals so that this can be developed into an online monitoring technique
	AE Energy	Correlation with Ra - 0.86; Correlation with PD - 0.71		Error percentage - 13.5%	

References

Akagaki, T. and Kato, K. (1988). Simulation of flow wear in boundary lubrication using a vickers identation method. *Tribology Transactions*, 31(3):311–316.

Azouzi, R. and Guillot, M. (1997). On-line prediction of surface finish and dimensional deviation in turning using neural network based sensor fusion. *International Journal of Machine Tools Manufacture*, 37(9):1201–1217.

Baghbanan, M. R., Yabuki, A., Timsit, R. S., and Spelt, J. K. (2003). Tribological behavior of aluminum alloys in a vibratory finishing process. *Wear*, 255:1369–1379.

Beggan, C., Woulfe, M., Young, P., and Byrne, G. (1999). Using acoustic emission to predict surface quality. *The International Journal of Advanced Manufacturing Technology*, 15:737–742.

Bhushan, B. (2000). *Modern Tribology Handbook, Two Volume Set*. Mechanics & Materials Science. Taylor & Francis.

Bhushan, B. (2001). *Modern tribology handbook: Materials, coatings, and industrial applications*. Number v. 2 in The Mechanics and Materials Science Series. CRC Press.

Buttle, D. and Scruby, C. (1990). Characterization of particle impact by quantitative acoustic emission. *Wear*, 137(1):63–90.

Cariapa, V., Park, H., Kim, J., Cheng, C., and Evaristo, A. (2008). Development of a metal removal model using spherical ceramic media in a centrifugal disk mass

finishing machine. *International Journal of Advanced Manufacturing Technology*, 39(1-2):92–106.

Chang, Y., Hashimura, M., and Dornfeld, D. (1996). An investigation of the ae signals in the lapping process. *CIRP Annals-Manufacturing Technology*, 45(1):331–334.

Ciampini, D., Papini, M., and Spelt, J. K. (2007). Impact velocity measurement of media in a vibratory finisher. *Journal of Materials Processing Technology*, 183(2-3):347–357.

Ciampini, D., Papini, M., and Spelt, J. K. (2008). Characterization of vibratory finishing using the almen system. *Wear*, 264(7-8):671–678.

Ciampini, D., Papini, M., and Spelt, J. K. (2009). Modeling the development of almen strip curvature in vibratory finishing. *Journal of Materials Processing Technology*, 209(6):2923–2939.

Coker, S. A. and Shin, Y. C. (1996). In-process control of surface roughness due to tool wear using a new ultrasonic system. *International Journal of Machine Tools and Manufacture*, 36:411 – 422.

Cundall, P. (October 1971). A computer model for simulating progressive, large-scale movements in blocky rock systems. *Proceedings of the International Symposium on Rock Mechanics, Nancy, France*.

Domblesky, J., Cariapa, V., and Evans, R. (2003). Investigation of vibratory bowl finishing. *International Journal of Production Research*, 41(16):3943–3953.

Domblesky, J., Evans, R., and Cariapa, V. (2004). Material removal model for vibratory finishing. *International Journal of Production Research*, 42(5):1029–1041.

Dornfeld, D., Lee, Y., and Chang, A. (2003). Monitoring of ultraprecision machining processes. *The International Journal of Advanced Manufacturing Technology*, 21(8):571–578.

Eberle, D., Wall, C., and Treuhaft, M. (2005). Applications of radioactive tracer technology in the real-time measurement of wear and corrosion. *Wear*, 259(1):1462–1471.

Ferrer, F., Idrissi, H., Mazille, H., Fleischmann, P., and Labeeuw, P. (1999). On the potential of acoustic emission for the characterization and understanding of mechanical damaging during abrasion–corrosion processes. *Wear*, 231(1):108–115.

Fitch, B. (2013). Anatomy of wear debris. *Machinery Lubrication*, 10.

Franek, F., Vorlaufer, G., Stadler, A., Jech, M., and Wopelka, T. (2008). Modelling and simulation of assisted tribometrology. *Tribology in Industry*, 30(3-4):37–47.

Gates, J. D. (1998). Two-body and three-body abrasion: A critical discussion. *Wear*, 214(1):139–146.

Gillespie, L. (1975). A quantitative approach to vibratory deburring effectiveness. *SME Tech. Report.*

Gillespie, L. (2007). *Mass finishing handbook*. Industrial Press.

Glaeser (1981). Wear experiments in the scanning electron microscope. *Wear*, 73:371–386.

Groover, M. (2010). *Fundamentals of Modern Manufacturing: Materials, Processes, and Systems*. John Wiley & Sons.

Hase, A., Mishina, H., and Wada, M. (2012). Correlation between features of acoustic emission signals and mechanical wear mechanisms. *Wear*, 292-293:144–150.

Hashemnia, K., Mohajerani, A., and Spelt, J. K. (2013). Development of a laser displacement probe to measure particle impact velocities in vibrationally fluidized granular flows. *Powder Technology*, 235:940–952.

Hashimoto, F. and Debra, D. B. (1996). Modelling and optimization of vibratory finishing process. *CIRP Annals-Manufacturing Technology*, 45(1):303–306.

Hokkirigawa, K. and Kato, K. (1988). An experimental and theoretical investigation of ploughing, cutting and wedge formation during abrasive wear. *Tribology International*, 21(1):51 – 57.

Huda, A., Yamada, K., Hosokawa, A., and Ueda, T. (2002). Investigation of tool-chip interface in turning using two-color pyrometer. *ASME journal of Manufacturing science and Engineering*, 124(1):200–207.

Inasaki, I. (1998). Application of acoustic emission sensor for monitoring machining processes. *Ultrasonics*, 36(1):273–281.

Ivantsiv, V., Spelt, J., and Papini, M. (2009). Mass flow rate measurement in abrasive jets using acoustic emission. *Measurement Science and Technology*, 20(9):095402.

Jackson, M. and Davim, J. (2010). *Machining with Abrasives*. SpringerLink : Bücher. Springer.

Jiaa, C. L. and Dornfeld, D. A. (1990). Experimental studies of sliding friction and wear via acoustic emission signal analysis. *Wear*, 139(1):403–424.

Kayaba, T. and Suzuki, S. (1976). An investigation of surface damages by rolling contact. *Technology Report*, 41(1):21–46.

Kuchle, A. (2009). *Manufacturing Processes 2: Grinding, Honing, Lapping*. RWTHedition. Springer.

Kyle Elmblad, A. K. and Petkovich, M. (2002). Mass finishing. In *Buff, Brush & Polishin Techniques*, Nashville, TN.

Li, X. (2002). A brief review: acoustic emission method for tool wear monitoring during turning. *International Journal of Machine Tools & Manufacture*, 42:157–165.

Longbottom, J. and Lanham, J. (2005). Cutting temperature measurement while machining - review. *Aircraft Engineering and Aerospace Technology*, 77(2):122–130.

Marinescu, I., Hitchiner, M., Uhlmann, E., Rowe, W., and Inasaki, I. (2006). *Handbook of Machining with Grinding Wheels*. Manufacturing Engineering and Materials Processing. Taylor & Francis.

Menezes, P. L., Kishore, and Kailas, S. V. (2008). Influence of roughness parameters on coefficient of friction. *Sadhana*, 33(3):181–190.

Miller, R. and McIntire, P. (1987). *Nondestructive Testing Handbook, 2nd edn*, volume 5. American Society of Nondestructive Testing, Columbus OH,.

Mohajerani, A. and Spelt, J. K. (2009). Edge rounding of brittle materials by low velocity erosive wear. *Wear*, 267(9-10):1625–1633.

Mohajerani, A. and Spelt, J. K. (2010). Numerical modeling of the edge rounding of brittle materials by vibratory finishing. *Wear*, 268(7-8):1002–1012.

Naeini, S. E. and Spelt, J. K. (2009). Two-dimensional discrete element modeling of a spherical steel media in a vibrating bed. *Powder Technology*, 195(2):83–90.

Naeini, S. E. and Spelt, J. K. (2011). Development of single-cell bulk circulation in granular media in a vibrating bed. *Powder technology*, 211(1):176–186.

Oh, J. H. and Lee, S. H. (2011). Prediction of surface roughness in magnetic abrasive finishing using acoustic emission and force sensor data fusion. *Proceedings of the Institution of Mechanical Engineers, Part B: Journal of Engineering Manufacture*, 225(1):853.

PAC, P. A. C. (Online). Acoustic emission research. *http://www.pacndt.com/index.aspx?go=research&focus=/capabilities/ae%20research.htm*. Accessed on 20-8-2014.

Pawade, R. S. and Joshi, S. S. (2012). Analysis of acoustic signals and surface integrity in high-speed turning of inconel 718. *Proceedings of the Institution of Mechanical Engineers, Part B: Journal of Engineering Manufacture 2012*, 226(3):3–27.

Rigney (1992). The roe of characterization in understanding debris generation. *Tribology Series*, 21:405–412.

Roylance, B. and Hunt, T. (1999). *The Wear Debris Analysis Handbook*. Coxmoor Publishing Company's Machine & systems condition monitoring series. Coxmoor Publishing Company.

Sangid, M., Stori, J., and Ferriera, P. (2011a). Process characterization of vibrostrengthening and application to fatigue enhancement of aluminum aerospace components, part i. experimental study of process parameters. *The International Journal of Advanced Manufacturing Technology*, pages 1–15.

Sangid, M., Stori, J., and Ferriera, P. (2011b). Process characterization of vibrostrengthening and application to fatigue enhancement of aluminum aerospace components, part ii: Process visualization and modeling. *The International Journal of Advanced Manufacturing Technology*, 53:561–575.

Scheffer, C., Kratz, H., Heyns, P., and Klocke, F. (2003). Development of tool wear monitoring system for hard turning. *International Journal of Machine tools Manufacture*, 43(1):973–985.

Sofronas, A. and Taraman, S. (1979). Model development and optimization of vibratory finishing process. *International Journal of Production Research*, 17(1):23–31.

Spurlock, M. (2006). Particle counting or ferrous density or both? *Practicing Oil Analysis*.

Wang, S., Timsit, R. S., and Spelt, J. K. (2000). Experimental investigation of vibratory finishing of aluminum. *Wear*, 243(1-2):147–156.

Webster, J., Marinescu, I., Bennett, R., and Lindsay, R. (1994). Acoustic emission for process control and monitoring of surface integrity during grinding. *CIRP Annals-Manufacturing Technology*, 43(1):299–304.

Willcox, M. and Downes, G. (Online). A brief description of ndt techniques. *http://www.turkndt.org/sub/makale/ornek/a%20brief%20description%20of%20NDT.pdf*. Accessed on 20-8-2014.

Yabuki, A., Baghbanan, M. R., and Spelt, J. K. (2002). Contact forces and mechanisms in a vibratory finisher. *Wear*, 252(7-8):635–643.

Zhao, X. and Bhushan, B. (1998). Material removal mechanisms of single-crystal silicon nanoscale and at ultralow loads. *Wear*, 223:66–78.

Appendix A

Supporting Data and Results

This section of appendix includes the experimental data and results which are not presented in the work chapters. These experiments further add value to the main hypothesis and conclusion obtained as explained in the previous chapters. The experiments and results obtained are categorized based on the chapter which they add value. The following section explains the experiments presented in chapter 4 but with a new material - T6061 Aluminium Alloy.

A.1 Masked Reference Method

This section explains the results obtained by testing the masked reference method on a different workpiece material T6-6061 Al-Alloy. The processing conditions are exactly the same as mentioned in chapter 4, except for the workpiece material. Figure A.1 shows the variation of Ra as the surface is polished. Figure A.2 shows the variation of peak valley height measured by the masked reference method. Figure A.3 shows the comparison of percentage change of Ra with the percentage change of plastic deformation calculated from the masked reference method.

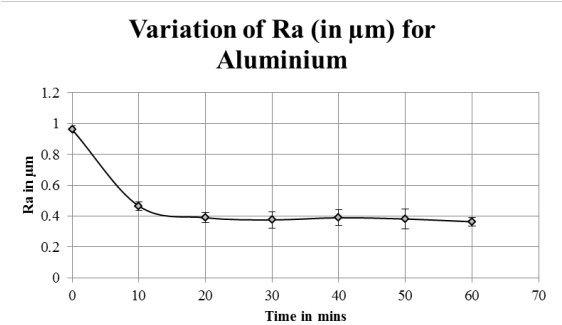

Figure A.1: Variation of Surface Roughness (Ra)

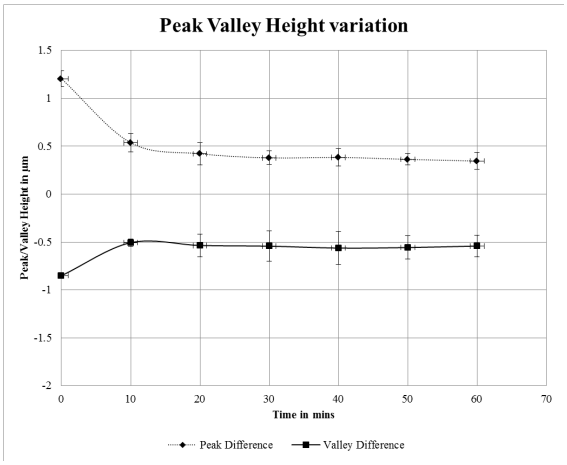

Figure A.2: Peak Valley Height Variation

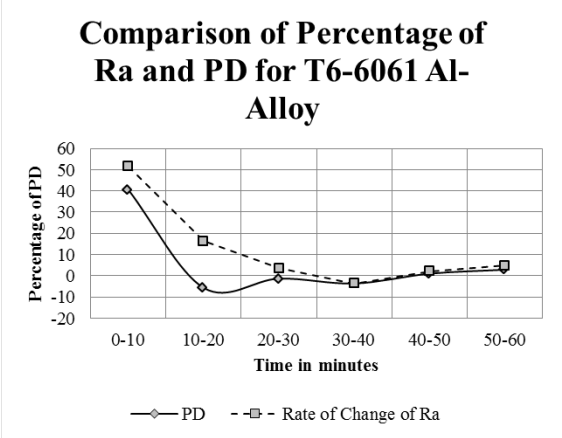

Figure A.3: Comparison of Percentage Change of Ra and PD

A.2 Wear Debris Analysis

The results obtained from the SEM analysis of the accelerated and analysis experiment described in Chapter 5 are presented in this section. The following figures are some of the magnified images of SEM pictures shown in figures 5.8 and 5.9.

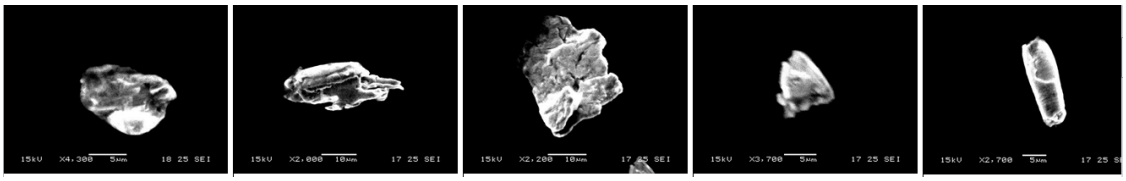

Figure A.4: SEM pictures of wear debris particles obtained after 30 mins for Accelerated Experiment

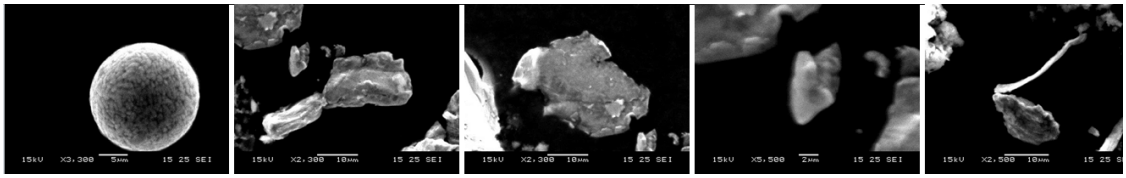

Figure A.5: SEM pictures of wear debris particles obtained after 60 mins for Accelerated Experiment

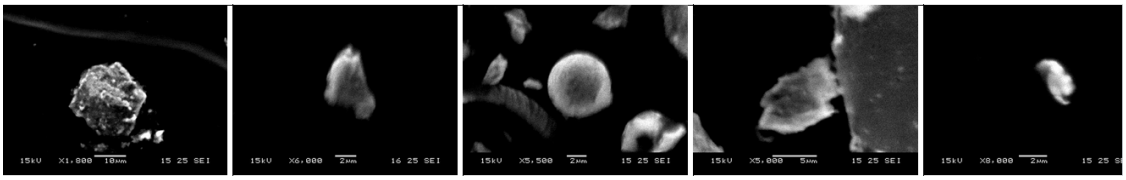

Figure A.6: SEM pictures of wear debris particles obtained after 90 mins for Accelerated Experiment

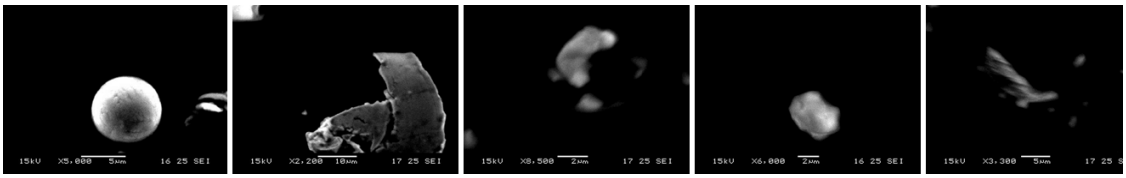

Figure A.7: SEM pictures of wear debris particles obtained after 120 mins for Accelerated Experiment

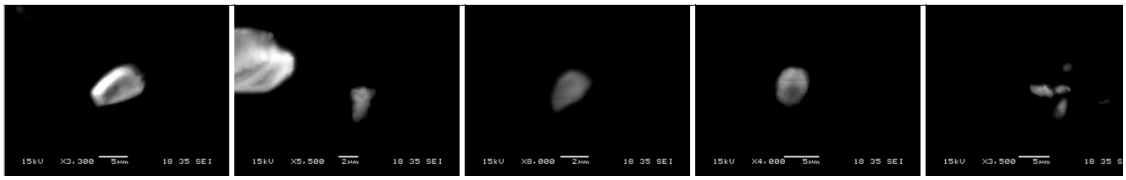

Figure A.8: SEM pictures of wear debris particles obtained after 150 mins for Accelerated Experiment

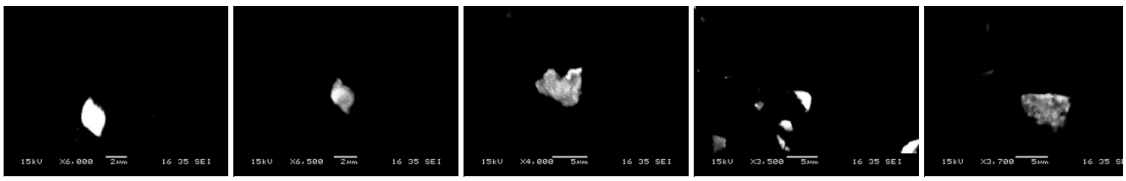

Figure A.9: SEM pictures of wear debris particles obtained after 180 mins for Accelerated Experiment

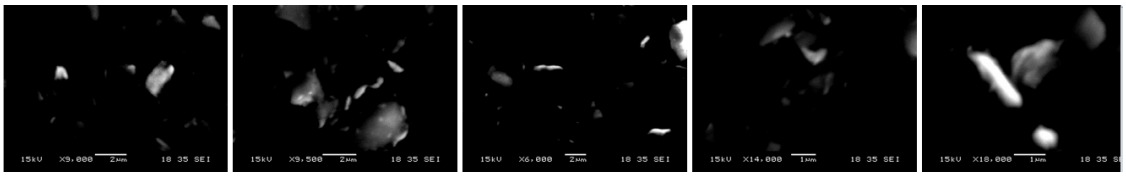

Figure A.10: SEM pictures of wear debris particles obtained after 210 mins for Accelerated Experiment

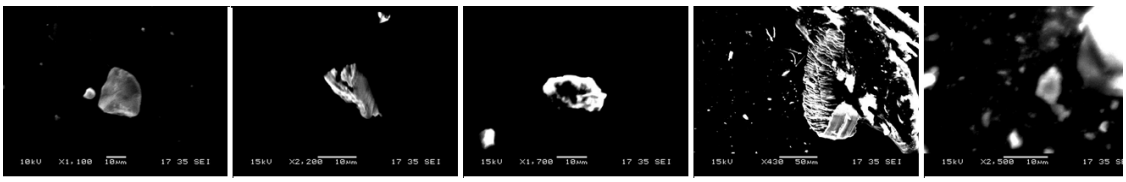

Figure A.11: SEM pictures of wear debris particles obtained after 30 mins for Analysis Experiment

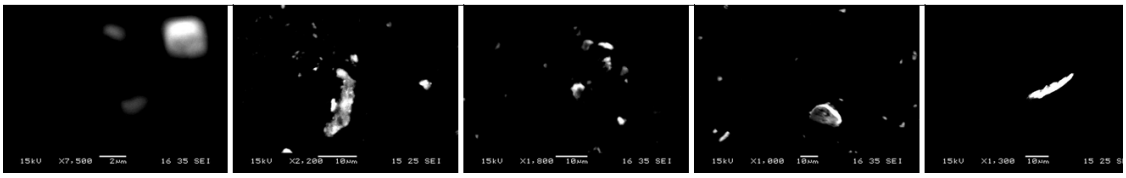

Figure A.12: SEM pictures of wear debris particles obtained after 60 mins for Analysis Experiment

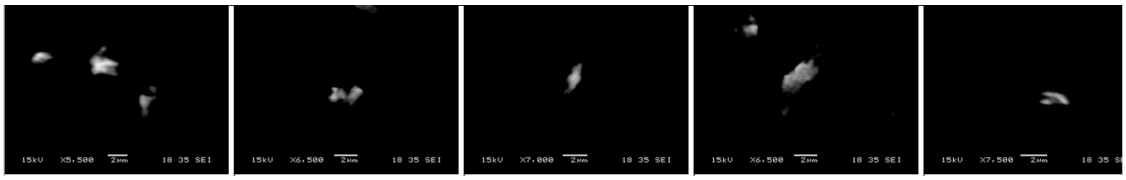

Figure A.13: SEM pictures of wear debris particles obtained after 90 mins for Analysis Experiment

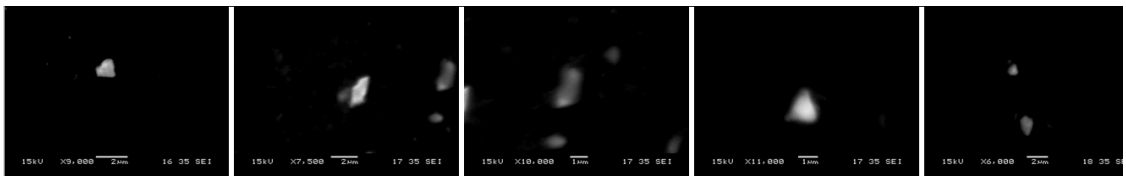

Figure A.14: SEM pictures of wear debris particles obtained after 120 mins for Analysis Experiment

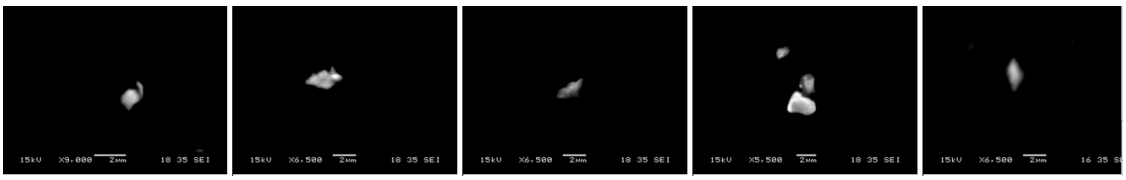

Figure A.15: SEM pictures of wear debris particles obtained after 150 mins for Analysis Experiment

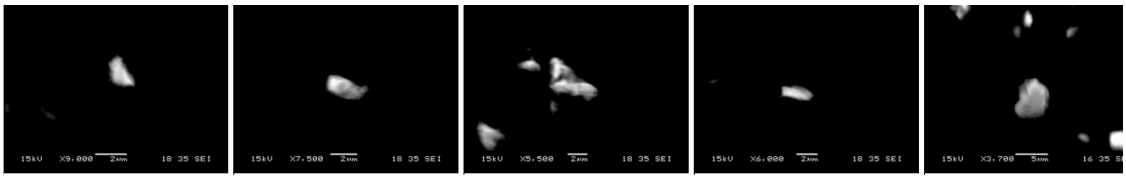

Figure A.16: SEM pictures of wear debris particles obtained after 180 mins for Analysis Experiment

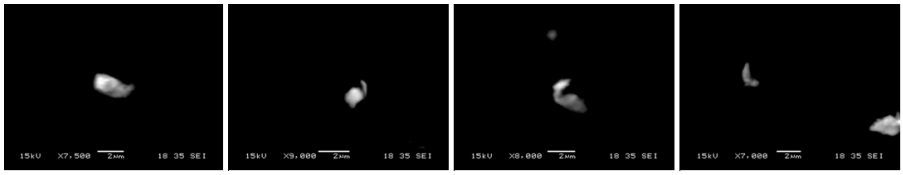

Figure A.17: SEM pictures of wear debris particles obtained after 210 mins for Analysis Experiment

A.3 Online Monitoring

A.3.1 PDT, HDT, HLT Calculation

This section presents a detailed description of the Peak Definition Time (PDT), Hit Definition Time (HDT) and Hit Lockout Time (HLT). This data is taken from user manual of Physical Acoustic Corporation Sensor.

The function of Peak Definition Time (PDT) also know as Rise Time Out (RTO) is to enable determination of the time of the true peak of the AE waveform. The PDT circuitry is a retriggerable one-shot, triggered by new signal maxima.

The main requirement is to avoid false measurements being made of a high velocity, low amplitude precursor, subject to this, PDT should be set as short as possible.

The function of Hit Definition Time is to enable the system to determine the end of the hit, close out the measurement processes and store the measured attributes of the signal. The HDT circuitry is a retriggerable one-shot, triggered by the threshold crossings. In most PAC systems the HDT must be at least twice the PDT.

The goal is to identify and describe events realistically. The HDT must be long enough to span over an intervals in which the signal to be measured falls below

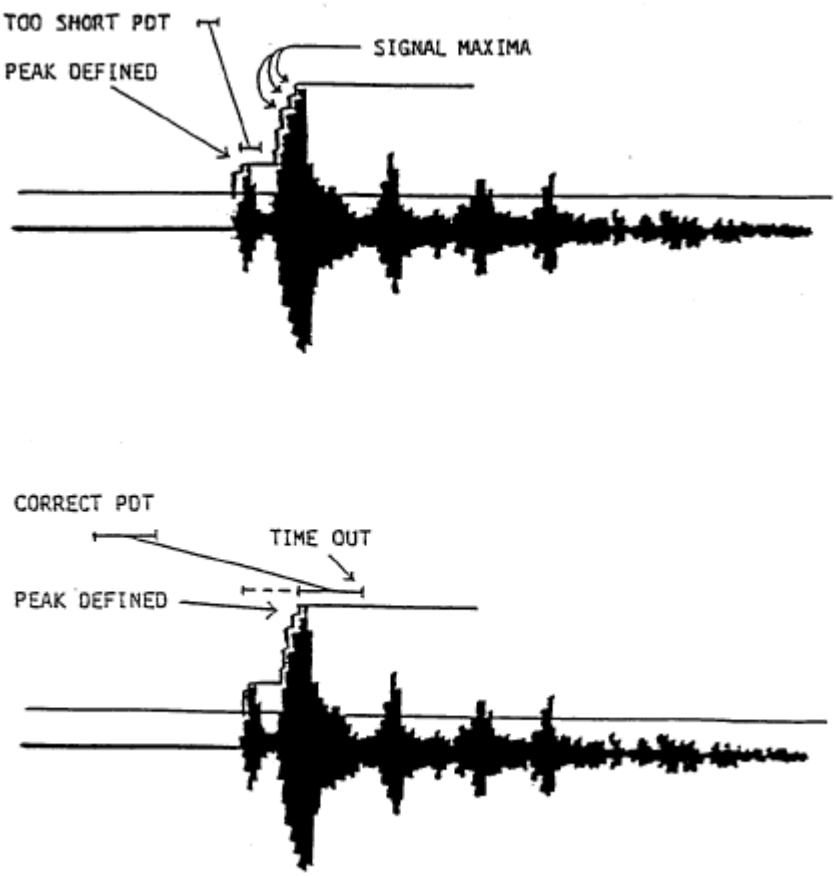

Figure A.18: Peak Definition Time Calculation

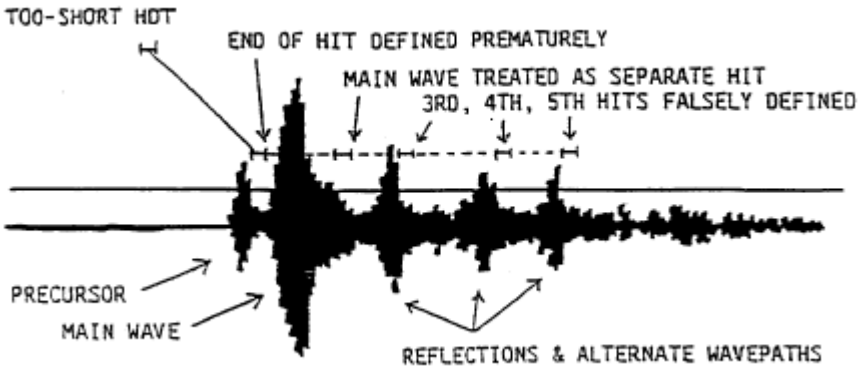

Figure A.19: Hit Definition Time

the threshold. Subject to this, the HDT should be set as short as possible in order to permit high data throughput rates and reduce the risk that two separate events will be treated as a single hit.

The function of Hit Lockout Time is to inhibit the measurement of reflections and late arriving parts of the AE signal, so that, data from wave arrivals can be

acquired at a faster rate.

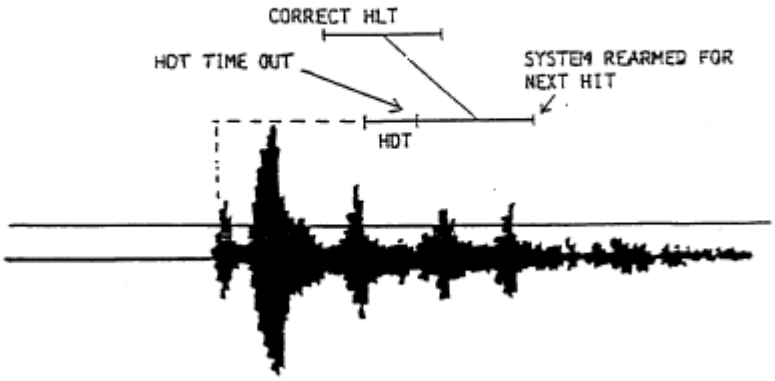

Figure A.20: Hit Lockout Time